Studies of nuclear reactions by micro-gas analytical methods

Anthony Robert Byrne

STUDIES OF NUCLEAR REACTIONS BY MICRO-GAS ANALYTICAL METHODS

by

ANTHONY ROBERT BYRNE, B.Sc.

Hatfield College

A Thesis presented in candidature of the Degree of Doctor of Philosphy under the supervision of G.R. Martin, B.Sc., F.R.I.C.

This research was performed during the period September 1961 to December 1964 at the Londonderry Laboratory for Radiochemistry in the University of Durham.

July, 1966

Chemistry Dept.,
University of Durham

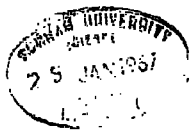

ABSTRACT

The development of an apparatus for the measurement of amounts of helium in the range 10^{-5} to 10^{-8} cc is described. Studies were made of the previously unmeasured average fission neutron cross section for the reaction $Fe^{56}(n, \alpha)Cr^{53}$ and a value of 0.39 mb. obtained from irradiations in B.E.P.O. at Harwell and D.F.R. at Dounreay. The nuclear reactions $Fe^{54}(n, p)Mn^{54}$ and $Fe^{54}(n, \alpha)Cr^{51}$ were also studied and values of the average cross section measured.

The absolute fission yields of Mo^{99} and Ba^{140} in the thermal neutron fission of natural uranium were determined using helium analysis of an irradiated uranium solution containing boric acid to obtain the number of fission events. The chemical separation of the nuclides and the counting and standardization procedures are fully described. The results, of 5.94 and 5.87% for Mo^{99} and Ba^{140}, respectively, and the errors involved, are discussed in the light of previous values.

The third section of the work was concerned with the calibration of photoneutron sources by destructive analysis of the beryllium cylinders for helium, also produced in the photo-reaction. A discussion of neutron source calibrations is included. The design, and experiments carried out with an apparatus which included a silver-palladium leak for hydrogen are described. Unfortunately this work was not completed, but suggestions are included for its conclusion.

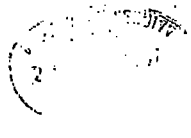

ACKNOWLEDGEMENTS

I would like to acknowledge my debt to the sound advice and ready encouragement given during this research by Professor G.R. Martin, formerly Reader in Radiochemistry in the University of Durham. Also to Mr. J.D. Hemingway for his friendly help and companionship.

I would also like to thank the (then) Department of Scientific and Industrial Research for the award of a Research Studentship.

INDEX OF CONTENTS

INDEX OF FIGURES

SECTION 1.

INTRODUCTION

1.1. General

This research was concerned with the application of a micro-analytical technique for measuring helium gas to three nuclear problems. The part played by the helium analysis differed in each study. In one of these studies, that of the magnitude of the average fission neutron cross section for (n, α) reactions in iron, the helium measured was the consequence of, and of direct interest to, the reaction. In the second problem, that of photo-neutron production in beryllium sources, the helium was produced as an associated product of the reaction under study. In the third, that of the absolute yields of Mo^{99} and Ba^{140} in thermal neutron induced fission of natural uranium, the helium analysis served as a tool for the measurement of one of the parameters required for the calculation. This was the number of fissions occurring in the sample. The helium measurement was the only link between these otherwise self-contained problems. To have attempted to write a chapter introducing the reader to the fundamentals and facets of these three distinct problems would have produced a fragmentary and chaotic effect. Hence this 'Introduction' is not so much an introduction to the problems as a summary of the work. Instead, each of the three problems is prefaced with its own relevant introduction.

1.2. Helium measurement

The study of inert gases in the atmosphere stretches back to the observation, in 1785, of Cavendish that about one part in 120 of the air refused to react on repeated sparking with oxygen. (This is remarkably close to the figure of 0.94% of argon in air). The development of apparatus for precise measurements on inert gases was excellently reviewed by Paneth[1] in 1953. The basic apparatus has remained unchanged, except for minor technical improvements, since the development by Glueckauf[2] in the early forties of the gas-solid chromatographic unit, termed the column, for separating the inert gases from one another and from residual traces of other gases. The last basic atmospheric research on the rare gases was the accurate determination of the xenon and krypton content of the air by Glueckauf and Kitt in 1956[3].

In this present research, the amounts of helium measured were in the range of 10^{-5} to 10^{-8} cc. at N.T.P., the 'blank' on the apparatus being normally about 1 to 2 x 10^{-9} cc.

1.3. The (n, α) reaction in iron

The aim of the work was to measure the average cross section for the reaction $Fe^{56}(n, \alpha)Cr^{53}$ with fission spectrum neutrons.

The meaning and importance of average fission cross sections is discussed. The apparatus used and results for helium production in natural iron and isotopically pure Fe^{56} are presented. In most of the experiments samples of about one gramme were irradiated at Harwell in B.E.P.O. Two samples were irradiated in the fast reactor, D.F.R., at Dounreay which has a large fast flux with a negligible thermal neutron component. The results obtained were in good agreement with simple cross section theory.

Average fission cross sections for the reactions $Fe^{54}(n, \alpha)Cr^{51}$ and $Fe^{54}(n, p)Mn^{54}$ were also measured on solutions of the irradiated natural iron used for helium analyses. The results are discussed in the light of previous values obtained by earlier workers.

1.4. Yields of the fission products Mo^{99} and Ba^{140}

The aim was to measure as accurately as possible the absolute fission yields of the nuclides Mo^{99} and Ba^{140} in the thermal neutron induced fission of natural uranium, that is, effectively in U^{235}. The helium apparatus was used to measure the extent of the $B^{10}(n, \alpha)Li^{7}$ reaction occurring in boric acid irradiated homogeneously with the uranyl nitrate solution. This, with a knowledge of the cross sections for the boron reaction and fission, and together with the proportions of boron and uranium, enabled the absolute number of fissions to be calculated. The radiochemical, counting and calibration procedures are fully described. The yields were determined to about $\pm$ 3% and the values are discussed in the light of previous measurements.

1.5. Calibration of photo-neutron sources

The aim of the work was to obtain an accurate (about $\pm$1%) absolute calibration of three of the six British beryllium (γ, n) sources by destructive analysis for helium. Measurement of the helium accumulating by the reaction

$$Be^{9} + \gamma \longrightarrow n + 2He^{4}$$

in a known time gives the neutron emission rate.

Various (α, n) and (γ, n) sources are discussed and methods of standardization briefly surveyed. The assumptions involved in the

application of the helium analysis to the standardization of the (γ, n) sources are discussed. Problems associated with micro-analysis of helium in large quantities of beryllium, and the method chosen and the apparatus constructed are described. Various tests and experimental runs performed are considered. The sources were not measured because of the failure of the palladium 'leak' apparatus for hydrogen removal and lack of time. Suggestions for completion of the work are included.

SECTION 2.

THE APPARATUS

2.1. Historical

Paneth[1] has reviewed the historical development of techniques for the measurement of micro quantities of inert gases. Early methods used manometric techniques or measurement of the intensity of the characteristic spectral lines[4]; both relied on very large sampling systems. The apparatus used in the work described here was a development of that used by Glueckauf and Paneth[5], which followed the introduction, by Glueckauf[2], of the fractionation 'column' for the separation of the inert gases from each other. This, together with a specially sensitive Pirani, or hot wire gauge, enabled them to show, from small bottled samples, that the helium and neon content of ground level air is a geophysical constant.

Later workers, using slightly modified apparatus, have measured the helium and neon contents of meteorites for cosmological studies (e.g. 6, 7); the helium, neon and argon content of stratospheric air for evidence of gravitational separation[8, 9]; and a whole range of problems associated with alpha particle production in nuclear reactions, ranging from spallation to studies of inert gas diffusion in metals (e.g. 10, 11).

2.2. General description

Before discussing the general scheme of the apparatus and its component parts, mention must be made of the salient features of the system. With the only exceptions of the mercury diffusion pumps and the Pirani gauges, the entire apparatus was built from soda (soft) glass. This was necessitated by the relatively high permeability of pyrex glass to atmospheric helium.

When taps were being fitted to the system, the key of the tap was always checked to make sure that it was soda glass, as many manufacturers use pyrex keys in soda barrels.

The Pirani gauges and galvonometer suspension were sensitive to vibration, so the bench on which the apparatus was built had deep foundations separate from those of the laboratory, and the rotary oil pumps were mounted independently of the bench with vibration damped vacuum leads to the apparatus.

The 'primary' pumping system consisted of a rotary oil pump and two mercury diffusion pumps connected to the various parts of the apparatus through a wide bore tube termed the manifold. This pumping system was duplicated at the other end of the manifold, so that different sections of the apparatus could be pumped out separately as the need arose. Another rotary oil pump was connected to the 'secondary' line, used for lowering mercury in the various Toepler pumps, the pipetting system and mercury cut-offs.

All stopcocks were lubricated with Apiezon N, except those which, being near to outgassing furnaces, required the higher temperature grease T. Permanent and semi-permanent cones and sockets were joined with Apiezon W wax.

2.3. The Block Diagram

The block diagram, Fig. 1, shows the main sections of the apparatus. A full description of each section, and its uses, follows under the separate section headings, but first a brief summary of the complete procedure is given here.

The helium containing specimen, usually in the form of a piece of metal of up to a few grammes in weight, was dissolved in an appropriate solvent in the dissolution vessel after this had been

FIGURE 1.

Schematic block diagram of the apparatus

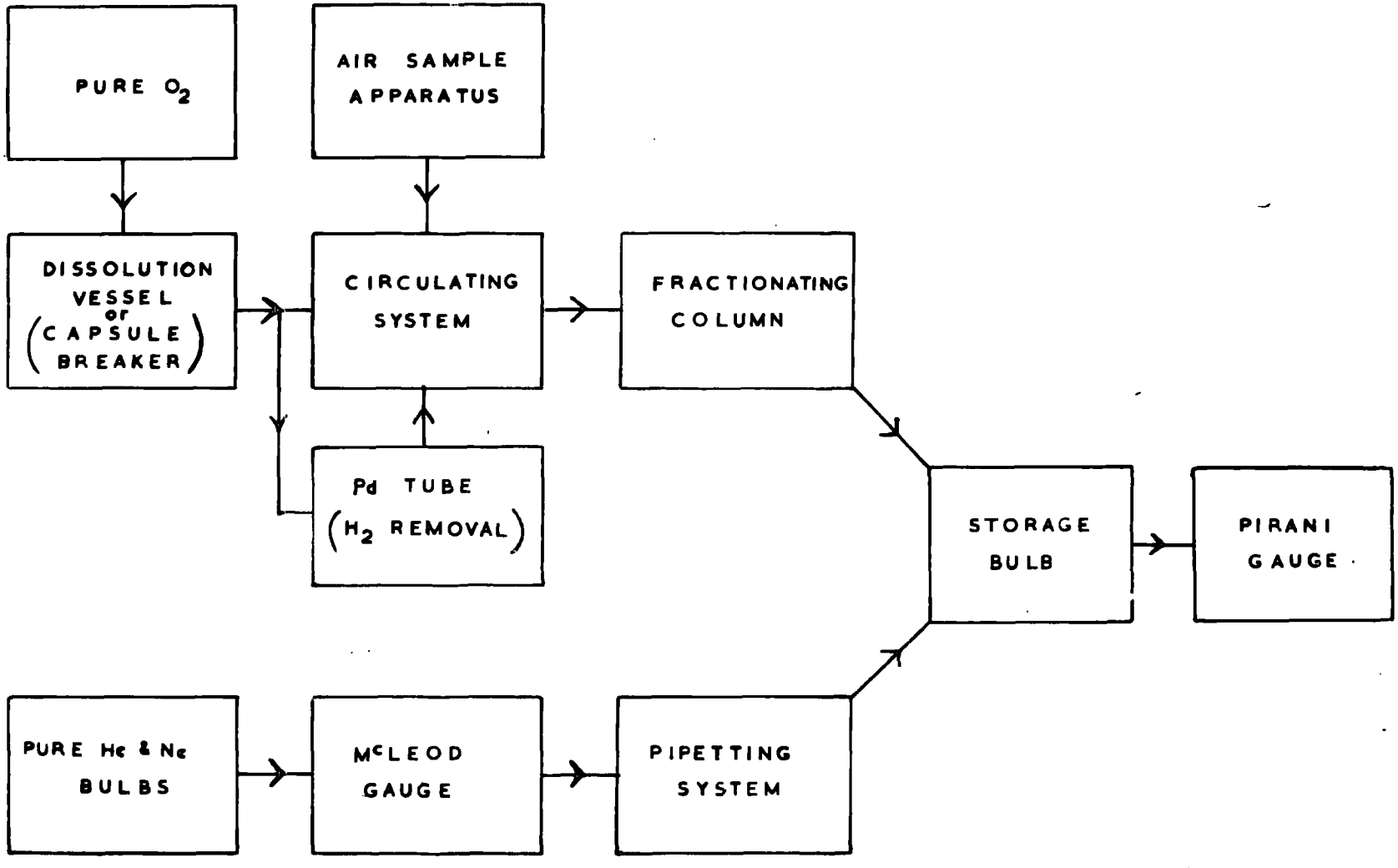
PURE O_2
AIR SAMPLE APPARATUS
DISSOLUTION VESSEL or (CAPSULE BREAKER)
CIRCULATING SYSTEM
FRACTIONATING COLUMN
Pd TUBE (H_2 REMOVAL)
STORAGE BULB
PIRANI GAUGE
PURE He & Ne BULBS
McLEOD GAUGE
PIPETTING SYSTEM

outgassed and flushed free from helium by the pure oxygen from the oxygen reservoir. (A blank run had, of course, been performed on the oxygen, before dissolution of the sample, to check the purity of the oxygen). The gases released by dissolution of the sample were flushed into the circulating system, where they were pumped magnetically over a hot palladium catalyst and the great bulk of the hydrogen (if any) removed as water. If very large amounts of hydrogen were released by the dissolution (for example, from large samples of beryllium) the bulk of this was first removed in the palladium diffusion leak section. The great bulk of the condensable gases was then adsorbed onto the cooled charcoal in the circulating system, and the helium, with a little oxygen, was transferred by Toepler pump into the first unit of the column. This section fractionated the helium from the neon (if any) and delivered the gas into the storage or compression bulb. The mercury was then raised in the bulb, compressing the pure helium into a small space above the measuring Pirani gauge. The tap above the gauge was opened and the galvonometer deflexion measured on a suitably sensitive scale.

Since the sensitivity of the gauge varied a little from day to day due to slight variations in temperature and voltage, and an ageing effect in the delicate filament, it was calibrated after each measurement with a known amount of helium. (Typical day to day variation was about 1%). This was measured out in the calibrated volumes of the McLeod gauge, diluted by the gas pipetting system, and finally allowed into the re-evacuated storage bulb. The deflexion obtained from this accurately known amount enabled the unknown helium sample to be determined by simple ratio.

The function of the air apparatus was to allow a known volume of air, and hence helium, into the circulating system to make

periodic checks on the correct functioning of the apparatus.

A full description of these various sections now follows.

2.4. The oxygen reservoir

The apparatus is shown in Fig. 2.

Oxygen has been used in this type of work for flushing solutions and as a carrier gas for two main reasons:

(i) it removed hydrogen by combination in the circulating system;

(ii) it was easily handled in the vacuum system by condensation with liquid nitrogen and adsorbtion on cooled charcoal.

The method of purifying oxygen from helium and neon was as follows. With taps T_1, T_2 and T_4 open and T_3 closed, the apparatus was rigourously evacuated (through T_1) for several hours, the charcoal bulb, which contained about 50 gms. of coconut charcoal, being baked out at about 300°C. After the charcoal had cooled and a hard vacuum obtained in the Toepler bulb attached to the pumping line, (i.e., a pressure of better than 10^{-6} cm. Hg. attained), T_4 was closed and oxygen gas from a cylinder admitted slowly into the system through T_3. Before opening T_3, the rubber connections and glass arms were thoroughly flushed out with oxygen via the mercury bubbler B, which acted as a non-return valve to prevent air entering the system should T_3 be opened too rapidly. When the pressure of oxygen in the system registered by the manometer had reached one atmosphere, T_3 was shut. The small bulb adjacent to tap T_2 was then surrounded with liquid nitrogen and the bulk of the oxygen condensed into it. A vapour pressure of 16 or 17 cms. of oxygen was then registered on the manometer. T_2 was closed and the charcoal bulb was also

FIGURE 2.

Apparatus for production of pure, helium-free oxygen

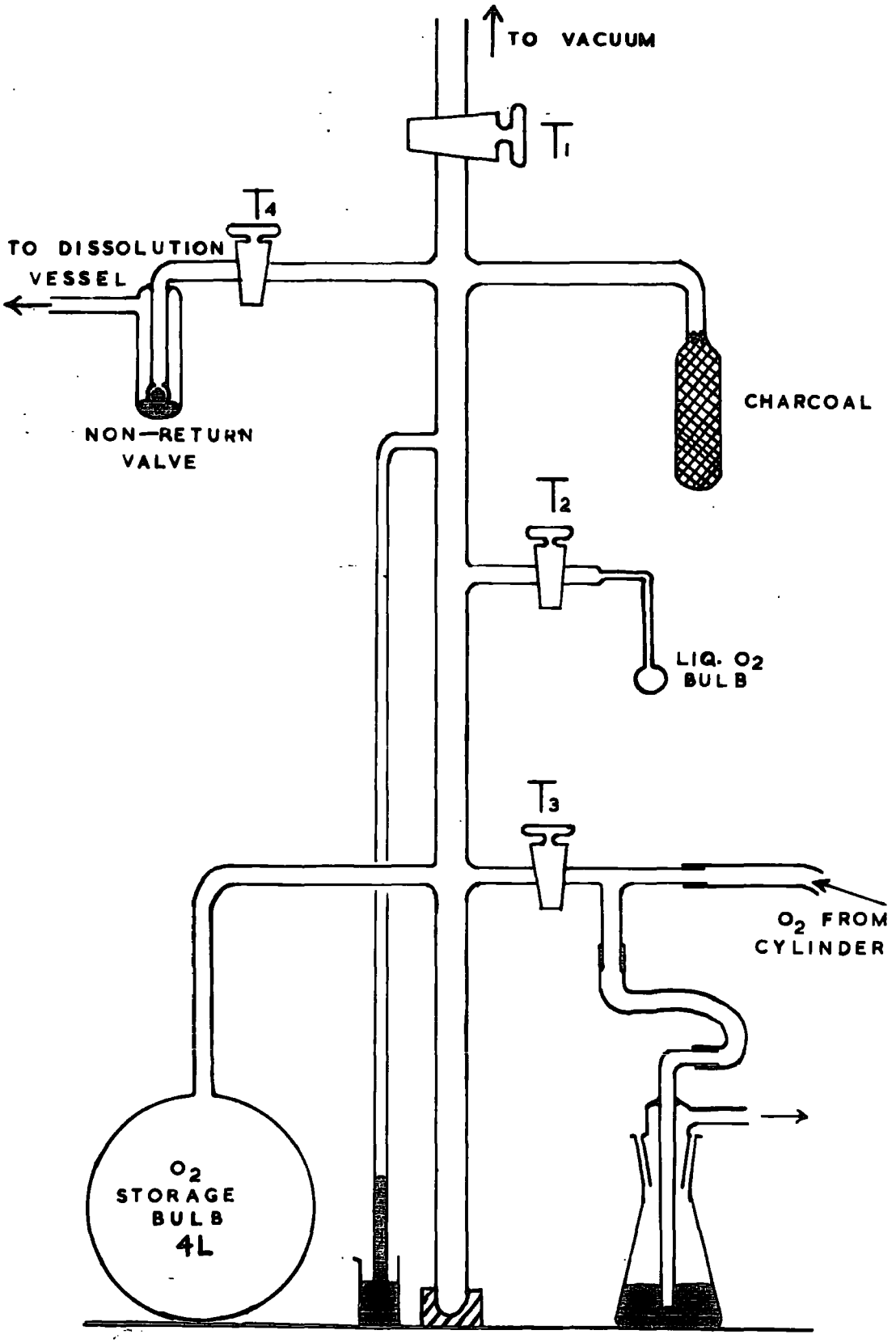
TO VACUUM
T1
T4
TO DISSOLUTION VESSEL
NON—RETURN VALVE
CHARCOAL
T2
LIQ. O2 BULB
T3
O2 FROM CYLINDER
O2 STORAGE BULB 4L

surrounded with liquid nitrogen. After a few minutes, the manometer showed less than 1 mm. oxygen pressure and T_1 was opened to the pumps. By this means, an appreciable proportion of the least adsorbable gases (helium and neon), together with a little oxygen, were pumped away. After about 15 minutes, T_1 was closed and the liquid nitrogen removed from around the charcoal, T_2 was opened and the liquid oxygen allowed to evaporate.

When the oxygen had all desorbed, and the pressure reached one atmosphere again, the liquid oxygen bulb was again cooled and the whole process of condensation, adsorbtion and pumping repeated.

In practice, it was found that 10 to 12 cycles were required to reduce the helium contamination to a level such that an oxygen sample of about 25 cc at N. T. P. contained around 1×10^{-9} cc of helium. This was the quantity of oxygen normally used in a run.

It appeared that the processes limiting the speed of purification were:

(a) the volume of the dead space in the liquid oxygen bulb;

(b) the solubility of helium in liquid oxygen;

(c) the adsorbtion of helium on the large mass of charcoal;

(d) back diffusion of helium past the pumps when relatively large quantities of oxygen were being pumped away.

By this method about four litres (the volume of the storage bulb) of substantially helium-free oxygen could be prepared at one or two centimetres below atmospheric pressure. Initially, electrolytically prepared cyclinder oxygen was used, as this should have less atmospheric contaminants, but after this was exhausted, ordinary

cylinder oxygen was used with equal success.

It was found that the oxygen slowly became recontaminated with helium from the walls and by diffusion through the glass, but two or three purification cycles per week were sufficient to maintain the purity level.

Oxygen being used for flushing was allowed out of the system through T_4 and the bubbler. The latter prevented any back diffusion of gas from the delivery tube into the pure supply.

2.5. The Dissolution Vessel

Three different types of dissolution vessel were used in the course of the work. Since their design and operation are integrally connected with the type of investigation, they are fully described below in the relevant chapters.

(a) A small dissolution vessel which contained about 100cc of solvent, used for samples of iron up to about a gramme. This is described below in Section 3 on cross section measurements.

(b) A vessel of fundamentally the same design as in (a), but capable of holding 1 litre of reagent. This was used for runs on large quantities of beryllium, circa 6 gms. In conjunction with this, was the hydrogen removing palladium diffusion apparatus. Both of these are described in the work on photo-neutron sources in Section 5.

(c) A vessel designed for breaking open small irradiated glass capsules, containing a uranium and boron solution, under vacuum; and for flushing out the helium in this

solution as in (a) and (b). This was built for the studies of fission described in Section 4.

For the sake of continuity, however, we can describe the function of these pieces of apparatus as the release of helium from the samples and its transfer, by flushing with pure oxygen, into the circulating system. The solvent used in (a) and (b) depended on the nature of the specimen but was usually a saturated aqueous solution of potassium cupric chloride (K_2CuCl_4).

2.6. The Circulating System

The circulating system, Fig. 3, was designed to remove relatively small amounts of hydrogen (of up to about 20 cc at N. T. P.) from the gas flushed into it with the oxygen from the dissolution section.

In the work concerned with the dissolution of beryllium, the bulk of the hydrogen was removed by the palladium thimble device, but amounts of hydrogen of the above order were still present, as the diffusion became extremely slow when only a small pressure existed across the thimble. Diffusion was not practicable below a pressure of about 2 cms. of hydrogen. When iron samples had been dissolved, however, in K_2CuCl_4 reagent, the amount of hydrogen present, if any, in the carrier gas was very small.

The construction of the system is best understood by describing its operation:

The helium-carrying oxygen gas, together with the hydrogen, entered the system through tap T_1 after taps T_2 and T_4 had been closed. The gas gently bubbled past the mercury in the ventil V, acting as a non-return valve by being raised around the U bend just sufficiently to prevent the gas from forcing a permanent entry. The

FIGURE 3.

The circulating system

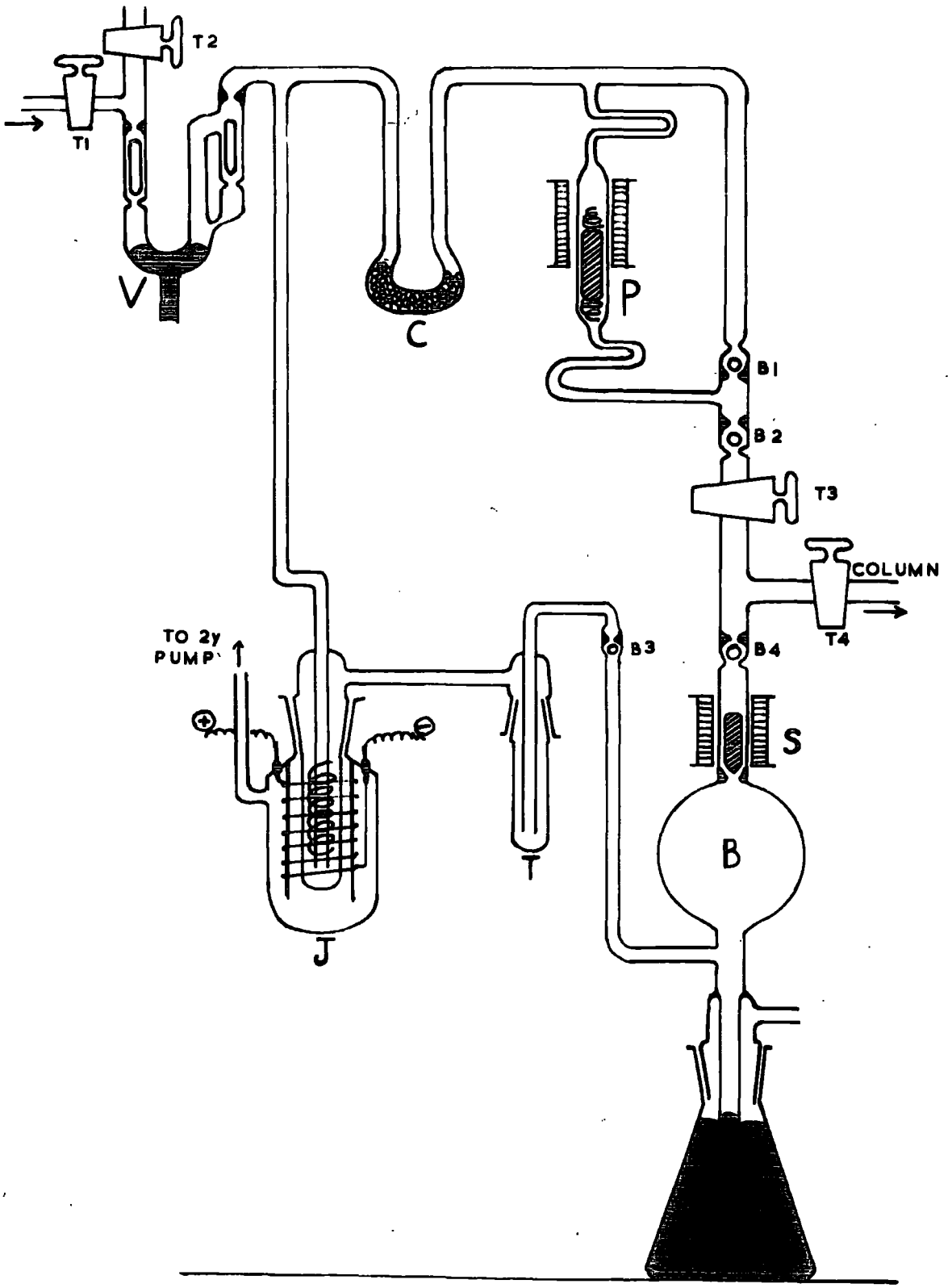
T2
T1
V
C
P
B1
B2
T3
COLUMN
T4
TO 2y
PUMP
B3
B4
S
B
T
J

gases were adsorbed on the nitrogen-cooled charcoal in C, which contained about 5 gms. of coconut charcoal previously baked out. This prevented the pressure from building up in the system, which would have vitiated the action of the ventil V. When all the gas had been flushed through V into the system, the mercury in V was raised until the ground glass floats seated in their sockets. The liquid nitrogen was then removed from around C and the gases desorbed.

The gas was now confined to what was in effect a closed circle or loop of tubing, around which it was caused to circulate by the magnetic pump P. A glass enclosed iron slug acted as a piston in its surrounding tube. When the solenoid was activated, the piston leapt up drawing gas through the ball valve B2 while B1 remained shut. When the solenoid was deactivated, the piston dropped, forcing gas past B1 while B2 was forced to shut. A make-and-break device supplied an intermittent current to the solenoid so that a continuous pumping action ensued, and the speed of the pump could be controlled at will. The springs above and below the piston, and the loops in the tubing were designed to absorb the shock of the plunger.

The float valve S was lifted from its seat above B magnetically to allow the free circulation of gas in an anti-clockwise direction around the loop.

The gas was thus forced through the catalysing system J. This was a spiral of palladium wire wound around the inner tube of a trap. Outside the trap and joined to it by the cone and socket was a wire wound jacket. The heater current was adjusted by a rheostat until the element glowed a dull red and the palladium spiral was heated by radiation to about three or four hundred degrees. The whole system was immersed in a water bath. In practice, the heating

of the trap was not found to add any helium to the oxygen blank, but an initial degassing was always undertaken.

At the temperature of the palladium, any hydrogen combined with the excess oxygen and the water formed was trapped out in T. The trap was not actually immersed in nitrogen as this would have condensed the oxygen, but was surrounded by a Dewar flask containing a few ccs of nitrogen at the bottom, to keep it well below $0^{\circ}C$.

When large quantities of hydrogen were present, the mercury level in B could be seen to rise as the hydrogen was removed. Usually circulation was continued for 15 to 20 minutes.

The furnace was now switched off and circulation terminated. C was re-immersed in nitrogen and the trap T topped up. Tap T_3 was closed and the mercury raised in the Toepler bulb B to around the float valve S. When the solenoid surrounding it was de-activated, the float rested on the mercury. The mercury was then sucked down to below the side arm, leaving the float trapping a collar of mercury above B which retained the gas formerly in B to the section between S, T_3 and T_4. The mercury was held down for a few seconds to allow the gas in the rest of the circulating system to re-equilibrate with the volume B, and then a further Toepler stroke was begun. 30 Toepler strokes were performed in all to ensure effectively complete transfer of the helium. The mercury in the column was lifted up to its starting position before the commencement of Toepler action, so that after three or four operations tap T_4 could be opened to allow the gas to equilibrate with the first charcoal of the column. This also helped to accommodate the oxygen which desorbed from C each time the charcoal was exposed to the evacuated space B.

Although the volume of the Toepler bulb B was such that only about 15 strokes should have been required to transfer 99.9% of the gas, its efficiency was lowered by retention of some of the helium on the charcoal at each stage.

Experimentally, it was found that 15 Toepler strokes left about 5% of the helium behind, and that 30 strokes resulted in a recovery of 99.8%.

These results were in fact consistent and led to the deduction that only about 20% of the helium was transferred at each stroke:-

We can say

$$F = (1 - x)^n$$

where F is the fraction of gas left behind after n cycles in which a fraction x is removed during each cycle.

Thus when $n = 15$, $F = 0.05$, so that

$$x = 0.18 \text{ (i.e., about 20\%)}$$

For 30 Toepler strokes

$$F = (1 - 0.18)^{30} = 0.0025$$

That is, 30 cycles should leave about 0.25% of the gas behind, in good agreement with experiment.

On the final Toepler stroke, the mercury was raised until the ball valves B3 and B4 seated, and the next stage, the separation of the gases transferred to the column, could be commenced.

It seems possible that small amounts of hydrogen remained in the gas unremoved, but it was shown experimentally that they did not pass through the column after a number of operations sufficient to deliver the neon fraction, and were hence of no importance.

2.7. The Fractionation Column

The column was basically a gas-solid chromatography unit, using liquid nitrogen cooled charcoal as the adsorbent.

2.7.1. General description

The column is shown in Fig. 4. It consisted of two parallel lines of tubing, each connected to a separate mercury reservoir. 15 vertical stems sprouted from each line, supporting bulbs of capacity about 25 ccs, viz. A_{1-15} and B_{1-15}. Below each of the bulbs A was a side arm connected to a small bulb C, containing about .75 gm. of activated coconut charcoal. These charcoal bulbs were grouped together into four clusters; the first, bulbs C_{1-3}, and the three others containing four bulbs each. This enabled the 15 bulbs to be cooled or degassed conveniently in four small Dewar flasks or four small furnaces (at about 300°C). Bulb C_1 hung below C_2 and C_3 so that it could be cooled separately; in this way it would hold back the condensable gases from the circulating system while the other bulbs were successively allowed to warm up to speed the passage of neon through the column once the helium had all been removed. In practice, no experiments were performed in which a complete neon recovery was required.

Each unit, of which there were 15, consisted of the equilibrium gas volume A_n, the charcoal bulb C_n and the gas transfer bulb B_n. The basic process was the exposure of the volume A_n, containing gas, to the charcoal C_n when equilibrium was established between the adsorbed (or condensed) and gas phases, and the transfer by Toepler action of the gas phase via the bulb B_n into the next unit, $(n + 1)$, where equilibrium was again established.

FIGURE 4.

The fractionating column

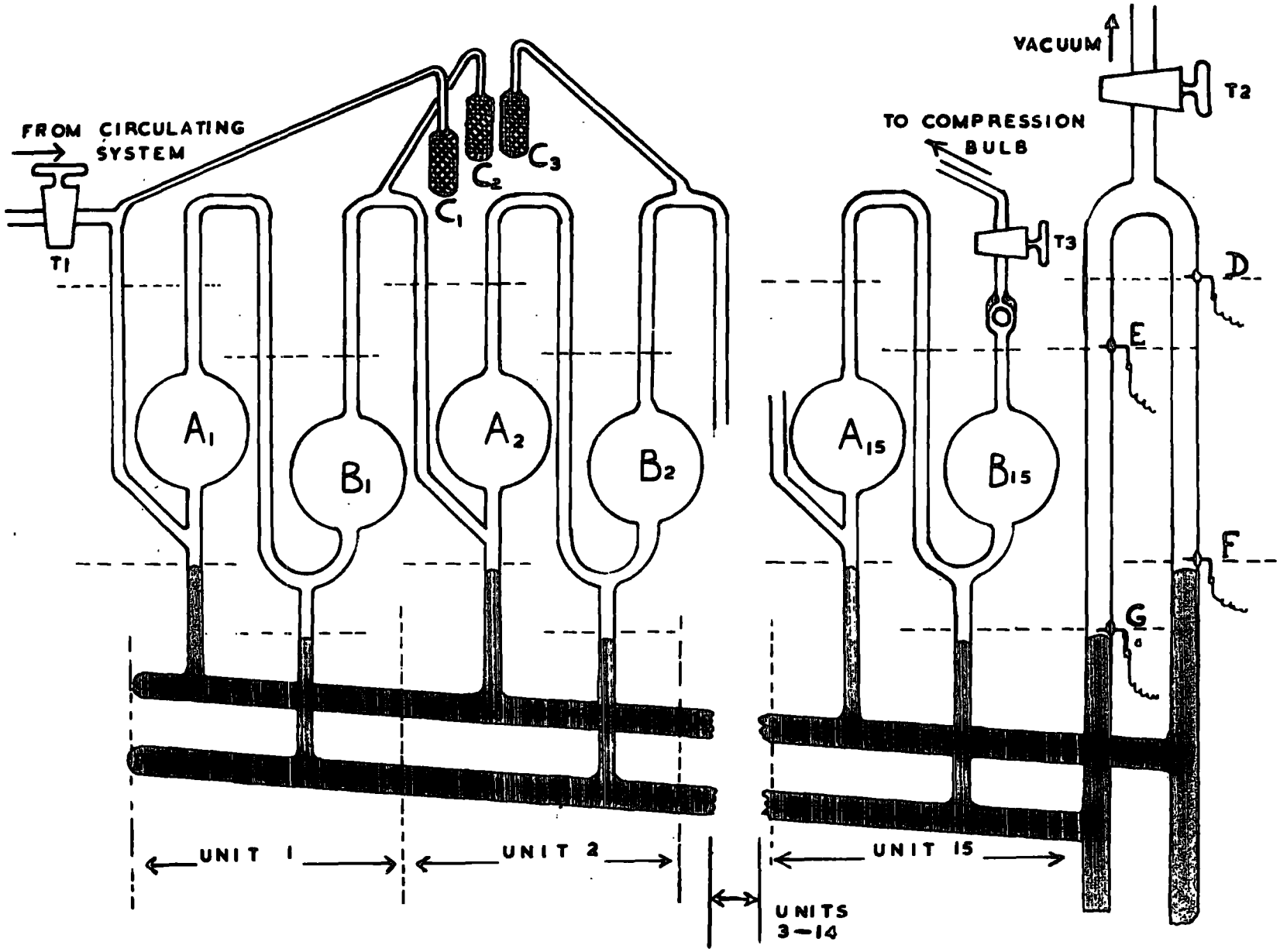
FROM CIRCULATING SYSTEM
T1
C1
C2
C3
A1
B1
A2
B2
A15
B15
VACUUM
T2
TO COMPRESSION BULB
T3
D
E
F
G
UNIT 1
UNIT 2
UNIT 15
UNITS 3—14

2.7.2. Operation of the column

With the mercury drawn down into its reservoirs, the apparatus had previously been evacuated through taps T_2 and T_3, and the charcoals outgassed. After a good vacuum had been obtained, the mercury was raised to levels E and D as described during the transfer of the helium sample into the first unit. Tap T_2 was shut but T_3, leading to the evacuated compression bulb, remained open so that the gas fractions were delivered into the compression bulb during the operation of the column. The helium sample was present in the glass tubing on each side of T_1 and partially adsorbed on C_1.

The mechanical operation of the column was fully automatic, but it could also be operated manually for special purposes or in an emergency. The movement of mercury in the column was controlled by magnetically operated valves, opening either to the vacuum pump, or to the atmosphere, and activated through a relay system by the electrical contacts made with the mercury at D, E, F, and G and two other common contacts, one on each stem.

On switching on the column mechanism from the 'hold-up' position, the mercury was sucked down the bulbs A away from contact D. When the mercury dropped below F, breaking contact, the relay system closed the valve to the pump and opened a valve to the atmosphere causing the mercury to rise back to D. When contact was renewed at D, the rise of the mercury in the bulbs A was terminated and the mercury sucked down the bulbs A away from E. This movement was similarly reversed after contact G was broken, and the mercury rose again to E, whereupon the mercury in the bulbs A once more began to fall. This process was continued until

35 cycles had been registered on the Post Office relay counting device. One cycle comprised the lowering and raising of mercury in both sets of bulbs, A and B.

When the mercury dropped below F, the gas adsorbed on charcoal C_1 was exposed to the volume A_1 and equilibrium was established between the two phases. (This was a rapid process, substantially complete in the five seconds or so for which the exposure lasted). The gas phase in A_1 was then driven by the rising mercury into the small section of tubing between the levels E and D. When the mercury then dropped below G, the great bulk of this gas was collected in the transfer bulb B_1. The rise of the mercury to E compressed the gas into the small section of tubing above the charcoal in C_2; when the mercury dropped from D, equilibrium was set up between the gas phase and adsorbed phase in A_2 and C_2. Simultaneously, equilibrium was re-established for the remaining gas in the first unit between C_1 and A_1. On the next operation, this second gas fraction would be pumped into the second unit and so on. The overall effect of this process was the rapid passage down the column of the least strongly adsorbed gas, helium, followed by the next least adsorbed gas, neon.

2.7.3. Theory and behaviour of the column

The theory of the column has been derived by Glueckauf[2]. This summary of his treatment is included for completeness.

Langmuirs isotherm is normally written

$$C_s = K_1 C_v/(1 + K_2 C_v) \qquad (1)$$

where C_s and C_v are the equilibrium concentrations in the solid and gas phases.

The amounts of gas are so small that we can write

$$C_s = \alpha C_v \qquad (2)$$

where α is the adsorbtion coefficient for the gas.

Consider a quantity of helium A_o, allowed to equilibrate between a volume V and a mass of adsorbent S. Then the gas in the gas phase, A_1, will be given by

$$A_1/A_o = VC_v/(VC_v + SC_s)$$

i.e. $$A_1 = A_o[1/(1 + SC_s/VC_v)$$

$$A_1 = A_o[1/(1 + \alpha S/V)] \qquad (3)$$

or $$A_1 = A_o a \qquad (4)$$

where a is the fraction of the gas in the gas phase,

A_1/A_o, termed the distribution factor:

$$a = 1/(1 + \alpha S/V) \qquad (5)$$

Similarly, for a second gas B (e.g., neon),

$$b = B_1/B_o = 1/(1 + \beta S/V) \qquad (6)$$

Glueckauf has shown that the best separation of two gases in one unit may be considered to have been achieved when the maximum proportion of one substance would have to be transferred to the other phase in order to produce equal ratios of the two gases in both phases.

This condition indicates that (a - b) should be a minimum; that is

$$d(a - b)/d(S/v) = 0 ;$$

the solution of which, in accordance with equations (5) and (6) above is

$$V/S = \sqrt{\alpha\beta} \qquad \text{——————————} \quad (7)$$

This result also leads to the result, from (5) and (6) that

$$(a + b) = 1 \qquad \text{——————————} \quad (8)$$

Equation (7) defines the design parameters S and V for the separation stage. α and β, the adsorbtion coefficients, are quoted by Glueckauf as 10.6 and 110.7 for helium and neon respectively in units of $cc.gm.^{-1}$. These values were remeasured in an experiment described below and values very similar in magnitude obtained.

Now V on the column was about 25 cc so that S should be 0.73 gm.

The actual weight of charcoal used in the bulbs was about 0.8 gm (to allow for the volume of the side arm tubing).

Glueckauf considers the amounts of material in the various units, m, after n operations and derives the following expressions:

$$A_n^m (V) = \frac{A_o (n - 1) !}{(m - 1) ! (n - m) !} a^m (1 - a)^{n - m} \quad \text{——} \quad (9)$$

$$A_n^m (S) = \frac{A_o (n - 1) !}{(m - 1) ! (n - m) !} a^{m - 1} (1 - a)^{n - m + 1} \quad \text{——} \quad (10)$$

$A_n^m (V)$ and $A_n^m (S)$ refer to the amount of gas in the volume or solid phases in the m^{th} unit after n operations. For a system of m units, the amount of gas A transferred to the storage bulb after n operations

is

$$A_T = A^m_m + A^m_{m+1} + A^m_{m+2} + \ldots\ldots + A^m_n \text{ —— (11)}$$

the summation beginning at the m^{th} process since no gas can be delivered until m operations have been performed.

Also, the amount left on the column must be

$$A_R = A^m_{n+1} + A^m_{n+2} + A^m_{n+3} + \ldots\ldots + A^m_{\infty} \text{ —— (12)}$$

Similar expressions hold for gas B.

In the course of fractionation of two gases A and B, the successive fractions delivered to the storage bulb are

$$F_x = A^m_x + B^m_x$$

consisting of a mixture of both gases.

As the process continues, both the quantities A^m and B^m go through a maximum, as illustrated by the helium and neon curves in Fig. 5, and the air sample curve Fig. 6. (Both these curves were obtained experimentally). In reality, the function is a step function, not a smooth curve as drawn.

Consider the meaning of the term 'best separation' for a column of a given number of units, m. The earlier the fractionation is stopped, the purer will be the helium, but its delivery less complete. The best point at which to stop is reached when the amount of helium still to be delivered is equalled by the amount of neon contamination.

FIGURE 5.

Fractionation curves for helium and neon

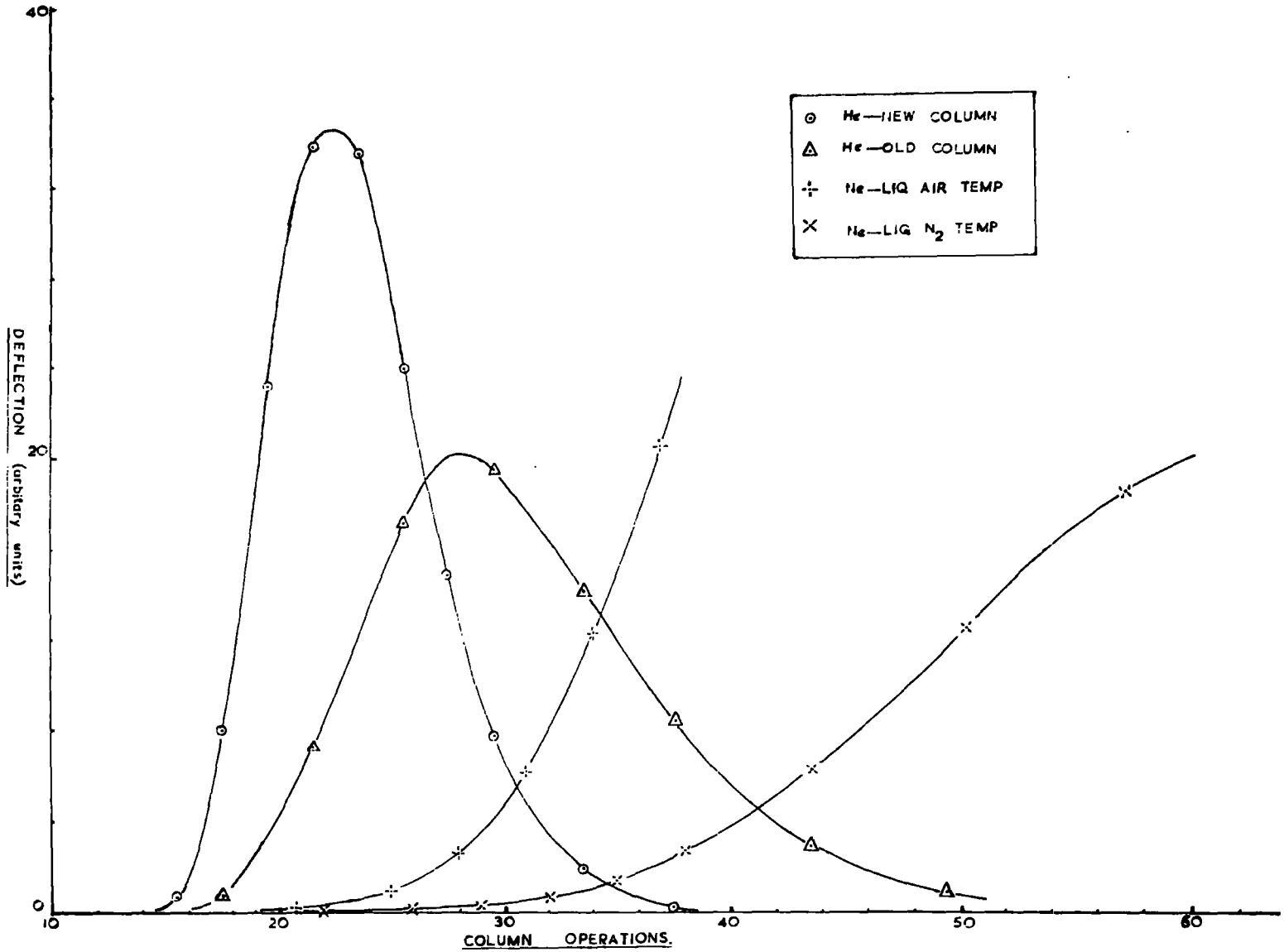
40
20
0
DEFLECTION (arbitary units)
10
20
30
40
50
60
COLUMN OPERATIONS.
He—NEW COLUMN
He—OLD COLUMN
Ne—LIQ AIR TEMP
Ne—LIQ N_2 TEMP

FIGURE 6.

Fractionation curve for an air sample

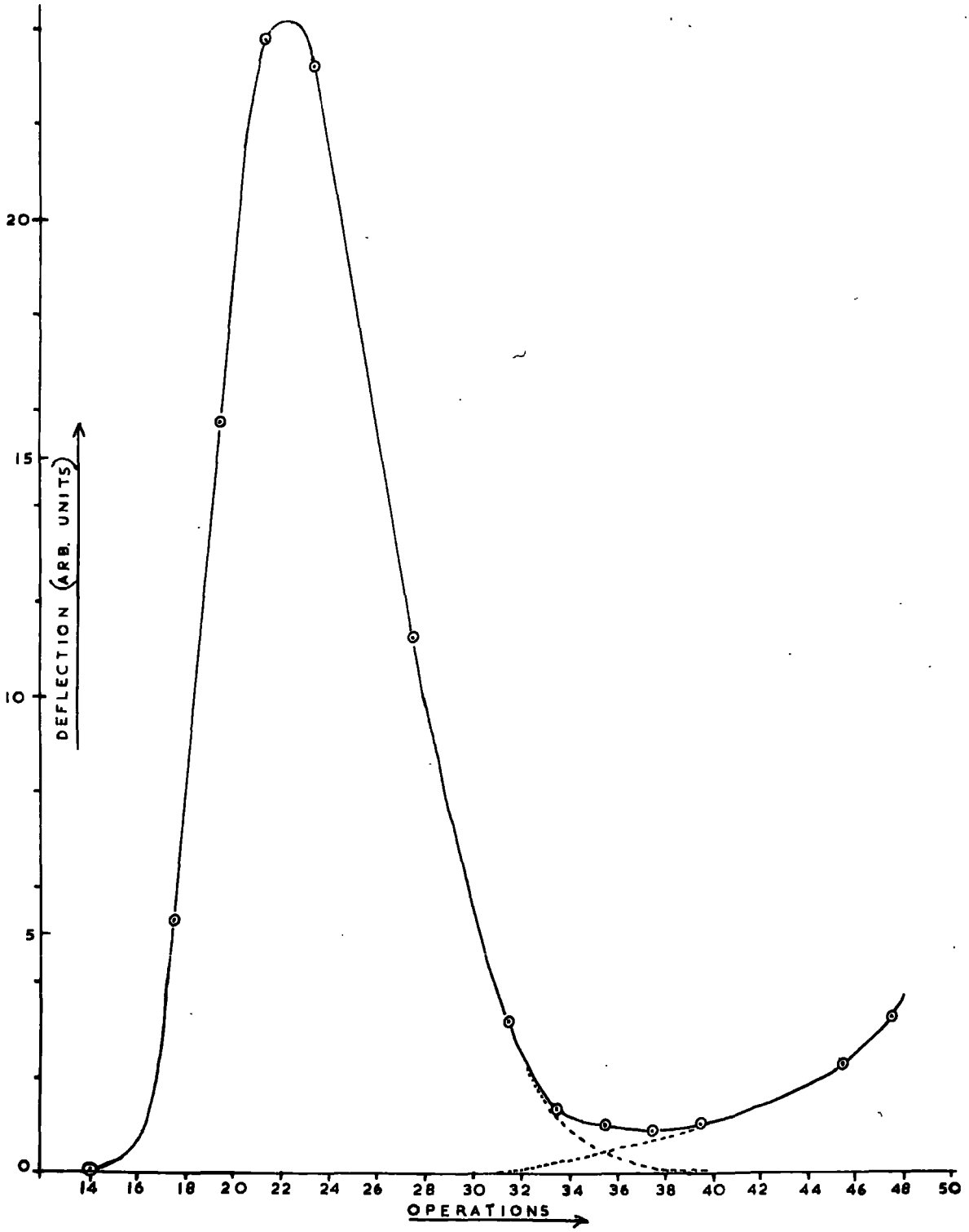
DEFLECTION (ARB. UNITS)
0
5
10
15
20
14
16
18
20
22
24
26
28
30
32
34
36
38
40
42
44
46
48
50
OPERATIONS

Glueckauf showed that this condition occurs when

$$n = 2m - 1 + [\log A_o/B_o]/[\log(1 - b)/(1 - a)] \quad \text{——— (13)}$$

so that if the initial amounts of the gases A_o and B_o are of the same order,

$$n \approx 2m \quad \text{——————— (14)}$$

All the above expressions are applicable to an ideal system, obeying Langmuirs Isotherm, having zero dead space, 100% equilibration and transfer, and identical units. In practice, the column is calibrated experimentally. The column contained 15 units, i.e. m = 15, so equation (14) indicates that fractionation should be stopped at about operation 30. Fig. 6 indicated that the actual best separation was achieved at operation 35.

2.7.4. Modifications made to the column

The apparatus initially produced the helium and neon chromatograms of Fig. 5; the helium curve being that plotted as 'old column' and the neon curve that at 'liquid air temperature'. These curves showed very poor resolution between helium and neon, and an air sample check on the functioning of the helium separation was almost impossible. The helium 'tail' was also excessive even if no neon were present in a sample for analysis (as was the case in almost all the samples). The charcoal used in the column was placed in a simple experimental system to enable the adsorption coefficients α and β to be determined. This simply consisted of connecting a gramme of the charcoal to the large McLeod gauge, which was of known volume, and measuring the change in pressure of the helium or neon when the charcoal was cooled in liquid nitrogen for about an hour.

The following values were obtained:

$\alpha = 10.7$; $\beta = 116$ where the units used were $gm.cc^{-1}$. These are in excellent agreement with the values quoted by Glueckauf:

$\alpha = 10.6$; $\beta = 111$.

Clearly then, the charcoal was not at fault.

It was then realized that the dead space in the tubes connecting the equilibrium volumes, A_n, to the next charcoal, C_{n+1}, was an important factor in the separation. When the mercury dropped round the 'T' junction at level G in the column, a good deal of the gas would not pass forward into the next unit. To ensure this transfer was almost complete, the bulbs B_n were built into the tubing.

The much improved passage of helium achieved by this modification is shown in Fig. 5 under points marked 'new column'.

It will also be noticed from the same figure, that the passage of neon through the column was retarded by the modification, though to some extent this was due to the use of liquid nitrogen rather than liquid air, as coolant.

Some evidence was obtained that the passage of neon through the column is fairly sensitive to the temperature of the charcoal.

The ratio of successive fractions of gas delivered by the column's m^{th} unit, is, from equation (9) :-

$$A^m_{n+1} \Big/ A^m_n = n(1 - a) \Big/ (n - m + 1)$$

This equation enables the constant a, and similarly, b, to be determined from the experimental curve :-

$$a = 0.64$$

$$b = 0.24$$

These values are constant over a fairly wide range; e.g., a is 0.64 in the range from operation 18 to 29.

Now it has been shown that $(a + b) = 1$. The above figures, $(a + b) = 0.88$, show the deviation from ideal behaviour.

2.7.5. Percentage recovery of helium

In all the samples analysed for helium, there should have been no neon present. However, it was safer and quicker to measure the helium at operation 35 than to attempt to collect all the helium 'tail' which only amounts to about 1% of the helium. It was thus necessary to measure accurately what fraction of the helium in the circulating system was actually measured by the standardized procedure; namely 30 Toepler strokes in the circulating system and 35 operations of the column. (The only exception to this absence of neon was the analysis of air samples and this is discussed in the next section).

The following standardization procedure was adopted. A known amount of helium was measured out in the pipetting system and delivered to the compression bulb, C. (See Fig. 9). This was then collected in the small transfer pipette B by the joint action of the compression bulb and the mercury in T. Raising the mercury in the compression bulb followed by three Toepler strokes of T past tap T_2 transferred the bulk of the helium into B; a further lowering and raising of the mercury in the compression bulb and three more Toepler strokes of T ensured that over 99.95% of the helium had been transferred. T_2 was closed after the final stroke, (the mercury being brought up into the key of the tap), and the pipette B removed from the apparatus at the B.10 joint. It was then re-fitted on another B.10 cone attached to the circulating system through a tap. The space

between the taps was thoroughly evacuated and then the helium in B could be allowed into the circulating system.

The helium remaining in the pipetting system was not pumped away but a second fraction cut off in the second pipette P_2. From the known volumes, this consisted of 98.0% of the first fraction previously transferred via B to the circulating system. Thus a comparison of the first fraction passing through the column with the second directly measured eliminated the necessity of measuring the amount of helium in the McLeod gauge absolutely. The percentage efficiency of the helium procedure followed with the gas transferred to the circulating system was given by

$$\frac{D_1}{D_2} \times 98.0\%$$

D_1 being the helium run through the column;

D_2 being the 2nd helium fraction, equal to 98.0% of the first;

the amounts of helium being measured by their deflexions D_1 and D_2 on the galvonometer connected to the Pirani gauge.

Two such calibration experiments showed the efficiency to be 98.8%. This is in accordance with the experimental observations that 1.0% of the helium was not delivered by operation 35 and a small amount of approximately 0.2% was not transferred into the column from the circulating system, as mentioned above.

2.7.6. Air analyses

Since it was established by Glueckauf and Paneth in 1944[5] that the helium content of the atmosphere at ground level is constant, the air of the laboratory has served as a helium standard

and a convenient check on the correct working of the apparatus.

Below are tabulated some of the results of such measurements in the Londonderry Laboratory:-

Glueckauf 1944	$5.24 \times 10^{-6} \pm 0.03$ cc/cc	(5)
Glueckauf 1945	$5.239 \times 10^{-6} \pm 0.004$ cc/cc	(5)
Reasbeck 1953	$5.285 \times 10^{-6} \pm 0.01$ cc/cc	(7)
Hall 1958	$5.279 \times 10^{-6} \pm 0.006$ cc/cc	(12)

(The errors quoted being standard errors of means).

The above results, except Hall's, ultimately depended on the ratio of nitrogen plus argon to total air, which had previously been determined to be constant. Hall used a small air space between two greased taps which was of known volume, and measured the helium directly. This method was used initially by the present author, but low and divergent results led to a realization of the likely errors inherent in the method. A rather serious error could be introduced by the small amount of grease extruded from the taps into the side arms of the air pipette, which was necessarily small on account of the limited handling capacity of the measuring system. It was discovered that up to 3 or 4% of the volume of about 0.2 cc could be filled with grease from well-turned taps.

Accordingly, a new greaseless air sampling system was built using a mercury cut-off.

FIGURE 7.

The air sampling apparatus

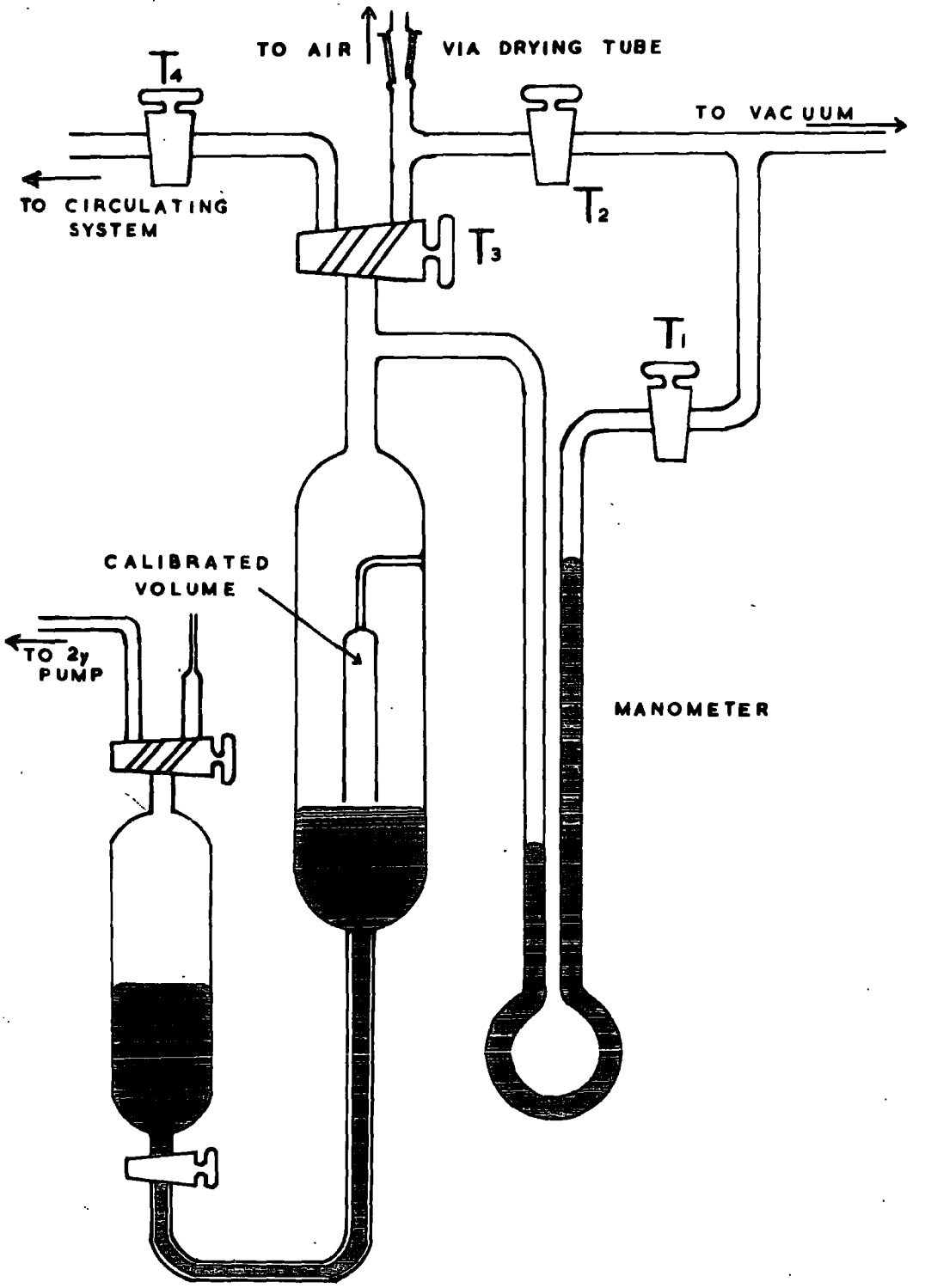
TO AIR
VIA DRYING TUBE
T4
TO VACUUM
TO CIRCULATING SYSTEM
T2
T3
T1
CALIBRATED VOLUME
TO 2y PUMP
MANOMETER

2.7.7. The Air Apparatus (See Fig.7)

This consisted of a calibrated volume sealed into a mercury cut-off and connected to a manometer. The volume was actually 2.749 cc. The method of use was as follows:-

The apparatus was evacuated through taps T_1, T_2 and T_4, the two-way tap T_3 being turned several times to remove any gas from its bores. The mercury in the cut-off was brought as close as possible to the bottom, open lip of the calibrated volume. T_2 was then closed and T_3 turned to the position shown in the diagram. A drying tube containing magnesium perchlorate connected T_3 to the atmosphere through a tap above and below the drying agent. The top tap was opened to the atmosphere and closed again after a few seconds. This portion of dry air was then allowed into the system through the bottom tap and the process repeated once. This produced a pressure of about 9 cms. of dry air in the calibrated volume and manometer. The pressure was read on the manometer with a travelling microscope and a meniscus correction applied. The mercury was then raised more than 9 cm. above the open end of the calibrated volume and the excess air pumped away through T_3 and T_2. The importance of bringing the mercury as near to the lip as possible was to avoid a change in pressure in the air cut-off as the mercury was lifted up to the cut-off point.

T_3 was then turned to connect the calibrated volume section to the circulating system. When a good vacuum had been obtained in the circulating system and the connecting tubing, the mercury could be lowered in the cut-off to allow the trapped air to pass into the circulating system. The usual analysis procedure was

then carried out and the helium found expressed as ccs per cc of air admitted.

It can be pointed out that this was an occasion where two primary pumping systems were useful; pumping out the unwanted air through T_2 could be done while the circulating system and column were being evacuated in preparation for the measurement.

2.7.8. Results of air analyses

Air samples were measured at regular intervals during the work to check the correct functioning of the apparatus. Below, some of the results are listed:-

He found in cc (N. T. P.) per cc (N. T. P.) of dry air:-

(1) 5.30×10^{-6}

(2) 5.27×10^{-6}

(3) 5.20×10^{-6}

(4) 5.30×10^{-6}

(5) 5.30×10^{-6}

(6) 5.19×10^{-6}

Average $= 5.26 \times 10^{-6} \pm 0.02(3)$ cc / cc

where the error is the standard deviation; the result quoted with the standard error of the mean is 5.26 ± 0.01 cc / cc.
This compares well with the results listed above.

The air sample curve and the pure helium curve, Figs. 6 and 5, were used to evaluate the correction required to the gas measured at operation 35. From the experimentally determined value of b and the known relation between successive fractions, the amount of neon evolved by operation 35 was determined. It turned out that,

within the uncertainty of the measurements, the helium not delivered was just balanced by the neon present (in terms of deflexion of the gauge).

The shape of the neon fraction was found to vary slightly according to the 'age', i.e., the temperature, of the liquid nitrogen used on the column charcoals. This was a small effect and was further reduced by always using fresh nitrogen on the column.

In view of these small uncertainties of the order of ¼% the results above are quoted to 3 significant figures only, as the fourth figure, i.e., parts in 5000, is of little value.

It should be pointed out that these uncertainties do not apply to the rest of the helium analysis work, where no neon was involved.

The accuracy with which the helium content of neon containing samples could be measured depended on the size of the minimum between the helium and neon fraction peaks. In the apparatus under discussion, this was about 4% of the helium peak height. A similar apparatus in the Londonderry Laboratories achieved a considerably better separation for no clear reason. The possibility of achieving much better separation for such work by the use of more selective adsorbents, i.e., molecular sieves, is worthy of consideration.

2.8. The McLeod Gauge and Pipetting System

The normal amounts of helium measured during this work varied from about 1×10^{-6} to 1×10^{-8} cc at N.T.P., though 'blanks' on the oxygen apparatus were as low as 1×10^{-9} cc. The pipetting system shown in Fig. 8 was capable of measuring out amounts

of helium from 1×10^{-5} to 1×10^{-8} cc for calibration of the Pirani gauge.

The Mc Leod gauge R, with a bulb of over 800 cc, was normally used for measuring the pressure in various sections of the apparatus connected to it through tap T_1 and the manifold of the vacuum line. It was also used in conjunction with the pipettes to measure out a known amount of helium.

As regards its first use, as a pressure gauge, a 'stick' in the instrument represented a pressure of better than 5×10^{-7} cm. of mercury; the pressure P_1 in the system will be given

$$\text{by} \quad P_1 = \frac{P_2 V_2}{V_1}$$

where V_1 is the volume of the bulb.

P_2 is the pressure difference between the open and closed limbs when the gas is confined in a volume V_2 in the closed limb. When the mercury was brought to the topmost, or first, etch mark (the volume V_2 being 0.2 cc) no pressure difference could be read off between the closed and open levels on a telescope reading to better than 0.002 cm.

$$\text{Hence} \quad P_1 < \frac{0.2 \times .002}{800}$$

$$\text{or} \quad P_1 < 5 \times 10^{-7} \text{ cm.}$$

The operation of the calibrated Mc Leod in conjunction with the system of pipettes for measuring out helium (or neon) was as follows.

FIGURE 8.

The gas storage bulbs, the McLeod gauge and gas pipetting system

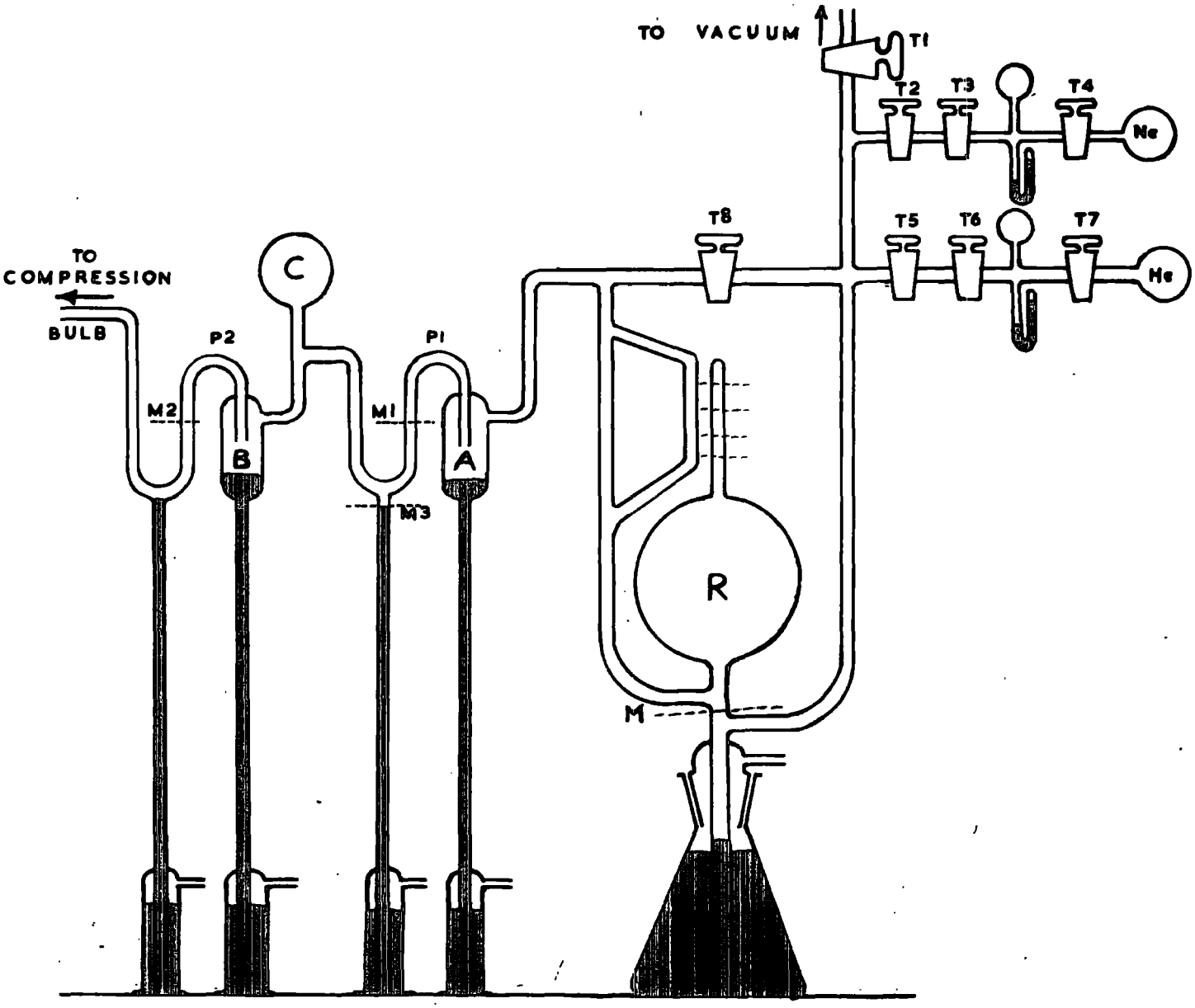
TO VACUUM
T1
T2
T3
T4
Ne
T5
T6
T7
Ne
T8
TO
COMPRESSION
BULB
C
P2
P1
M2
M1
M3
B
A
R
M

The apparatus was pumped out rigorously through T_1 and through the compression bulb section until a hard vacuum was obtained. Naturally, taps T_3 and T_6 were kept closed, confining the helium and neon to the small bulb fitted with a manometer (which was maintained at about 3 or 4 cms. pressure). Taps T_2, T_5 and T_8 were open. The mercury in the pipettes A and B was raised to the levels shown, and to the etch marks M_1 and M_2 in the two other limbs. T_2 was then closed and T_3 opened and closed, allowing a small amount of helium to be trapped between T_2 and T_3. T_1 was closed and the helium allowed into the Mc Leod bulb by opening T_2. (A similar procedure with taps T_5 and T_6 was followed for neon). T_1 was then opened to the pumps for an interval dependent on the amount of helium required, to remove excess gas. The mercury was raised in R and if the volume of gas trapped in the closed limb was too large, the mercury was lowered and T_1 opened again for a brief interval.

The closed limb was marked with five etched lines marking off volumes from 0.2 to 1.0 cc; and a pressure difference of up to 10 cms. could be read off. After the bulk of the gas not trapped in the closed limb had been pumped away, the pressure difference between the open and closed levels was read off on a travelling microscope, after the mercury in the closed limb had been accurately aligned so that the bottom of the meniscus was exactly on the etch mark. The temperature of the gas was noted with a thermometer reading to $0.1^{\circ}C$ and the meniscus heights also measured so that a meniscus correction could be applied to the pressure reading.

After about 20 minutes when all the unwanted gas had been pumped away, T_8 was shut and the mercury level at M_1 checked. The mercury was then lowered in R as far as the mark M, allowing the measured helium to expand into a known volume comprised of the bulb, the side tubing between T_8, M and the first pipette to M_1. This volume was 883.87 cc. By raising the mercury in the cut-off A, the known volume of the pipette P_1 was isolated from the main bulk of the helium; the fraction was $\frac{2.947}{883.87}$. The helium in P_1 was then allowed to expand into the bulb C and second pipette P_2 by lowering the mercury from M_1 to the black wax mark M_3. This new volume exposed was 166.38 cc. The mercury level at M_2 was checked and the mercury in B then raised cutting off in P_2 a fraction $\frac{3.283}{166.38} \times \frac{2.947}{883.87}$ of the original helium. By lowering the mercury from M_2, this gas was expanded into the compression bulb which was of about one litre capacity. This gas was then measured in the Pirani gauge as described below.

The amount of gas originally in the McLeod gauge was

$$\frac{273.2\ PV}{76(273.2 + T)}$$

where P was the difference between the open and closed levels (in cms.) in the volume V (cc) in the gauge, measured at temperature T (^{o}C).

Hence the amount delivered to the compression bulb was

$$\frac{PV}{76} \times \frac{273.2}{(273.2 + T)} \times \frac{3.283}{166.38} \times \frac{2.947}{883.87}$$

or $$PV \times \frac{273.2}{(273.2 + T)} \times 8.657 \times 10^{-7} \text{cc at N.T.P.}$$

As regards the accuracy of the process, the errors involved (disregarding any systematic error in the calibrated volumes) were small; the alignment of the etch marks could be achieved, with a magnifying glass, to better than 0.2 mm., which was a negligible portion of the length of the pipettes. The McLeod gauge pressure was read to 0.002 cm., so that errors were only significant when low pressures were being read.

2.9. The Compression Bulb

The large one litre bulb C, (see Fig. 9), was connected to the column through tap T_1 and to the pipetting system through P_2; a tube led from the top of the bulb to the measuring Pirani gauge through T_6.

The method of use was as follows; if fractions from the column were to be collected, the mercury in the column was raised to its starting or 'hold-up' position, tap T_1 was opened and the bulb and tubing evacuated through tap T_4 until a hard vacuum was obtained. The mercury in the Toepler bulb T was permanently raised to the tap T_3 and the ball valve B_3, since this Toepler was only used on very rare occasions, for example, in the percentage recovery experiments on the column. The mercury in C was sucked down to its lowest level. The side arm leading to the pipettes was shut off by raising the mercury in P_2 to the mark M_2 as shown.

The helium fractions from the column were then collected in the bulb C, and the gas was then measured in the gauge as described below. The gas was then pumped away through taps T_4 and T_6 and the gauge calibrated with helium from the pipetting system, measured out as described above.

FIGURE 9.

The compression bulb, Toepler pump and the Pirani gauges

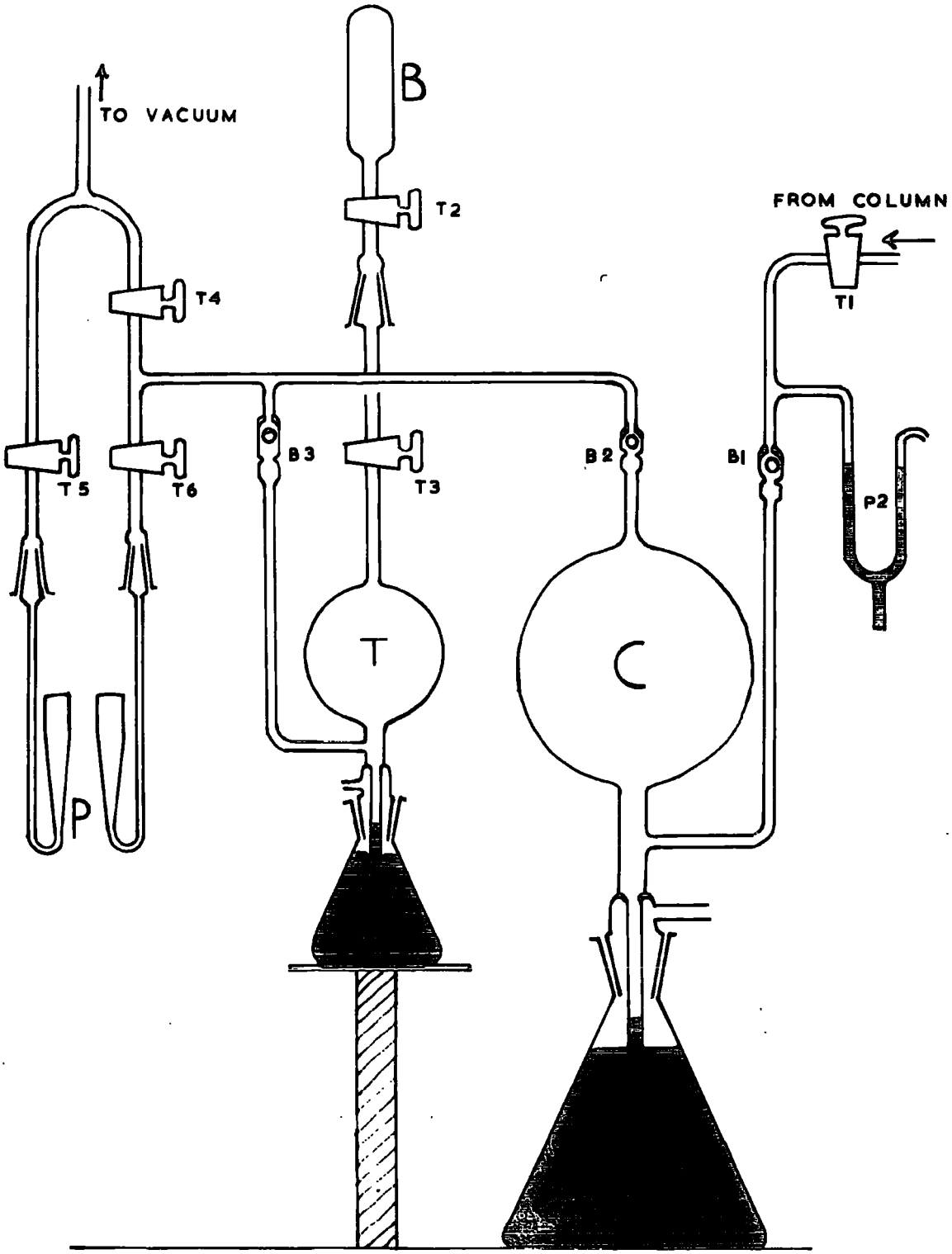
TO VACUUM
B
T2
FROM COLUMN
T1
T4
T5
T6
B3
T3
B2
B1
P2
T
C
P

The delivery of the gas fractions from the column to operation 35 took about one and a quarter hours, during which the bulb C was of course shut off from the pumps. Nevertheless, no appreciable accumulation of helium occurred by leakage or diffusion, as was shown by the very small blanks obtained on the column, usually around 1.5×10^{-9} cc of helium.

2.10. The Pirani Gauges

2.10.1. Design and Theory

The Pirani gauges, one of which is shown in Fig.10, were the only part of the apparatus, except the diffusion pumps, to be made of pyrex glass. This was because the pinch seal supporting the tungsten hooks and spring, and the Dewar seal round the top were incapable of surviving the thermal shock of immersion in liquid nitrogen when soda glass was used in their construction. Leakage of atmospheric helium was negligible, however, as the great bulk of the gauges was cooled in the nitrogen bath, and diffusion was very slow at such temperatures. The discussion of the theory of the sensitivity of the Pirani gauge has been excellently treated by Ellet and Zarbel[14]. Their results may be summarised as follows:

(1) In a bridge circuit operated at constant watt input, the galvonometer deflexion should be proportional to the pressure.

(2) The sensitivity of the gauge is proportional to the square root of the area of the wire.

(3) The wire should be as long as convenient and its resistance should be of the same order of magnitude as the galvonometer.

FIGURE 10.

The Pirani Gauge

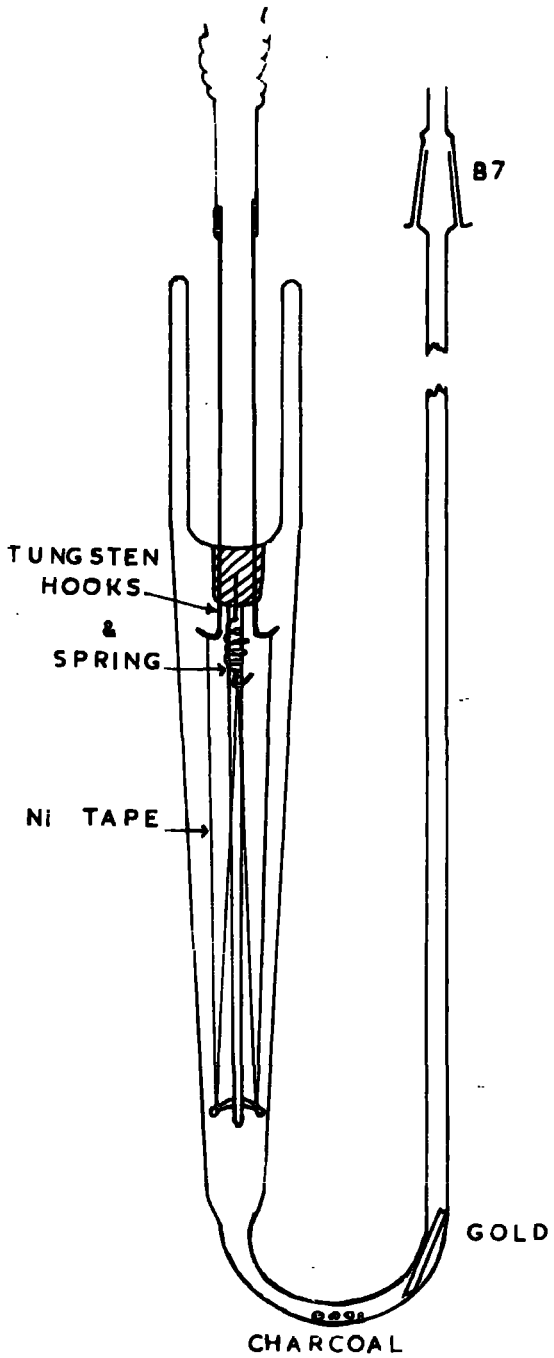
B7
TUNGSTEN
HOOKS
&
SPRING
Ni TAPE
GOLD
CHARCOAL

(4) The sensitivity of the gauge will be greater when the walls are cooled, though the relationship is a complex one.

These deductions were put into practice in the gauge shown in Fig.10. The W shaped filament enabled the greatest length of wire to be fitted into the volume of the gauge of 25 cc, which was as small as was possible to create the largest pressure change on admittance of the gas. The fine nickel filament was of flat section in accordance with (2), the section being 0.05 x 0.0003 mm. The gauge, with a compensating 'dummy', was immersed in a liquid nitrogen bath. Thin gold foil was placed in the gauge to give sacrificial protection to the soft soldered joints between the hooks and the tape from attack by mercury vapour. The charcoal served to mop up any trace of condensable gases (for example, from the tap grease), while its mass was so small relative to the volume of the gauge that only negligible amounts of helium were adsorbed.

2.10.2. Construction of the gauges

The tungsten hooks and spring, previously clad in glass, were pinched together at the end of a glass tube and the tape supporting rod fused on. The hooks were cleaned with molten sodium nitrite, washed and covered with copper by electroplating in a copper sulphate solution. This was necessary to get the solder to 'take'. The hooks were then tinned and the tube clamped at about 20° from the vertical. About 18 inches of the nickel tape was carefully unrolled onto a glass sheet. This was picked up and manoeuvered by two small glass rods having a dab of soft black wax on their ends. After making sure that the wire was free from kinks,

it was draped over the hook of the spring, down and over the supports at the end of the glass rod and up and over the tinned tungsten hooks. The glass rods were allowed to hang down to tension the tape. Small auxiliary weights of up to 5 grammes in all at each end of the tape could be added, though it was best to use glass rods of about this weight initially. After a few minutes, the tape was fused onto the hooks by touching the ends of the hooks cautiously with a hot soldering iron. A sharp tug on the pendant glass rod would snap off the excess tape at the hook. The wired-up inside of the gauge had then to be glass blown into its jacket by making the Dewar or ring seal around the top. The distance at which this seal was made from the pinch seal had to be sufficient to prevent the heat from the joint melting the solder on the tungsten hooks.

After inserting three or four small pieces of charcoal and a small roll of gold foil, the gauges were attached to the apparatus through the black-waxed B7 joints.

The life of the measuring gauge was normally about four to six months, while the compensating or 'dummy' gauge lasted almost indefinitely.

2.10.3. The Pirani gauge circuit

The two Pirani gauges P_1 and P_2 formed part of a double Wheatstone network as shown in Fig.11. The compensating or 'dummy' gauge never had gas admitted to it and was kept at a good vacuum. By being subject to exactly the same environment as the measuring gauge, spurious deflexions due to stray electric or magnetic fields, vibration or changes in temperature or incident light flux were avoided or at least minimised.

The switch S_2 was almost invariably kept in the vertical position so that the second bridge arm consisting of R_5, R_6 and R_7 was inoperative. This arm was used for checking purposes only; for example to check the free swinging of the galvo spot without having to wait for the Pirani gauges to settle down.

The accumulator shown provided a voltage of one volt across the Piranis and this could be checked on the terminals shown. As mentioned above, a gauge constructed as described had a resistance of 150 to 250 ohms. R_1, R_5 and R_2, R_6 were respectively 150 and 50 ohms high stability wire wound resistors, while the variable resistors R_3, R_4 and R_7 were decade boxes of up to 1000 ohms. The galvonometer G was a sensitive quartz fibre suspension instrument, throwing a light spot onto a metre scale just under a metre away. Its internal resistance was about two thousand ohms, as deduced from its sensitivity to various values of the range box, R.B. This contained resistors from zero to 25,000 ohms, thus providing an approximately twelve-fold sensitivity range for normal use. Thus, if a one cm. deflexion on the most sensitive scale corresponded to about 1×10^{-8} cc of helium, (as it did), a 50 cm. deflexion on the least sensitive scale would be 600×10^{-8} or 6×10^{-6} cc of helium. Larger amounts of helium than this were never measured but could have been accommodated by an auxiliary shunt across the galvonometer. In practice, a 500 ohm shunt was connected directly across the galvonometer to protect it from violent fluctuations when the gauges were being immersed in, or withdrawn from the liquid nitrogen bath. The advantage of the system described was that the galvonometer was maintained in a constant resistance circuit giving slight over-damping, thus avoiding the difficulties of

FIGURE 11.

The Pirani gauge circuit diagram

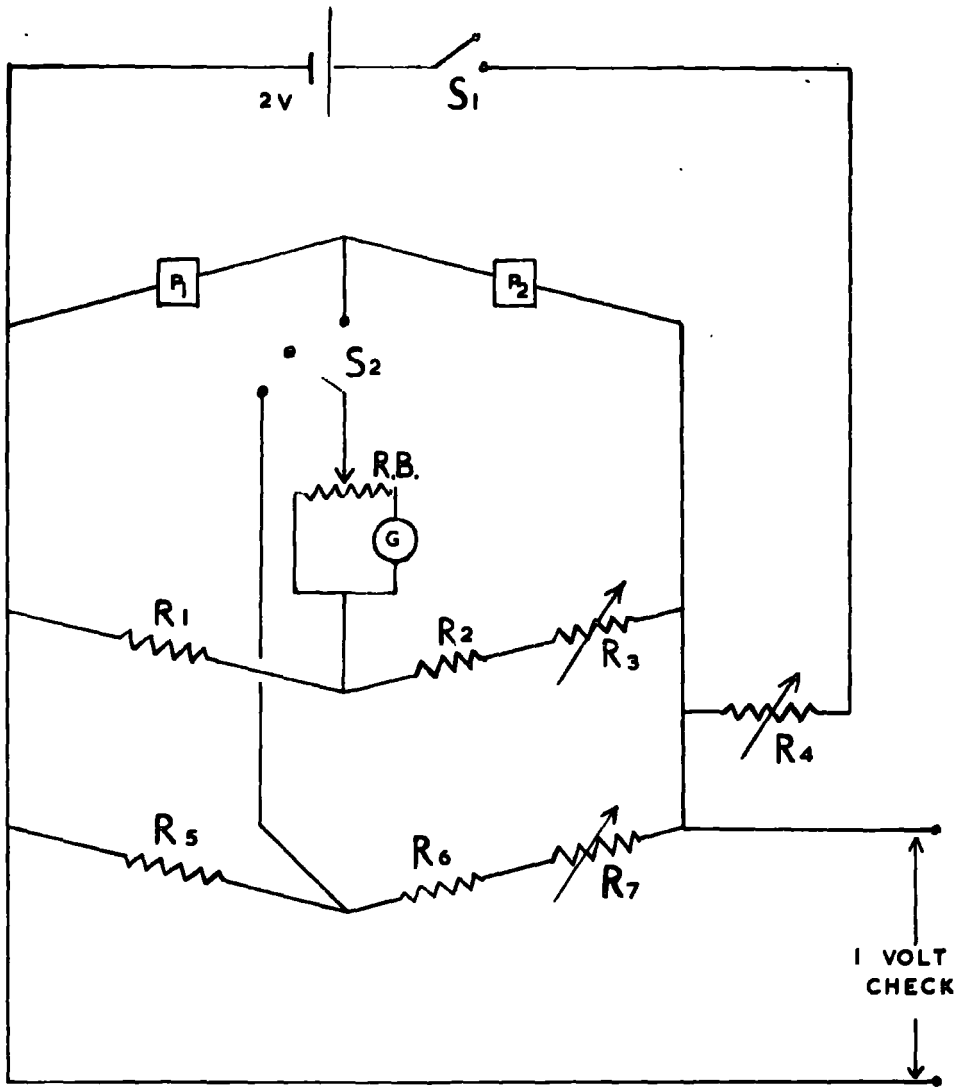

R.B. = RANGE BOX

R_1, R_5 = 150 Ω (HIGH STABILITY RES.)

R_2, R_6 = 50 Ω (" " ")

R_3, R_4, R_7 = ↑1000Ω (VARIABLE DECADE RES.)

under-damping which would occur on the sensitive scales of an ordinary series resistance sensitivity system. The latter system was initially in use on the apparatus but was changed to that described.

Before immersing the gauges in a tall two litre Dewar of liquid nitrogen, the galvonometer range box was turned to the least sensitive range and the shunt brought into operation. The current was switched on through the Piranis by S_1 and they were slowly surrounded by the coolant. R_3 was altered to keep the light spot on the scale during the initial rapid drifting. The galvonometer spot drift gradually decreased with time, but it normally took four hours before measurements on a sensitive scale were practicable.

2.10.4. Use of the gauges

The gauges were first rigourously evacuated through the taps T_5, T_6 and T_4 above the B7 sockets; see Fig. 9. The charcoal in the gauges was outgassed with a small gas flame for about five minutes. After about fifteen more minutes the pressure was checked on the McLeod gauge and if a 'stick' was obtained, the taps T_5 and T_6 were shut. T_5, the tap to the compensating gauge, remained shut throughout all the measuring procedures.

The current was switched on through the gauges and they were immersed as described above. When stability had been attained, they were ready for use.

The helium fractions from the column had been collected in the compression bulb C, with the mercury in T raised to T_3 and B3 beforehand, and the pipette P_2 shut off as shown. The mercury in C was brought to the lower fixed mark, namely the internal seal just above the reservoir. T_6 was then opened and the helium allowed to

equilibrate between C and the Pirani gauge. A small deflexion (about 5% of the deflexion to be measured) occurred; the reason for this procedure is explained later. T_6 was then closed and the mercury raised in C to the ball valves B_1 and B_2, compressing the helium between these and the ball valve B_3 and the taps T_6 and T_4. The small fraction of the gas trapped in the side arm above B_1 was a constant fraction of the total and hence immaterial.

T_6 was then opened and the galvonometer swing measured (on a suitably sensitive scale). Since the deflexion slows down in an exponential fashion, the readings of the spot were noted at minute intervals for five minutes. The deflexion could be extrapolated to infinite time, but in practice, since the calibration was always performed with a nearly equal amount of helium, the reading after five minutes was taken as the actual swing. The use of nearly equal swings in the calibration also made corrections for the non-circularity of the scale unnecessary.

T_6 was shut and the mercury drawn down in C to the lower fixed mark. T_6 was again opened and the galvonometer spot swung back to its original position. The readings of the 'up' and 'down' strokes of the mercury were repeated in this manner until sufficient statistical accuracy had been achieved. The reason for opening T_6 initially should now be clear; if this had not been done, the initial 'up' reading would have been greater than subsequent readings, since the gas would have been expanding into a vacuum and not the equilibrium pressure of the gas at the lower fixed mark.

The opening of tap T_6 for the 'up' and 'down' readings was strictly regulated by a stop-watch; in this way, the drift of the spot in a direction contrary to the subsequent reading was always of

an equal magnitude. Some random spurious movements of the spot occasionally occurred, but by noting the reading every minute, spurious results were usually detected and the reading ignored. If very small deflexions were being measured on the sensitive scale, this problem was more important and a larger number of swings was measured; the fluctuations should then have cancelled out in the average. Some Pirani gauges did not suffer much from this trouble, being very stable, but others were rather temperamental.

After the measurement, the helium was pumped away through taps T_4 and T_6, about ten minutes being sufficient for complete removal. The gauge was then calibrated with an almost equal quantity of helium from the pipetting system in an analogous manner.

All measurements were made in the dark, relieved only by a small electric lamp, for two reasons:

(i) the light spot was easier to read

(ii) the gauges were sensitive to the incident light flux and variations in this could cause spurious deflexions of several mm. on the most sensitive scale.

The gauge here described has some disadvantages, notably its short life and difficulty of manufacture. An attempt was made to replace the heated filament with a thermistor. Thermistors have successfully been used in differential gas analysis, for example by Walker and Westenburg[113]. Two types were tried; 'Stantel, type A' and 'Stantel, type U' of respectively 100 and 25 milliwatts consumption. The latter type when soldered into a small hollow brass cylinder as the vacuum envelope, and immersed in an ice bath at $0^{\circ}C$, was found to be some five times less sensitive

to helium than the normal Pirani gauge. Leaks in the metal to metal joins proved extremely vexatious when immersion in liquid nitrogen was attempted. Stability was not good for the 'U' type and could not be achieved at all with the 'A' type, so the experiments were abandoned.

Another type of gauge using a vertical stainless steel jacket containing a single strand of the nickel tape, soft-soldered at each end, was also tried. In practice this turned out to be almost as difficult to make as the glass gauge, and the glass-metal seal through which the filament passed failed to withstand immersion in liquid nitrogen.

2.11. Some notes on the apparatus

The apparatus has been dismantled on the termination of this research. An improvement worth incorporating into a rebuilt model is thermostatic control of the laboratory atmosphere. One reason is the greater accuracy of gas volume and pressure measurements that would ensue. Secondly, for long tap life, that is, long intervals between regreasing the keys, the taps should only be turned between about 19 and 23°C. This applies to Apiezon N grease whose viscosity is very temperature dependent. High temperatures are also inimical to the grease in the 'wedge' type of tap where the key has the pressure of the atmosphere holding it against the barrel; the apparatus contained some taps of this type. Silicone grease is not recommended because, being colourless, it is very difficult to judge the condition of a tap or whether it is 'streaked', that is, a potential atmospheric leak. It is also difficult to remove from glassware.

The apparatus was a bulky and complex vacuum system containing about one hundred greased taps. Because of the experimental handling difficulties, its slowness and lack of versatility, this type of apparatus has been largely displaced by mass spectrometers. However, for extremely accurate absolute measurements on very small amounts of gas, it is still unrivalled. For example, Hoffman and Nier[114], who measured He^3 and He^4 in meteorites, quote their mass spectrometer accuracy as $\pm$ 5% on samples of about 3×10^{-6} cc. Reynolds[115], using similar apparatus for argon and xenon, quotes similar values; more recently (in 1965) Lipschutz[133] has published results on iron meteorites.

2.12. Errors

It has been stated above that the accuracy of helium measurements is better than 1%. Consider the expression used for calculating the amount of helium:

$$\text{Helium} = k_1 k_2 \frac{PD_1}{D_2}$$

k_1 is the volume calibration constant, D_1 and D_2 are the average galvonometer deflexions for the sample and the standardizing helium, P is the pressure of the standardizing helium, read off by microscope, and k_2 the percentage recovery (or efficiency) factor for the apparatus. The accuracy will depend on the amount of helium to be measured, but 1×10^{-7} cc is a typical figure. In such a case, P is about 2 cm. and D_1 and D_2 about 10 cm. P can be read to 0.002 cm. and gives rise to an error of 0.1%. D_1 and D_2 can be read to 0.02 cm. and each is compounded of at least 6 readings; this leads to a small error. However, it is more realistic to assess

limits of spurious errors due to instability in the gauges. The criterion adopted is that at least 3 pairs of averages of D lie within one percent; this was always achieved in practice. On this criterion the worst case leads to a maximum standard error of the mean of 0.4%.

In addition, a possible error of up to 0.2% exists in the percentage recovery factor of 98.8%, derived in Section 2.7.5.

Treating these errors as standard errors, the total error is 0.6%. Thus for normal use, we can say that results are accurate to better than 1%. This is borne out by comparison of the results obtained with different apparatuses, and also by the results of air analyses.

SECTION 3.

AVERAGE CROSS SECTIONS FOR THE FISSION NEUTRON REACTIONS $Fe^{56}(n, \alpha)Cr^{53}$, $Fe^{54}(n, \alpha)Cr^{51}$ AND $Fe^{54}(n, p)Mn^{54}$

3.1. Introduction

The (n, α) and (n, p) reactions induced by fast neutrons from a nuclear reactor are usually referred to as threshold reactions. This is something of a misnomer since in many cases there is no energy threshold as the reactions are exoergic. However, a threshold exists insofar as emission of charged particles is normally prevented by the Coulomb barrier below excitation energies of a few Mev.

Threshold reactions are of great importance in reactor technology and in the production of radionuclides. They are commonly used to monitor fast fluxes [for example, the $Ni^{58}(n, p)Co^{58}$ reaction] and to determine the energy spectra of unknown fluxes. Their occurrence in structural materials, moderators or coolants leads to undesirable effects, such as the weakening of metals by the growth and diffusion of gas bubbles[15], or the accumulation of activity or of neutron 'poisons'. A knowledge of the cross sections of such reactions is clearly vital, not least in the economic production of artificial radionuclides.

The work here described was primarily concerned with value of the cross section for fission neutrons of the reaction $Fe^{56}(n, \alpha)Cr^{53}$, notably from the standpoint of its use in reactor structures. Cr^{53} is stable and measurement of the cross section

was made by direct estimation of the helium produced in iron samples subjected to a known neutron flux. [This method can be applied to all (n, α) reactions with stable products, provided that enough helium results to be measurable]. This important cross section has not been previously experimentally determined; the value found in the literature is an extrapolated one [e.g. (24), (137)]. This extrapolated value and a value derived from a theoretical excitation function of Bullock and Moore (116) are discussed below.

Irradiation of samples of iron of natural isotopic composition led to the measurement of the average cross sections of the reactions $Fe^{54}(n, \alpha)Cr^{51}$ and $Fe^{54}(n, p)Mn^{54}$. The results obtained are compared with previous results [in the case of $Fe^{54}(n, \alpha)$, only one previous measurement seems to have been reported] and with values obtained by integration of their excitation functions.

3.2. Average cross sections, $\bar{\sigma}$

A fission spectrum of neutrons has an energy range from zero to about 20 Mev. Their distribution as a function of energy E is well represented by the expression

$$N(E) = e^{-E} \sinh \sqrt{2E} \qquad (1)$$

To calculate the reaction rate per atom of target, R, one also needs to know the way in which the cross section, $\sigma(E)$, varies with energy, i.e., the excitation function for the reaction. One can say

$$R = \int_0^\infty \sigma(E)\, N(E)\, dE \qquad (2)$$

The average cross section for a fission spectrum of neutrons, $\bar{\sigma}$, is defined as the constant cross section which will give the same reaction rate:

$$R = \bar{\sigma}\int_0^{\infty} N(E)\,dE \qquad \text{(3)}$$

$$\text{or } \bar{\sigma} = \frac{\int_0^{\infty} \sigma(E)\, N(E)\,dE}{\int_0^{\infty} N(E)\,dE} \qquad \text{(4)}$$

The total flux distribution in a reactor is not of course represented by equation (1), but contains a much larger proportion of low energy neutrons due to scattering. However, the equivalent fission flux, Fe, say, for a reaction with a threshold of several Mev, where there is little distortion of the flux from that represented by equation (1), may be used to calculate the proportion of neutrons in a given energy range, say E_1 to E_2:

$$N_{E_1}^{E_2} = \frac{Fe\int_{E_1}^{E_2} e^{-E}\sinh\sqrt{2E}\;dE}{\int_0^{\infty} e^{-E}\sinh\sqrt{2E}\;dE} \qquad \text{(5)}$$

Hughes[19] and Mellish[25] have shown that it is probable that the fast flux in a reactor is very close to a fission flux given by equation (1), above two or three Mev.

Until fairly recently, measurements of $\bar{\sigma}$ for various threshold reactions suffered from the lack of an agreed standard or reference cross section; e.g. see Rochlin[16]. However, Mellish[17] has shown that many apparently discordant results are in reasonable agreement if they are normalized to a value of 60 mb. for the reaction $S^{32}(n,p)P^{32}$. Boldemann[18] quotes the following values of $\bar{\sigma}$ calculated from their respective excitation functions:-

Table 1.

Reaction	$\bar{\sigma}$ (calculated) in mb.
$S^{32}(n, p)P^{32}$	60 ± 3
$Al^{27}(n, \alpha)Na^{24}$	0.59 ± 0.04
$Ni^{58}(n, p)Co^{58}$	108 ± 8
$Fe^{56}(n, p)Mn^{56}$	0.89 ± 0.09
$P^{31}(n, p)Si^{31}$	31 ± 1

He showed that the above values were consistent with the experimental results of his measurements in a fission spectrum obtained from a neutron converter.

3.3. Threshold reactions in iron and simple theory

The three neutron induced reactions studied which occur in iron are listed in Table 2 with some of their properties:-

Table 2.

Reaction	Half life	E_T (Mev)	E_{eff} (Mev)
$Fe^{56}(n, \alpha)Cr^{53}$	stable	-0.27	9.7
$Fe^{54}(n, \alpha)Cr^{51}$	27.8 days	-0.86	9.1
$Fe^{54}(n, p)Mn^{54}$	314 days	-0.16	4.3

E_T, the threshold energy, is defined as $-\frac{(A+1)Q}{A}$ where A is the atomic weight of the target nucleus and Q, the energy balance for the reaction, is derived from the isotopic mass tables in Wapstra[20].

Negative values indicate exoergic reactions but the excitation of the compound nucleus from neutrons of low kinetic energy is not sufficient to overcome the potential barrier to charged particle emission. The probability of penetration of this barrier, or penetrability, P, is given by Bethe[21] as

$$P = \exp - \left[\left(\frac{4z Ze^2 \sqrt{M}}{\hbar \sqrt{2E}} \right) \left(\cos^{-1} \left(\frac{E}{B} \right)^{\frac{1}{2}} - \left(\frac{E}{B} \right)^{\frac{1}{2}} \left(1 - \frac{E}{B} \right)^{\frac{1}{2}} \right) \right] \quad (6)$$

where z = charge on emitted particle

E = energy of emitted particle

M = mass of emitted particle

Z = nuclear charge of final nucleus

B = barrier height

e = electronic charge

$\hbar$ = $h/2\pi$ (h is Planck's constant)

The height of the barrier, B, is equal to the electrostatic potential energy of the particle and residual nucleus at contact, and is shown by Hughes[22] to be given by

$$B = \frac{0.96 z Z}{(A)^{1/3}}$$

Hughes[23] introduced the concept of the Effective Energy, E_{eff}, which he found useful for correlating and predicting values of $\bar{\sigma}$ for (n, α) and (n, p) reactions. The only previously known value of $\bar{\sigma}$ for the reaction $Fe^{56}(n, \alpha)Cr^{53}$ was based on Hughes' extrapolations. Using equation (6), P may be calculated for various reactions. This is shown diagrammatically in Fig. 12(a) with the neutron distribution function N(E). Assuming that the cross section is proportional to P,

FIGURE 12.

(a) The penetrability function and the effective energy, E_{eff}

(b) The variation of $(E_{eff} - E_T)$ with atomic number Z, for (n, p) and (n, α) reactions

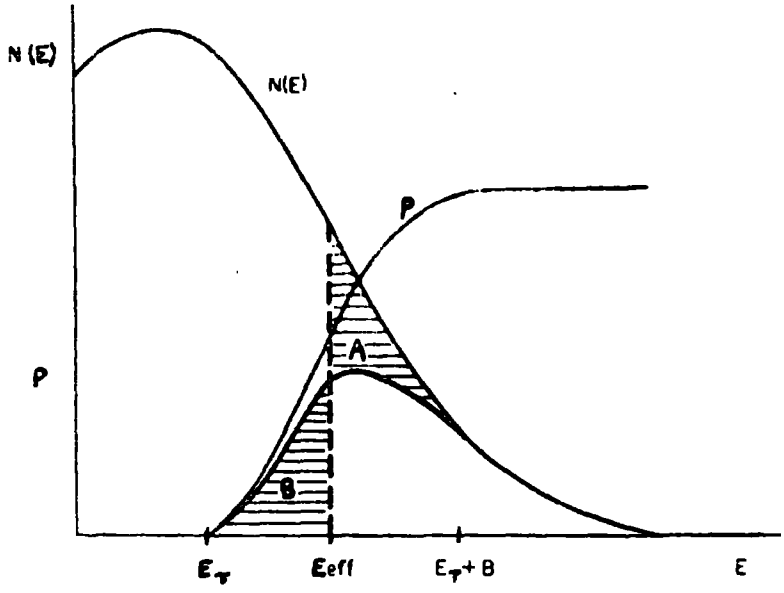
N (E)
N(E)
P
P
A
B
E_T
Eeff
E_T + B
E

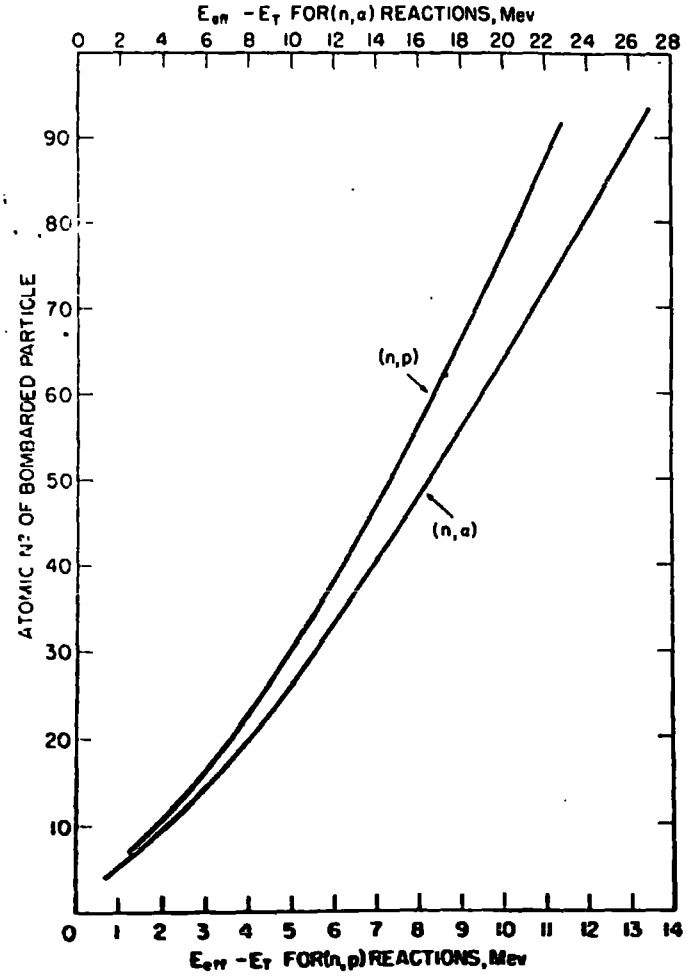
E_{eff} - E_T FOR(n,α) REACTIONS, Mev
0 2 4 6 8 10 12 14 16 18 20 22 24 26 28
90
80
70
60
50
40
30
20
10
ATOMIC Nº OF BOMBARDED PARTICLE
(n,p)
(n,α)
0 1 2 3 4 5 6 7 8 9 10 11 12 13 14
E_{eff} - E_T FOR(n,p) REACTIONS, Mev

the reaction rate will be given by P x N(E) which is also plotted in the figure as the weighted yield curve. E_{eff} is drawn where area A is equal to area B, and can be expressed as the threshold energy above which the reaction occurs with unit penetrability, while neutrons of lower energy contribute nothing to the reaction. E_{eff} is always greater than E_T and $(E_{eff} - E_T)$ is independent of E_T. Hughes' plot of $(E_{eff} - E_T)$ against Z, the atomic number of (here) the target is shown in Fig. 12(b) for (n, α) and (n, p) reactions. Now it would be possible from N(E) and $(E_{eff} - E_T)$ to predict the cross section $\bar{\sigma}$ if the value at unit penetrability, σ_o, were known.

$$\bar{\sigma} = \sigma_o \frac{\int_{E_{eff}}^{\infty} N(E)\,dE}{\int_{0}^{\infty} N(E)\,dE} \qquad (7)$$

Now σ_o, on a simple treatment, should be proportional to the nuclear area, πR^2, and in general will be some fraction of it because of competing modes of decay in the compound nucleus. The nuclear size is also proportional to $(A)^{2/3}$. If now the experimental values of $\bar{\sigma}$ are plotted against E_{eff}, the points lie on a curve which is the integral of the fission spectrum, $\int_{E}^{\infty} N(E)\,dE$, in accordance with equation (7) and the assumptions about E_{eff}. The quantity plotted (see Fig. 13) is not the observed cross section $\bar{\sigma}$ but a factor $\frac{25}{(A)^{2/3}}$ is introduced to normalize $\bar{\sigma}$ to a standard sized nucleus for which $(A)^{2/3} = 25$, i.e. $A = 125$.

Thus from this curve we can derive unknown values of $\bar{\sigma}$ from E_{eff}, obtained ultimately from the function for P, equation (6). By this method we are usually within a factor of two of the observed cross section.

FIGURE 13.

The variation of the average cross section, $\bar{\sigma}$, (normalized to a standard nucleus of atomic mass of 25), for (n, α) reactions, with E_{eff}

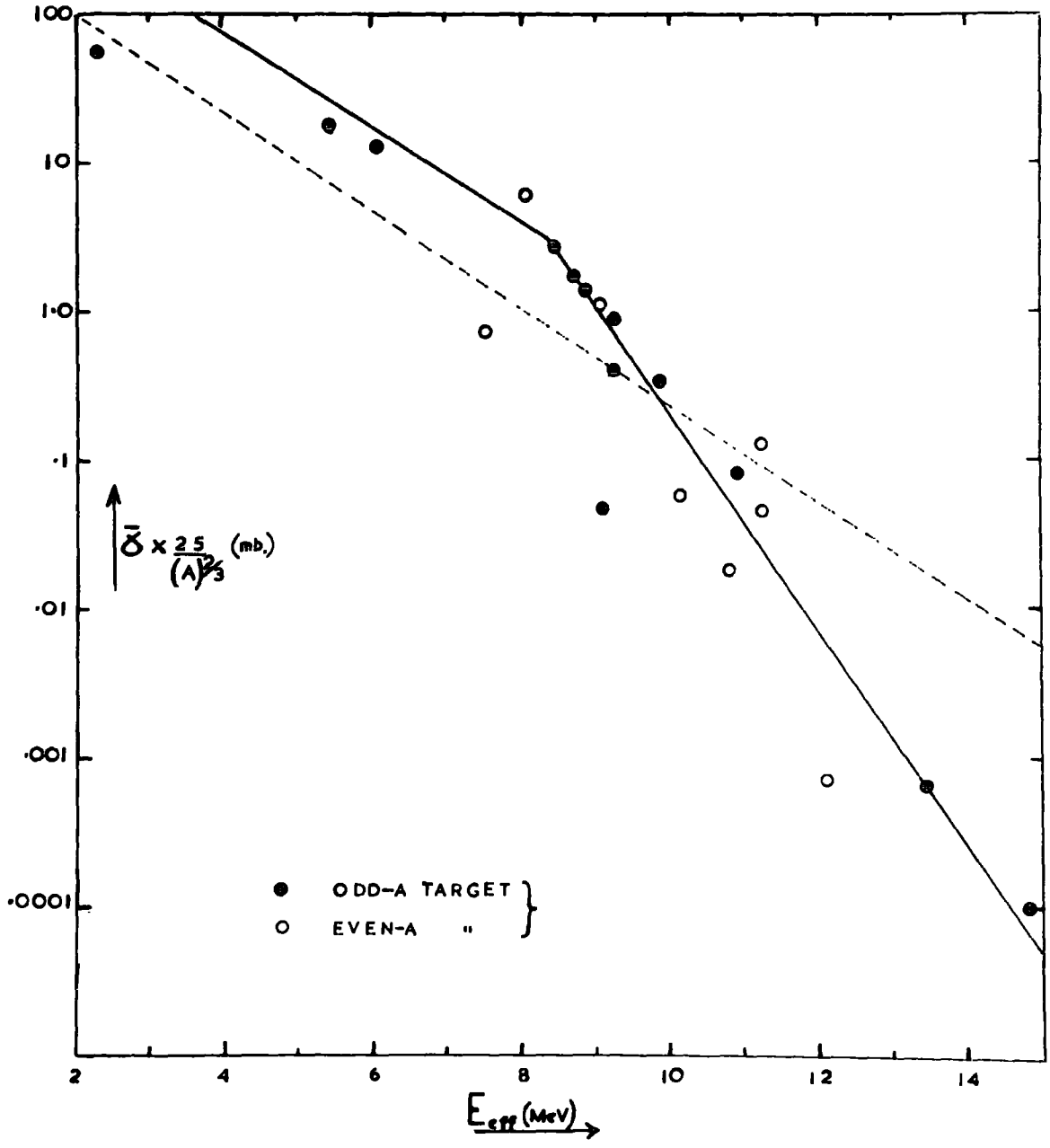
100
10
1·0
·1
·01
·001
·0001
$\bar{\sigma} \times \frac{25}{(A)^{2/3}}$ (mb.)
ODD-A TARGET
EVEN-A "
2
4
6
8
10
12
14
E_{eff} (MeV)

Roy and Hawton[24] published in 1960 an extensive compilation of values of $\bar{\sigma}$. They plotted all known experimental values of $\bar{\sigma}$ against E_{eff} of Hughes and found, for (n, p) reactions, two parallel straight lines represented the data for even and odd A targets fairly well, though their slopes were considerably different from that given by the integral of the fission spectrum. Their plot for (n, α) reactions, shown in Fig. 13, has two sections of different slope, the dotted line being the fission spectrum integral.

For (n, α) reactions on the isotopes of iron they list the following values of $\bar{\sigma}$:-

Table 3.

Fe isotope	% occurrence	$\bar{\sigma}$ (n, α) in mb.
54	5.84	(a) 0.6, (b) 0.74
56	91.68	0.35
57	2.17	3.5
58	0.31	0.01

For Fe^{54}, the experimental value of $\bar{\sigma}$ (n, α) of Mellish[25] is listed as (b); the extrapolated value is given as (a). In the compilation of $\bar{\sigma}$ values of Alter and Weber[137], $\bar{\sigma}$ [Fe^{56}(n, α)] is also listed as 0.35 mb., presumably quoting Roy and Hawton.

3.3.1. Integration of the excitation function (A)

In a more fundamental treatment, Bullock and Moore[116] have calculated curves of the variation of cross section with neutron energy, i.e. excitation curves for a number of reactions including Fe^{56}(n, α)Cr^{53}. They published two curves for the reaction based on different assumptions about C, the constant in the Fermi expression for nuclear level densities:-

FIGURE 14.

The excitation function for the $Fe^{56}(n, \alpha)$ reaction

(Ref. 116)

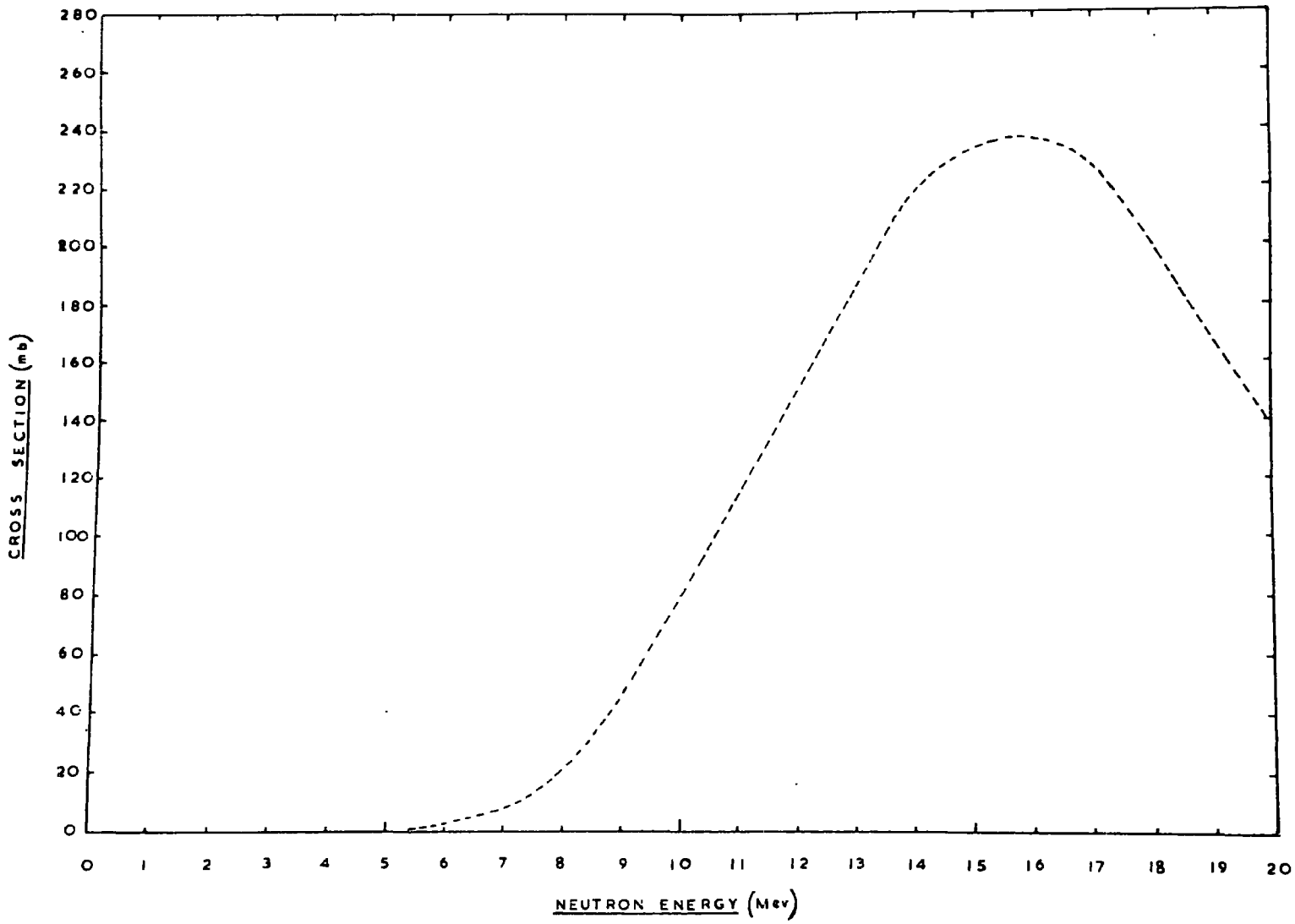
CROSS SECTION (mb)
280
260
240
220
200
180
160
140
120
100
80
60
40
20
0
0 1 2 3 4 5 6 7 8 9 10 11 12 13 14 15 16 17 18 19 20
NEUTRON ENERGY (Mev)

$$\rho(E) = C \exp(2\sqrt{aE}) \qquad (8)$$

where a and C are constants. In the first, they applied values of C, derived strictly for odd atomic masses only, by Blatt and Weisskopf[117]; in the second, they modified this so that

$$\tfrac{1}{2}C_{\text{ODD-ODD}} = C_{\text{ODD-EVEN}} = 5C_{\text{EVEN-EVEN}} \qquad (9)$$

The second of their two excitation functions is shown in Fig. 14. From this we can derive a value of $\bar{\sigma}$ for the reaction. The probability of finding a neutron of energy E per Mev can be calculated from the expression

$$N(E) = 0,48\, e^{-E} \sinh \sqrt{2E} \qquad (10)$$

By multiplying the cross section at various energies by this probability, a weighted yield curve is produced which on integration gives $\bar{\sigma}$, since

$$\bar{\sigma} = \int_0^\infty \sigma(E)\, N(E)\, dE \Big/ \int_0^\infty N(E)\, dE$$

and the neutron probabilities are normalized for $\int_0^\infty N(E)\, dE$ to be unity. An empirical formula which also has been used to represent the fission neutron energy spectrum by Hinves and Parker[135], based on the experimental work of Cranberg et al.[136] is

$$N(E) = 0.4572 \exp(-E/0.965) \sinh(2.9E)^{\frac{1}{2}} \qquad (11)$$

The following Table 4. may now be drawn up; the use of both equations 10 and 11 is tabulated.

Table 4.

E in Mev	σ(E) in mb.	N(E) per Mev Equation 10	N(E) per Mev Equation 11	σ(E)x N(E) Equation 10	σ(E)x N(E) Equation 11
6	$\approx$1	1.89×10^{-2}	1.84×10^{-2}	0.0189	0.0184
7	8	9.31×10^{-3}	8.77×10^{-3}	0.0745	0.0702
8	20	4.42×10^{-3}	4.10×10^{-3}	0.0884	0.0820
9	45	2.07×10^{-3}	1.89×10^{-3}	0.0932	0.0850
10	80	9.53×10^{-4}	8.56×10^{-4}	0.0762	0.0685
11	115	4.38×10^{-4}	3.84×10^{-4}	0.0504	0.0442
12	150	1.99×10^{-4}	1.70×10^{-4}	0.0298	0.0255
13	185	8.95×10^{-5}	7.48×10^{-5}	0.0165	0.0139
14	218	3.95×10^{-5}	3.26×10^{-5}	0.0086	0.0071
15	235	1.75×10^{-5}	1.41×10^{-5}	0.0041	0.0033
16	237	7.73×10^{-6}	6.07×10^{-6}	0.0018	0.0014
17	225	3.9×10^{-6}	2.6×10^{-6}	0.0009	0.0006

Below 6 Mev, σ becomes negligible, while above 17 Mev N(E) becomes so small that the product N(E)σ(E) becomes negligible.

Graphical integration of the weighted yield curves gives the values of $\bar{\sigma}$ [Fe^{56}(n, a)] as

(i) 0.46 mb. (from Equation 10)

(ii) 0.42 mb. (from Equation 11)

Thus to summarise, the simple theory of Hughes developed by Roy and Hawton[24] leads to an estimated value of $\bar{\sigma}$ [Fe^{56}(n, a)] of 0.35 mb.;

the theoretical treatment of Bullock and Moore[116] leads variously to the values of 0.46 and 0.42 mb., according to the neutron distribution used.

A similar treatment of the excitation functions for $Fe^{54}(n, p)$ and $Fe^{54}(n, \alpha)$, but based on published experimental work, is given below in the relevant sections (3.9.1.and 3.9.2.).

3.4. Measurement of helium in the irradiated iron

The samples were in the form of either thin (about 0.01 in.) pure sheet iron of natural isotopic composition, or spheres of 0.1 to 1 gramme. This amount of iron was dissolved within an hour by a cold aqueous saturated solution of potassium cuprichloride, provided that the iron was agitated to prevent the accumulation of thick copper deposits on the surface. Nash and Baxter[26] list various iron solvents but K_2CuCl_4 was found very satisfactory especially since no hydrogen was evolved, and a clear solution was obtained. The copper originally displaced was redissolved by the cupric ions, the net effect being a partial reduction of the solvent to the cuprous state. At first, the K_2CuCl_4 solution contained about 10% mercuric chloride as this mixture dissolved iron a little faster than K_2CuCl_4 alone, but the drawback of a grey sludge which formed led to the adoption of K_2CuCl_4 solution alone.

3.4.1. The dissolution flask used in this work is shown in Fig. 15. The flask normally contained about 100 cc of reagent. Two or three samples or blanks were placed in the sample arms, connected to the flask by an extension tube, to protect the samples from accidental splashing with reagent during the outgassing of the solution. A small glass enclosed iron slug (not shown in the figure) was placed at the

FIGURE 15.

The Sample Dissolution Vessel

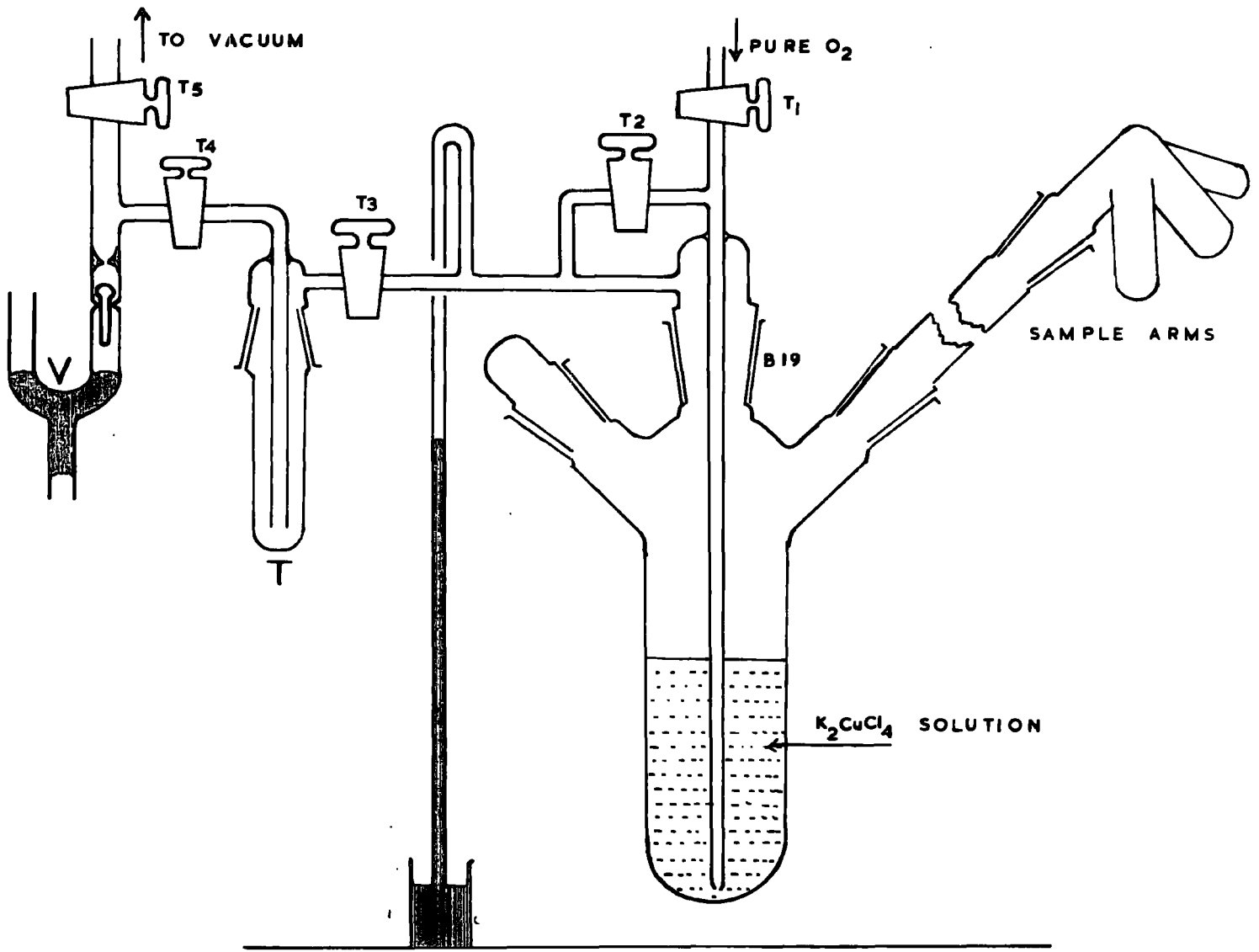
TO VACUUM
PURE O_2
T5
T4
T3
T2
T1
V
T
B19
SAMPLE ARMS
K_2CuCl_4 SOLUTION

bottom of the flask. This was used for stirring the solution and agitating the sample, and was also helpful in outgassing the solution when the flask was first evacuated.

3.4.2. Experimental

With tap T_2 open and T_1 shut, the apparatus was evacuated through T_3, the water trap T and taps T_4 and T_5. Dissolved gas was rapidly evolved by rolling the glass enclosed slug up and down the flask walls with a magnet. All traces of helium were removed from the solution by flushing with pure oxygen as follows. Taps T_3 and T_2 were closed, and T_1 opened extremely cautiously to allow oxygen to bubble slowly from the tip of the tube immersed in the solution. By careful adjustment of T_1 (in conjunction with the drawn-down tip of the tube) an excellent flushing action was achieved, the oxygen bubble spreading from wall to wall across the flask in its passage to the surface. When an oxygen pressure of about 1.5 cm. was registered on the manometer, T_1 was closed and the flask evacuated through T_3 with trap T surrounded by liquid nitrogen.

This flushing procedure when repeated a further nine times would remove all the atmospheric helium from the flask and solution. The effectiveness of this flushing and the purity of the oxygen was then tested by flushing the flask nine times to 1.5 cm. pressure, and allowing the oxygen to bubble through the ventil V into the circulating system after each of the nine flushes, tap T_5 being closed. The oxygen was condensed on the cooled charcoal of the circulating system to prevent a back pressure building up in the circulating system. This oxygen was then examined for any traces of helium by operation of the apparatus as previously described. If the

helium found was not negligible compared with the expected helium content of the sample to be dissolved, then the oxygen was further purified.

Having achieved a successful oxygen blank, the sample was drawn down magnetically into the solution. It was stirred by positioning a small intermittent electro-magnet (operated from the voltage supply to the circulating system's magnetic pump) against the flask about two inches above the bottom. When the sample was completely dissolved, the solution was flushed out in exactly the same manner as that described above for the oxygen blank. The helium content of a known weight of target was thus determined.

3.5. Neutron flux measurements

Most of the neutron irradiations were done at Harwell in B.E.P.O. and the flux monitored by the pile operators with nickel [$Ni^{58}(n, p)Co^{58}$] and cobalt [$Co^{59}(n, \gamma)Co^{60}$] for fast and thermal neutrons respectively. Two of the batches of samples were monitored for fast neutrons by the author with the $S^{32}(n, p)P^{32}$ reaction.

About 100 mg. of $LiSO_4.H_2O$ was encapsulated in a silica tube and irradiated alongside the iron samples. After irradiation they were broken open under a solution of $(PO_3)^{3-}$ and $(HPO_2)^{2-}$ carriers in dilute hydrochloric acid. Bromine water was added, the solution was stirred and warmed nearly to boiling point. It was then carefully transferred to a volumetric flask; the beaker was washed out several times with acidified carrier solution and the washings added to the flask. The flask was made up to the mark and reweighed to obtain the weight of P^{32} solution. A suitable weight of this solution was then taken and diluted in a 50 cc flask with carrier solution and

a 10 cc aliquot counted in a standardized liquid Geiger counter.

Then the fission flux, $\bar{\Phi}$, in neutrons per sq.cm.per minute, will be given by

$$A = \epsilon . f . N_s . \bar{\sigma} . \bar{\Phi} (1 - e^{-\lambda T}) e^{-\lambda t} \quad \text{——————} (12)$$

where A is the measured activity (c.p.m.)

ϵ is the counting efficiency

f is the fraction of the activity counted

N_s is the number of S^{32} atoms

$\bar{\sigma}$ is the average cross section for $S^{32}(n, p)P^{32}$

λ is the decay constant for P^{32} (half life 14.55 days)

T is the irradiation time

t is the time from irradiation to counting.

The value of $\bar{\sigma}$ for the $S^{32}(n, p)P^{32}$ reaction is often quoted as 60 mb. or occasionally as 65 mb.; this value is commonly used as a reference cross section for all other threshold reactions, as indeed we are using it here for reactions in iron. Values of the fast flux calculated by Harwell are referred to $\bar{\sigma}$ as 65 mb.[27] so although 60 mb. is perhaps more commonly used, all fluxes and cross sections in this work are referred to $\bar{\sigma}$ as 65 mb. unless noted otherwise.

3.6. The reaction $Fe^{56}(n, \alpha)Cr^{53}$

3.6.1. Irradiations and helium results

Initially, samples of pure sheet iron of natural isotopic composition were irradiated. The results are collected in Table 5 below. The fast neutron dose measured by Harwell is termed D_H, and that measured at Durham by D_D; the thermal dose is D_T. The agreement between D_H and D_D is excellent in view of the different

standardization and counting techniques involved (using nickel and sulphur monitors respectively).

The value of $\bar{\sigma}$ for Fe(n, α) reactions is calculated from

$$N_{He} = N_{Fe} D_F \bar{\sigma} \qquad (13)$$

where N_{He} is the number of helium atoms measured,

N_{Fe} is the number of iron atoms irradiated,

and D_F is the fission neutron dose (neutrons $cm.^{-2}$).

Table 5.

No.	Weight (g.)	Type	Code	He content (cc /g.)	D_H	D_D	D_T
0	0.905	Nat. Fe	Blank 1	0.27×10^{-8}	0		
0	1.60	Nat. Fe	Blank 2	0.33×10^{-8}	0		
1	0.564	Nat. Fe	55A(i)	12.2×10^{-8}	3.93×10^{17}	4.02×10^{17}	4.79×10^{17}
2	0.531	Nat. Fe	(ii)	17.7×10^{-8}			
3	0.569	Nat. Fe	55B(i)	21.4×10^{-8}	3.99×10^{17}	4.14×10^{17}	4.73×10^{17}
4	0.498	Nat. Fe	(ii)	2.11×10^{-8}			

The results called Blanks 1 and 2 were preliminary measurements of the initial helium content of the unirradiated foil. It will be noticed that this was quite small, being about 3×10^{-9} cc/g. The iron foil thickness was about 0.01 inches. Samples 55A and 55B were two rolls of foil each divided into (i) and (ii) for duplicate analysis. The helium contents of these halves do not agree well and their sums for A and B are not in agreement either. No precautions against thermal neutron reactions or recoil alphas from the

environment were taken, so it may be that part of the disagreement is between the outside and inside halves of the roll. It seems likely that result 4 is incorrect, since in the light of following measurements, it indicates a value of $\bar{\sigma}$ much too small. The thermal flux almost certainly accounts for the inconsistent results. Although it was requested that the samples be cadmium wrapped before irradiation, this was not done. Now the cross section for slow neutron produced alpha particles in boron from the reaction $B^{10}(n, \alpha)Li^{7}$ is at least 10^{6} times as great as the fast neutron cross section in iron (760 barns to less than 0.7 mb., say), so that the presence of a boron impurity of only one part in 10^{7} will produce a 10% excess of helium when the slow neutron flux is the same as the fast neutron flux.

Another question which arises in the presence of a considerable slow flux is the magnitude of the cross section for the reaction $Fe^{56}(n, \alpha)$ with slow neutrons. Some charged particle reactions are known to occur even with such low energy neutrons. The reaction has been investigated by study of tracks in iron coated or iron loaded nuclear emulsions. Hanni and Rossel[118] claimed to find a cross section of 40 ± 20 mb. Longchamp[119] repeated the work in 1952 and expressed his results as $0.1 \text{ mb.} \lesssim \sigma \lesssim 0.24 \text{ mb.}$ Faraggi[120] in attempting to decide between these results, failed to observe the reaction and ascribed previous values to lack of discrimination between alpha particles and protons in the emulsion. He concluded that σ was less than 10^{-2} mb. It would therefore seem that the reaction is not of significance.

Unfortunately, the second set of irradiations, set out below in Table 6, were commenced before the results of Table 5 had been obtained in full, and again the cadmium wrapping was omitted

by the pile operators. However, runs 6 and 7 were attempts to assess the thermal neutron contribution since they were given a much smaller fast neutron dose. It had been intended also to etch the surface of the iron samples to just beyond a depth equivalent to the range of recoil alpha particles, but the samples had been granulated to facilitate reactor loading and the weight loss would have been too great. All three samples were isotopically pure iron 56.

Table 6.

No.	Type	Code	Weight (g.)	He (cc / g.)	D_H	D_T
5	Fe^{56}	-	0.461	13.8×10^{-8}	1.45×10^{18}	4.22×10^{18}
6	Fe^{56}	'1st melt'	0.0481	179×10^{-8}	1.38×10^{16}	1.37×10^{19}
7	Fe^{56}	'2nd melt'	0.333	118×10^{-8}	1.58×10^{15}	3.34×10^{18}

It will be noticed that the results of 6 and 7 are not consistent; 7 received about one tenth of the fast dose and about one quarter of the thermal dose of 6, yet contained about two thirds as much helium. Result 5 is too low on the basis of the thermal flux alone using either 6 or 7 as a comparison. The helium measurements were almost certainly correct since after the measurement of sample 7, the correct functioning of the apparatus was checked by dissolution of a piece of beryllium of known helium content. The helium content of the beryllium was known from independent measurements by a colleague with a similar apparatus; the two results agreed to within 1%.

A probable explanation lies in the impurities in the isotopically pure iron, and boron in particular. Isotopically separated

elements are known to have high impurity levels, as Boldeman[18] found in titanium and Martin[28] has pointed out. Recoil alphas were of no importance, since result 6 was obtained on centre of a larger roughly spherical iron sample, the outer layers of which had been dissolved in an abortive measurement.

The third series of measurements, listed in Table 7, show better agreement.

Table 7.

No.	Type	Code	Weight (g.)	He (cc / g.)	D_H	D_D	$\bar{\sigma}_H$(mb.)	$\bar{\sigma}_D$(mb.)
8	Nat. Fe	C (i)	0.437	4.39×10^{-8}	3.19×10^{17}	3.18×10^{17}	0.352	0.354
9	Nat. Fe	(ii)	0.457	3.94×10^{-8}			0.309	0.310
10	Nat. Fe	E (i)	0.454	8.59×10^{-8}	3.35×10^{17}	3.32×10^{17}	(0.64)	(0.64)
11	Nat. Fe	(ii)	0.452	6.68×10^{-8}			(0.50)	(0.50)
12	Fe^{56}	D	0.739	4.92×10^{-8}	3.03×10^{17}	3.15×10^{17}	0.406	0.390
13	Fe^{56}	Dounreay 1	0.0383	6.19×10^{-6}	4.02×10^{19}		0.384	
14	Fe^{56}	Dounreay 2	0.224	6.46×10^{-6}	4.02×10^{19}		0.402	
15	Fe^{56}	Blank	0.126	$<5 \times 10^{-10}$	-		-	

Samples 8 to 12 were irradiated in B.E.P.O., and were wrapped in thin iron sheet and sealed into an evacuated silica tube before irradiation. Samples 8, 9 and 12 were also wrapped in cadmium sheet, but not 10 and 11. 10 and 11 produced roughly twice as much helium on irradiation. 10 consisted of the outer layers, and 11 the inner layers, of a single sample of rolled sheet. From their

helium contents it appears that some shielding effect was present. Samples 8 and 9 were produced by cutting the roll across the middle so the smaller helium content variation cannot be due in their case to an effect of this type. Samples 13 and 14 were specimens of Fe^{56} irradiated in the fast reactor D.F.R. at Dounreay. This reactor has a flux with virtually no thermal neutron component.

All the samples 8 - 15 were etched before dissolution with sulphuric acid to remove about 5 $mg.cm.^{-2}$. Sample 15 was a blank on the iron 56 and showed a negligible initial helium content.

3.6.2. Conclusions

Results 12, 13 and 14 are in excellent agreement about the value of 0.39 mb. for the reaction $Fe^{56}(n, \alpha)Cr^{53}$. The agreement achieved between irradiations in different reactors is a solid ground for the reliability of the result. However, it is surprising that the results 8 and 9 of natural iron irradiation should be rather smaller (an average of 0.33 mb.). Table 3, given earlier in Section 3.3., indicates that the contributions of iron 54 and 57 to the reaction would lead to a higher result for $\bar{\sigma}(n, \alpha)$ for natural iron. Fe^{57}, like Fe^{56}, gives a stable chromium isotope by (n, α) reaction and so the extrapolated value derived by Roy and Hawton[24] cannot be determined experimentally except by a helium analysis method on separated or enriched Fe^{57}. However, Fe^{54} gives Cr^{51} by (n, α) reaction and the reaction cross section has been determined by Mellish et al.[25] as 0.74 mb. Since this cross section is of interest to the interpretation of the helium measurements, and since Mellish's result appears to be the only reported value, the measurement was repeated. The method and results are described below in the next section (3.7.). It suffices here to say that the result was higher than that of Mellish and so the problem of the result 8 and 9 remains.

Table 8.

Helium contents, neutron doses and cross sections for iron samples

No.	Type	Code	Weight (g.)	He content (cc / g.)	D_H	D_D	D_T	$\bar{\sigma}_H$(mb.)	$\bar{\sigma}_D$(mb.)
0	Nat. Fe	Blank 1	0.905	0.27×10^{-8}	-	-	-	-	-
0	Nat. Fe	Blank 2	1.60	0.33×10^{-8}	-	-	-	-	-
1	Nat. Fe	(i) 55A	0.564	12.2×10^{-8}	3.93×10^{17}	4.02×10^{17}	4.79×10^{17}		
2	Nat. Fe	(ii)	0.531	17.7×10^{-8}					
3	Nat. Fe	(i) 55B	0.569	21.4×10^{-8}	3.99×10^{17}	4.14×10^{17}	4.73×10^{17}		
4	Nat. Fe	(ii)	0.498	2.11×10^{-8}					
5	Fe^{56}		0.461	13.8×10^{-8}	1.45×10^{18}	-	4.22×10^{18}		
6	Fe^{56}		0.0482	179×10^{-8}	1.38×10^{16}	-	1.37×10^{19}		
7	Fe^{56}		0.333	118×10^{-8}	1.58×10^{15}	-	3.34×10^{18}		
8	Nat. Fe	(i) 'C'	0.437	4.39×10^{-8}	3.19×10^{17}	3.18×10^{17}	Cd. wrapped	0.352	0.354
9	Nat. Fe	(ii)	0.457	3.94×10^{-8}				0.309	0.310
10	Nat. Fe	(i) 'E'	0.454	8.59×10^{-8}	3.35×10^{17}	3.32×10^{17}		(0.64)	(0.64)
11	Nat. Fe	(ii)	0.452	6.68×10^{-8}				(0.50)	(0.50)
12	Fe^{56}	'D'	0.739	4.92×10^{-8}	3.03×10^{17}	3.15×10^{17}	Cd. wrapped	0.406	0.390
13	Fe^{56}	Doun-reay 1	0.0383	6.19×10^{-6}	4.02×10^{19}		-	0.384	
14	Fe^{56}	" 2	0.224	6.46×10^{-6}	4.02×10^{19}		-	0.402	
15	Fe^{56}	Blank	0.126	$< 5 \times 10^{-10}$	-		-	-	

It must be said that the earlier results 1 to 7 are of little value. In the absence of Cd shielding, the most likely interpretation is the presence of variable amounts of impurities, most probably boron.

Something must be said of the different neutron spectra of B.E.P.O., a graphite moderated thermal reactor and D.F.R., a fast reactor. It could be argued that the 'harder' spectrum of D.F.R. raises results 13 and 14 above 8 and 9, while 12 is larger than it ought to be because of residual thermal neutron and epi-thermal reactions with boron impurities. This is to place too much emphasis on the one result 12, while ignoring the agreement of 8 and 9 with 13 and 14. Also the spectra of B.E.P.O. and D.F.R. are known to be quite close to a fission spectrum at least up to 10 Mev from about 3 to 4 Mev, [for example, Wright[150]].

Measurement and calculation of pile neutron spectra are not much better than 10% so it is rather fruitless to discuss the anomalies in the results quantitatively in terms of the spectra involved.

To summarise, a value of $\bar{\sigma}[Fe^{56}(n, \alpha)]$ of 0.39 mb. has been found, which while not entirely satisfactory, represents a vast improvement on the previous position where only a dubious extrapolation existed.

Great accuracy cannot be attained in the measurement of small average cross sections but the scatter of the experimental values and the agreement between B.E.P.O. and D.F.R. is good.

3.7. The $Fe^{54}(n, \alpha)Cr^{51}$ reaction

The K_2CuCl_4 solution containing sample 4 was washed out of the dissolution vessel with concentrated hydrochloric acid and added to the similar residues of sample 3. This gave a joint solution of the known weight of irradiated iron called '55B'. The other activities present besides Cr^{51} were Fe^{59}, Mn^{54} and a little Fe^{55}; all shorter lived isotopes like Mn^{56} having decayed away in the month since irradiation. It would have been better to have used the solution of samples 8 and 9 which had been cadmium wrapped, but this investigation was begun before 8 and 9 had been irradiated. This would have avoided any danger of production of Cr^{51} by $Cr^{50}(n, \gamma)$ reaction with thermal neutrons on any chromium impurity in the iron. The possible influence of this reaction is discussed later.

Cr^{51} decays by electron capture and weak γ emission; it exhibits a photo-peak at 0.32 MeV on a NaI (Tl) crystal scintillation counter. This was completely swamped by the Compton and back-scatter peaks of the other activities which are present in much higher concentrations. It was necessary therefore to separate the Cr^{51} activity to measure it. The procedure for separation of chromium is based on that of Brookshier and Freund[30].

3.7.1. Chemical procedure

(1) A known fraction of the iron solution was pipetted (5 cc) into a beaker containing 50 mg. of Cr^{3+} carrier. NH_4OH was added until the copper hydroxide redissolved as the cupramine complex, and the solution was boiled briefly and cooled.

(2) After filtering and discarding the filtrate, the precipitate (iron and chromium hydroxides) was washed into a beaker with

dilute H_2SO_4. Boiling with $S_2O_8^{=}$ converted the Cr (III) to Cr (VI) and the solution was cooled and NaOH added. The Cr (VI) solution was filtered to remove the $Fe(OH)_3$ and evaporated down to 20 cc.

(3) The solution was acidified with HCl and buffered to pH 1.7 $\pm$ 0.1 (pH meter) with NaCl-HCl buffer. After cooling to below 10°C, the solution was transferred to a separating funnel, 50 cc ethyl acetate were added and a few drops of 5% H_2O_2 and the solution shaken to extract the violet perchromic acid into the organic layer.

(4) The extraction was repeated and the organic fractions combined; then the chromium was stripped by addition of NaOH and back extraction into the aqueous phase. This solution was evaporated to small volume and made up to 25 ml. in a volumetric flask.

The chemical yield of the separation was determined by titrating an aliquot of the separated Cr (VI) solution, added to acidified KI solution, with sodium thiosulphate. The titration was carried out according to the method of Vogel[31].

The purity of the separated Cr^{51} was checked by examination of its γ spectrum in a hundred channel pulse height analyser connected to a NaI crystal. Negligible high energy components were detected and the shape of the spectrum was in excellent agreement with that given in Heath[32]. Routine counting was done in a $1\frac{1}{2}$ inch well-type crystal using a single channel to count the photo-peak. The half life was checked and found to be in good agreement with the accepted value of 27.8 days. The crystal had previously been calibrated for Cr^{51} under identical operating conditions[38].

3.7.2. Results

The cross section $\bar{\sigma}$ for the production of Cr^{51} will

be given by

$$I = N_{Fe^{54}} \bar{\sigma} \int \phi (1 - e^{-\lambda T}) e^{-\lambda t} \qquad \text{(14)}$$

where I is the absolute disintegration rate of Cr^{51} in the iron solution containing $N_{Fe^{54}}$ target atoms of Fe^{54}, at a time t after an irradiation of duration T in a flux density of $\int \phi$.

Also $$I = \frac{A}{f} \times \frac{100}{y} \times \frac{100}{c} \times \frac{1}{p} \qquad \text{(15)}$$

where A is the measured activity of a fraction f of the extracted Cr^{51}, obtained in chemical yield, y%. Also c is the counting efficiency (%) and p the fraction of the initial irradiated iron solution.

Two extractions were made, and the values of $\bar{\sigma}$ for $Fe^{54}(n, \alpha)Cr^{51}$ found were

(a) $\bar{\sigma}$ = 1.52 mb.

(b) $\bar{\sigma}$ = 1.49 mb.

Mean value = 1.50 mb.

Relative to $\bar{\sigma}$ for $S^{32}(n, p)P^{32}$ of 60 mb., $\bar{\sigma}$ = 1.38 mb.

3.7.3. Conclusions

The accuracy of the above results is not high: the counting relied on a previous calibration and is accurate to about 5%. Errors in the chemical determinations and dilutions probably amount to 3% and in the flux determination to about 5%. The total accuracy is thus better than 10% (standard error 8%).

Mellish et al.[25] determined this cross-section as 0.74 mb. [relative to $S^{32}(n, p)$ as 60 mb.], or 0.80 mb. [relative to $S^{32}(n, p)$ as 65 mb.]. Mellish (whose work seems to be the only published value) measured $\bar{\sigma}$ in a fission flux under two conditions; in the first, the thermal flux and the fast flux were approximately equal (inside the slug) and, secondly, in an irradiation position where the fission flux was only 0.17 of the thermal flux. The identical results showed thermal reactions were not significant. The thermal neutron cross-section for $Cr^{50}(n, \gamma)Cr^{51}$ is 16 barns[33] and the isotopic abundance 4.3%. Thus for a thermal dose equal to the fast dose (as in samples 3 and 4) the presence of one part chromium in a thousand of iron would produce a spurious fast cross-section of about 0.7 mb. However, analysis of the iron by the suppliers, United Steel, showed less than 5 p.p.m. chromium. Thus this is not the reason for our larger answer of 1.5 mb. It should be pointed out that since 1958, the date of Mellish's publication, most of his results have proved to be rather low. This is touched upon in the next section, on $Fe^{54}(n, p)Mn^{54}$. Another independent result would be instructive.

3.8. The $Fe^{54}(n, p)Mn^{54}$ reaction

Partly because it was convenient to perform (having a solution which had received a known neutron dose) and partly as a check on the $Fe^{54}(n, \alpha)Cr^{51}$ result, it was decided to measure the $Fe^{54}(n, p)Mn^{54}$ cross section. As regards the latter point, it had been noticed that Mellish[25] had measured the (n, p) cross section at the same time as the (n, α) and it was instructive to see how the latter would agree with the result we obtained. Also, Mellish's result[34] for the (n, p) reaction of 46 mb. is considerably lower than the four recent results quoted in Boldeman[18] which have an average of 62 mb., and the two most recent results of 65 and 66 mb.[35, 18] seem to indicate a measure of re-evaluation worth investigating. The results of Martin and Clare[151, 152] of 67 and 68 mb. confirm this upward trend [all values quoted here relative to $S^{32}(n, p)$ as 60mb.].

3.8.1. (i) By subtractive γ-spectrometry

The solution of natural iron samples 3 and 4 showed the main features of a mixture of Mn^{54} and Fe^{59}. The continuous line in Fig. 16 shows the shape of the γ spectrum of the mixture. The contribution of Cr^{51} is negligible relative to their peak heights. Peak A is assigned to the 0.84 MeV peak of Mn^{54} and peaks B and C to the 1.10 and 1.29 MeV peaks of Fe^{59}.

In order to count the Mn^{54} peak, the Fe^{59} component must be 'peeled off'. An Fe^{59} source was prepared by extraction of the iron from the mixture with di-isopropyl ether in 6N HCl[36]. The organic layer was stripped with water and evaporated down to a suitable small volume. The Fe^{59} source was then counted on the multichannel analyser at exactly the same settings. Both spectra are plotted on semi-log paper as this allows the Fe^{59} component to be normalized and subtracted by simple superimposition. The Fe^{59}

FIGURE 16.

Gamma spectra of Fe^{59} and Mn^{54} by pulse height analyses

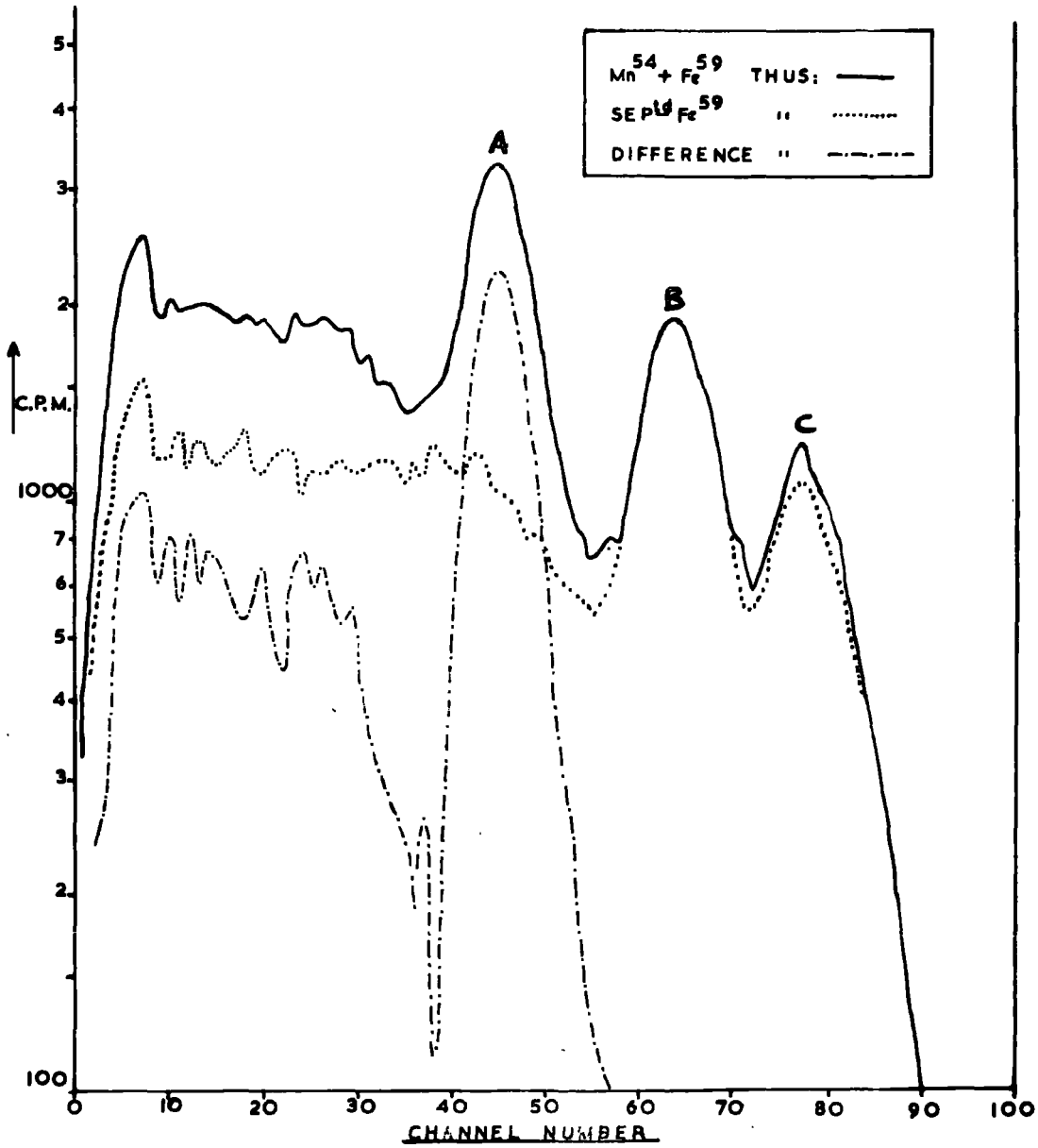
$Mn^{54} + Fe^{59}$ THUS:
SEP'D Fe^{59} "
DIFFERENCE "
A
B
C
C.P.M.
5
4
3
2
1000
7
6
5
4
3
2
100
0
10
20
30
40
50
60
70
80
90
100
CHANNEL NUMBER

source spectrum, shown as the dotted line in Fig. 16, is moved on top of the unbroken line until the Fe^{59} peaks B and C are superimposed. The Fe^{59} curve is then traced through onto the mixed spectrum and subtraction produces the dashed spectrum of Mn^{54}.

The counting arrangement was standardized by counting a Mn^{54} solution which had previously been standardized absolutely[38] by 4π X-ray-γ coincidence counting. The Mn^{54} spectrum obtained by subtraction was identical with the spectrum of the standard Mn^{54}. It will be noticed that the Fe^{59} peaks do not correspond exactly, but the effect is small and probably due to variations in amplifier gain. As a check on the radionuclidic purity of the extracted Fe^{59}, a second extraction was performed on the sample once extracted. The spectrum of the repurified solution was unchanged.

3.8.2. (ii) By chemical separation of manganese

An aliquot of the solution of irradiated iron was added to a known amount of Mn (II) carrier solution (as sulphate) and a little chromium (III) carrier.

(1) NH_4OH was added until the copper (from the K_2CuCl_4 reagent) was complexed, and then the solution was filtered. The precipitate was washed carefully twice to remove all chloride ion [which prevents precipitation in (2)] with dilute NH_4OH.

(2) The precipitate was dissolved in concentrated HNO_3, with a drop of H_2O_2 if necessary. Solid $KClO_3$ was added and the solution boiled cautiously to precipitate MnO_2 which was washed twice with HNO_3 and centrifuged.

(3) The precipitate was dissolved in the minimum of HCl with 5 drops of added 5% H_2O_2; ferric iron holdback carrier was added

and the solution taken to dryness to remove HCl. The residue was redissolved in concentrated HNO_3 and MnO_2 re-precipitated, as in (2).

(4) The precipitate was washed twice with concentrated HNO_3 and once with water, then filtered onto a tared glass paper and washed successively with hot water, alcohol and ether. It was then dried in a dessicator and weighed as $MnO_2.H_2O$.

The MnO_2 precipitates were counted by dissolution in dilute HCl, with a little H_2O_2, and transfer of the solution to a $1\frac{1}{2}$ inch well-type NaI crystal, which was standardized with the absolutely calibrated Mn^{54} solution.

3.8.3. Results and conclusions

Relative to $\bar{\sigma}$ for the $S^{32}(n,p)$ reaction of 65 mb. assumed in the flux measurements, the average fission cross section for $Fe^{54}(n,p)Mn^{54}$ was:-

By method (i), 3.8.1., (a) 66.4, (b) 65.4 mb.

By method (ii), 3.8.2., (a) 72, (b) 72, (c) 71 mb.

Hence mean, relative to S^{32} of 65 mb., is 69 mb.

and mean, relative to S^{32} of 60 mb., is 64 mb.

This result is in excellent agreement with recent measurements. Boldeman[18] lists the following values of $\bar{\sigma}$ $[Fe^{54}(n,p)]$, relative to $\bar{\sigma}$ $[S^{32}(n,p)]$ of 60 mb., after correction to the now accepted value of 314 days for the Mn^{54} half life[121]:-

Rochlin[16], (1959)	60 mb.
Passel and Heath[37], (1961)	58 mb.
Hogg and Weber[35], (1962)	65 mb.
Boldeman[18], (1963)	66 mb.

Since then, Clare et al.[151] and Martin and Clare[152] found 67.5 and 68.3 mb. respectively.

The agreement between these values and the value of 64 mb. found speaks for itself. Mellish's value of 46 mb. indicates that his value for $\bar{\sigma}$ $Fe^{54}(n, \alpha)Cr^{51}$ may be too low at 0.74 mb. The disagreement between this and the result of 1.38 mb. here reported may be thus partly alleviated.

3.9. Integration of published excitation functions, (B)

In a recent paper, Salisbury and Chalmers[134] published their own experimental results and a compilation of previous values of cross sections for $Fe^{54}(n, p)$ and $Fe^{54}(n, \alpha)$ at various bombarding energies. These are reproduced in Fig. 17 (a) and (b). [For references see (138) to (147)]. Following the treatment of 3.3.1., we may derive values of $\bar{\sigma}$ by integration.

3.9.1. $Fe^{54}(n, p)Mn^{54}$

The values of σ given in Table 9 are derived from the dashed line (due to Salisbury and Chalmers) of Fig. (17)(a).

FIGURE 17.

(a) Excitation function for the reaction $Fe^{54}(n, p)Mn^{54}$, from Ref. (134)

(b) Excitation function for the reaction $Fe^{54}(n, \alpha)Cr^{51}$ (134)

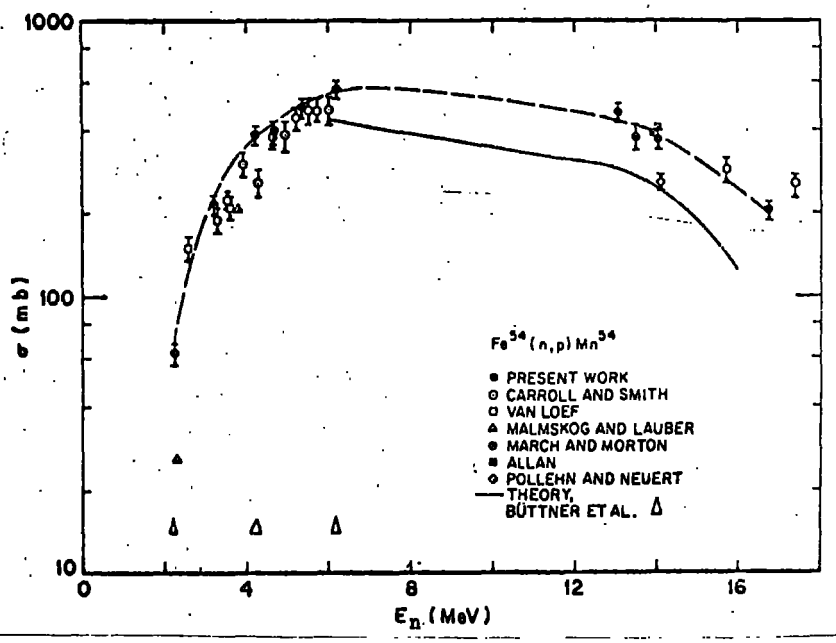
1000
100
10
σ (mb)
0
4
8
12
16
E_n (MeV)
$Fe^{54}(n,p)Mn^{54}$
PRESENT WORK
CARROLL AND SMITH
VAN LOEF
MALMSKOG AND LAUBER
MARCH AND MORTON
ALLAN
POLLEHN AND NEUERT
THEORY, BÜTTNER ET AL.

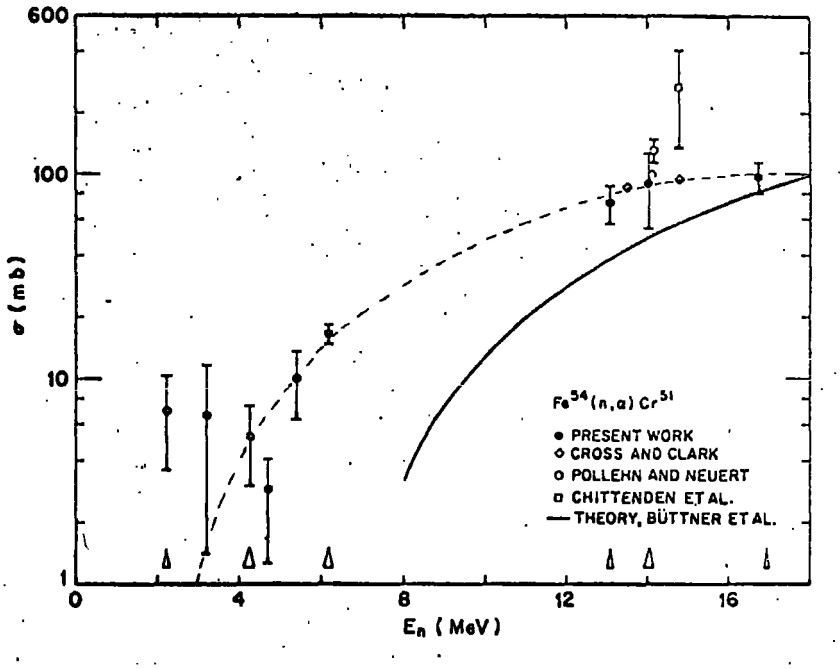
600
100
10
1
σ (mb)
0
4
8
12
16
E_n (MeV)
$Fe^{54}(n,\alpha)Cr^{51}$
PRESENT WORK
CROSS AND CLARK
POLLEHN AND NEUERT
CHITTENDEN ET AL.
THEORY, BÜTTNER ET AL.

Table 9.

E (Mev)	σ(E) mb.	N(E) Eqn. (10)	N(E) Eqn. (11)	σ(E) x $N(E)_{10}$	σ(E) x $N(E)_{11}$
2	0				
2.5	106	1.84×10^{-1}	1.84×10^{-1}	19.5	19.5
3	185	1.38×10^{-1}	1.38×10^{-1}	25.5	22.5
3.5	225	1.02×10^{-1}	1.02×10^{-1}	28.0	28.0
4	335	7.40×10^{-2}	7.38×10^{-2}	24.8	24.7
5	450	3.84×10^{-2}	3.75×10^{-2}	17.3	16.9
6	530	1.89×10^{-2}	1.84×10^{-2}	10.0	9.75
7	580	9.31×10^{-3}	8.77×10^{-3}	5.40	5.08
8	550	4.42×10^{-3}	4.10×10^{-3}	2.43	2.25
9	540	2.07×10^{-3}	1.89×10^{-3}	1.12	1.02
10	510	9.53×10^{-4}	8.56×10^{-4}	0.49	0.44
11	480	4.38×10^{-4}	3.84×10^{-4}	0.21	0.18
12	460	1.99×10^{-4}	1.70×10^{-4}	0.09	0.08

Integration produces values of 89 mb. [Eqn. (10)] and 88 mb. [Eqn. (11), the Cranberg spectrum] for $Fe^{54}(n, p)Mn^{54}$. This can be regarded as fair agreement with the value found and the literature values. The weighted yield curve gives greatest weight to the low energy points where the slope is very steep and the points most uncertain.

3.9.2. $Fe^{54}(n, \alpha)Cr^{51}$

Here the situation is much worse experimentally, see Fig. (17)(b), and also the low energy σ values are very imprecise

leading to very great imprecision in $\bar{\sigma}$. The dotted line is an attempt by the present author to a best fit for the points; the full line is a theoretical function due to Buttner[144].

Table 10.

E(Mev)	$\sigma(E)_{ARB}$	$\sigma(E)_{(144)}$	$N(E)_{11}$	$\sigma(E)_{ARB} \times N(E)$	$\sigma(E)_{(144)} \times N(E)$
3	0	0		0	0
3.5	2.5	0	1.02×10^{-1}	0.25	0
4	4	0	7.38×10^{-2}	0.295	0
5	8	0	3.75×10^{-2}	0.30	0
6	13	0	1.84×10^{-2}	0.24	0
7	20	0	8.77×10^{-3}	0.175	0
8	27	3.1	4.10×10^{-3}	0.11	0.013
9	38	7.8	1.89×10^{-3}	0.07	0.015
10	45	12	8.56×10^{-4}	0.04	0.010
11	55	20	3.84×10^{-4}	0.02	0.008
12	63	27	1.70×10^{-4}	0.01	0.005
13	70	37	7.48×10^{-5}	0.005	0.003
14	87	47	3.26×10^{-5}	0.003	0.0015

Integration with the Cranberg spectrum of the dotted curve $[\sigma(E)_{ARB}]$ gives $\bar{\sigma}$ for $Fe^{54}(n, \alpha)Cr^{51}$ as 1.34 mb.; Buttner's curve gives 0.06 mb. The agreement between this value of 1.34 and our experimental value of 1.50 mb. is mainly fortuitous in view of the large uncertainties in the method. It does weigh slightly against the value of Mellish (0.80 mb.), as our dotted 'best fit' tends to underestimate the values of σ (E) at low neutron energies found by Salisbury and Chalmers[134].

SECTION 4.

ABSOLUTE FISSION YIELDS OF Mo^{99} AND Ba^{140} IN THE THERMAL NEUTRON INDUCED FISSION OF NATURAL URANIUM

4.1. Introduction

Since the discovery of the fission process, a vast amount of theoretical and experimental work has been done by physicists and chemists for mechanistic studies. The mass yield curve, that is, the proportions in which the various fission products are produced, is the fundamental fact which any theory of fission must reproduce and explain. Mass yield curves for heavy nuclei at low bombarding energies are typically asymmetric, as the familiar two-humped curve for the thermal neutron fission of U^{235}, Fig. 18(a), shows. The curve is not smooth at the maxima, and this fine structure, shown in more detail in Fig. 18(b) [data from Katcoff[39]], and Fig. (19), [data from Farrar and Tomlinson[72]], has been the subject of great and continuing discussion.

The following account is mainly concerned with the thermal neutron induced fission of U^{235}. Methods of measuring fission product yields are of two main types; radiometric (radiochemical) and mass spectrometric. Absolute measurements of both types consist of two main steps; (a), measurement of the number of fissions that have occurred in the sample and (b), measurement of the number of atoms of fission product or products in question that have been produced. Relative measurements simply

FIGURE 18.

(a) Mass distribution curve for thermal neutron fission of U^{235}

(b) Fine structure of U^{235} mass distribution curve (Ref. 39)

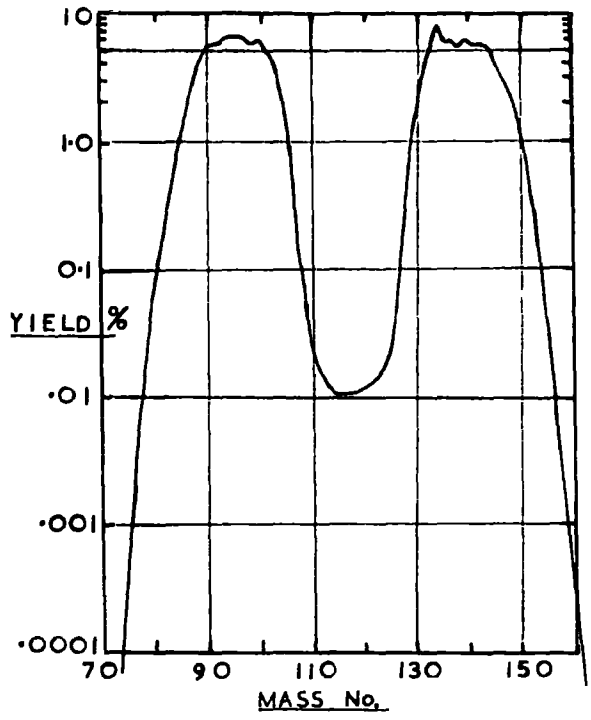
10
1·0
0·1
YIELD %
·01
·001
·0001
70
90
110
130
150
MASS No.

(a)

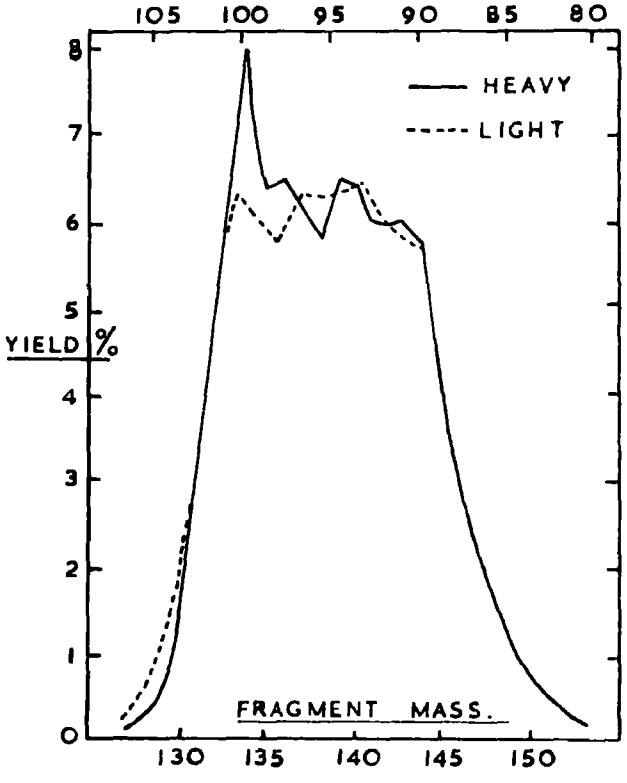
105
100
95
90
85
80
8
7
6
5
YIELD %
4
3
2
1
0
HEAVY
LIGHT
FRAGMENT MASS.
130
135
140
145
150

(b)

FIGURE 19.

Fine structure of U^{235} mass distribution curve, (ref. 72)

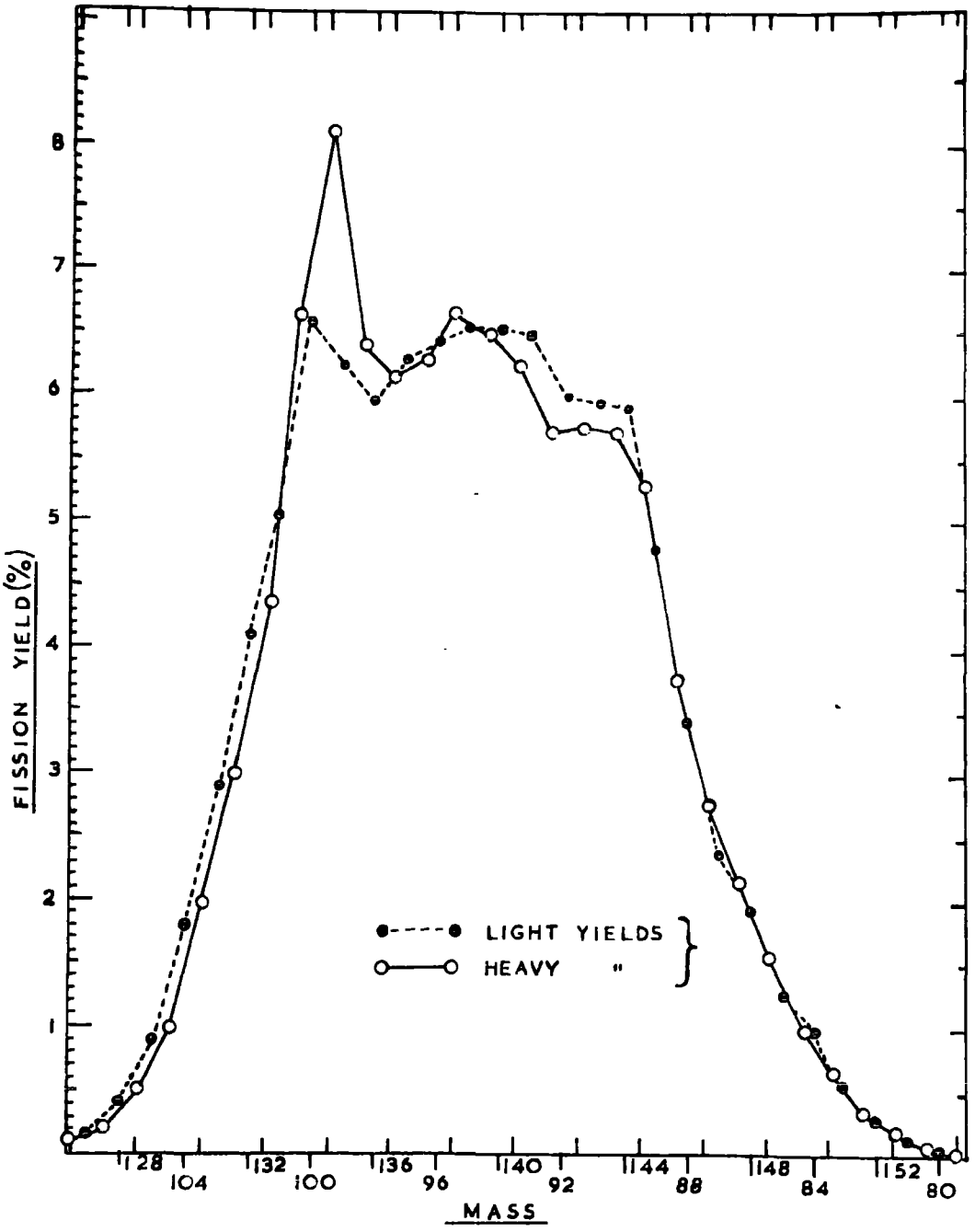
FISSION YIELD (%)
8
7
6
5
4
3
2
1
LIGHT YIELDS
HEAVY "
128
104
132
100
136
96
140
92
144
88
148
84
152
80
MASS

consist of step (b) performed on several nuclides from the irradiated sample. The terms radiometric and mass spectrometric really apply only to step (b), since methods common to both have been employed in (a). Common methods used in step (a) are:

(i) the use of a flux monitor, such as $Co^{59}(n, \gamma)Co^{60}$ or $U^{238}(n, \gamma)U^{239}$,

(ii) the use of the $B^{10}(n, \alpha)Li^{7}$ reaction to measure the change in the B^{10}/B^{11} ratio by spectrometry,

(iii) the use of a fission chamber (counter), or

(iv) the normalization method.

Methods (i) and (ii) also require a knowledge of the $U^{235}(n, f)$ cross section, which ultimately depends on a fission chamber measurement. A great deal of work has been done internationally to establish an accurate value of $\sigma_f(U^{235})$; its use is probably more accurate than employing a conventional fission chamber. Also the form of the uranium sample used in the method described below is difficult to reconcile with fission counter geometry. The normalization method (iv) entails relative measurements of the individual fission products by step (b) over the whole mass curve. Normalization of the sum of the yields to 200% total yield or 100% for both light and heavy peaks in the case of U^{235} follows.

As regards step (b), radiochemical methods entail the separation of a β^- emitting precursor of the stable chain product and absolute measurement of its number of atoms by the use of a calibrated counter. This is justified since it has been shown by Glendenin et al.[40], and Wahl[41], that the last two or three members

of the chain have virtually zero independent yields, that is, they are formed almost exclusively from the decay of their precursors. Mass spectrometric methods employ the isotope dilution technique to determine the number of atoms of a particular nuclide formed.

The complete radiochemical method using the normalization technique is generally quoted to an accuracy of $\pm$ 10%. Using methods (i) to (iii) in step (a), however, both the radiometric and mass spectrometric methods are claimed to be accurate to about $\pm$ 3%. These errors are discussed more fully in the next Section, (4.2.), after the method used has been described.

4.1.1. The present work : Mo^{99} and Ba^{140}

The two fission products chosen for study were Mo^{99} and Ba^{140}. Both nuclides have frequently been used as standards in relative yield work, though the yields, in particular for Mo^{99}, are not very well defined. Both appear in the fine structure region near the maxima of the light (Mo^{99}) and heavy (Ba^{140}) peaks. For these reasons, and because the method (see below) promised accurate values, these two nuclides were chosen. Also advantageous are their large yields, suitable half lives, ease of separation and relatively non-complex delay schemes.

4.2. The method

The method was radiometric in step (b) and used a new method of measuring the fission events, step (a). The use of the $B^{10}(n, \alpha)Li^{7}$ reaction has been mentioned above, the alteration in the B^{10}/B^{11} ratio being measured. This has usually taken the form, e.g. Yaffé et al.[42], of simultaneous irradiation of a vessel of BF_3 with the uranium sample close by. Knowledge of the cross sections

of $B^{10}(n, \alpha)$ and $U^{235}(n, f)$ enabled the number of fissions to be calculated. In the present work, boron as boric acid, was thermal neutron irradiated in an uranyl nitrate solution, and the helium produced by $B^{10}(n, \alpha)$ measured by the micro gas analysis apparatus. Having measured the helium produced in the solution, the fission products Mo^{99} and Ba^{140} were radiochemically separated using carrier solutions. Measurement of the numbers of their atoms was carried out by counting in a calibrated liquid Geiger counter. The counter was previously standardized for the two nuclides with known amounts of solutions of known absolute radioactive concentration, determined by $4\pi\beta^-$ counting of weightless sources.

Consider the accuracy of the method, especially with regard to mass spectrometric methods. The helium determination is accurate to better than 1%. Some errors occurring in mass spectrometric methods might be mentioned. The use of the B^{10}/B^{11} ratio change is of only fair accuracy; changes in the isotope ratio may be accurate to typically 0.1%, but the change of the ratio is of the order of 1.03 [42, 71]; i.e. an accuracy of about 3%. Long irradiations are required to achieve even this isotopic ratio alteration. The use of the isotope dilution technique, in itself is more accurate, (better than 1%), than absolute counting of the separated fission products but introduces other errors. Large samples and long irradiation periods are required to produce enough fission product to apply the dilution technique accurately. Large samples lead to large self-shielding corrections, and long irradiation periods are also clearly undesirable. It is interesting to note that Yaffé et al. in 1960 [71] changed over, for his more accurate

determination of Ba^{140}, from the B^{10}/B^{11} method of 1954[42], to a Co^{59} monitor technique, while retaining radiometric measurements on Ba^{140}.

4.2.1. Discussion of potential errors

In the method outlined above it is assumed that there is a constant relation between the number of fission product atoms produced and the helium produced. We must consider other processes occurring and show that they are negligible. Firstly, helium may be produced by other mechanisms than the reaction $B^{10}(n, \alpha)$. The use of an irradiation blank of encapsulated water was used to show that negligible amounts of helium were produced by heating or (n, α) reactions in the vessel or its aqueous contents. Some helium will be produced by ternary fission; Fulmer and Cohen[45] found that 0.3% of fission events gave rise to an alpha particle. However, this small figure is diminished to negligible proportions by the consideration that about twelve times as many $B^{10}(n, \alpha)$ events occurred in the solution as fissions, as a result of the proportions of boron and uranium used. Production of helium from decay of the uranium series (U^{238} and U^{234} need only be considered) gives rise to completely negligible amounts of helium from the 200 mg. of uranium per capsule in the period of less than a month which the irradiation and analysis encompassed.

Another point must be considered; thermal fission of U^{235} will produce a small fission spectrum of neutrons, some of which will produce fast fission of the U^{238}. The point is not that the fast fission yields of U^{238} in the region of the mass yield maxima are 5-10% different from thermal fission yields of U^{235} (since the

proportion of fast fissions is small) but that some fission events will have occurred for which no corresponding $B^{10}(n, \alpha)$ reactions have occurred (or with a very much smaller probability). By considering the worst case it can be shown that this is a negligible effect. On the very unrealistic assumptions that no fission neutrons escape and that the U^{238} is subjected to an unmoderated fission spectrum of neutrons (far from the case in a dilute aqueous solution, of course), one may proceed as follows. Since U^{238} has an almost constant fission cross section of about 0.5 barn above a threshold of 1.5 Mev[147] its average fission cross section will be roughly 0.25 barn. Knowing the amount of U^{238} and the thermal flux, it may be shown that less than one in a thousand fission events is due to U^{238} fast fission, even in this 'worst case' example.

The next sections are descriptions of the two vacuum systems, one for filling the capsules with a helium free solution containing a known ratio of boron to uranium, the other for breaking open the capsule after irradiation and flushing the gas into the main helium measuring section.

4.3. The filling apparatus

The filling apparatus shown in Fig. 20 was designed to fill five lead glass capsules with a helium free solution of uranyl nitrate containing boric acid.

The five capsules joined on the bottom of the filling chamber (only one is shown in the figure for the sake of clarity) were made of lead glass since all other glasses were unsuitable. Silica has much too large a permeability to helium; pyrex not only has a high permeability but also a considerable boron content. Soda glass

FIGURE 20.

Apparatus for encapsulation of a helium free solution of uranyl nitrate containing boric acid

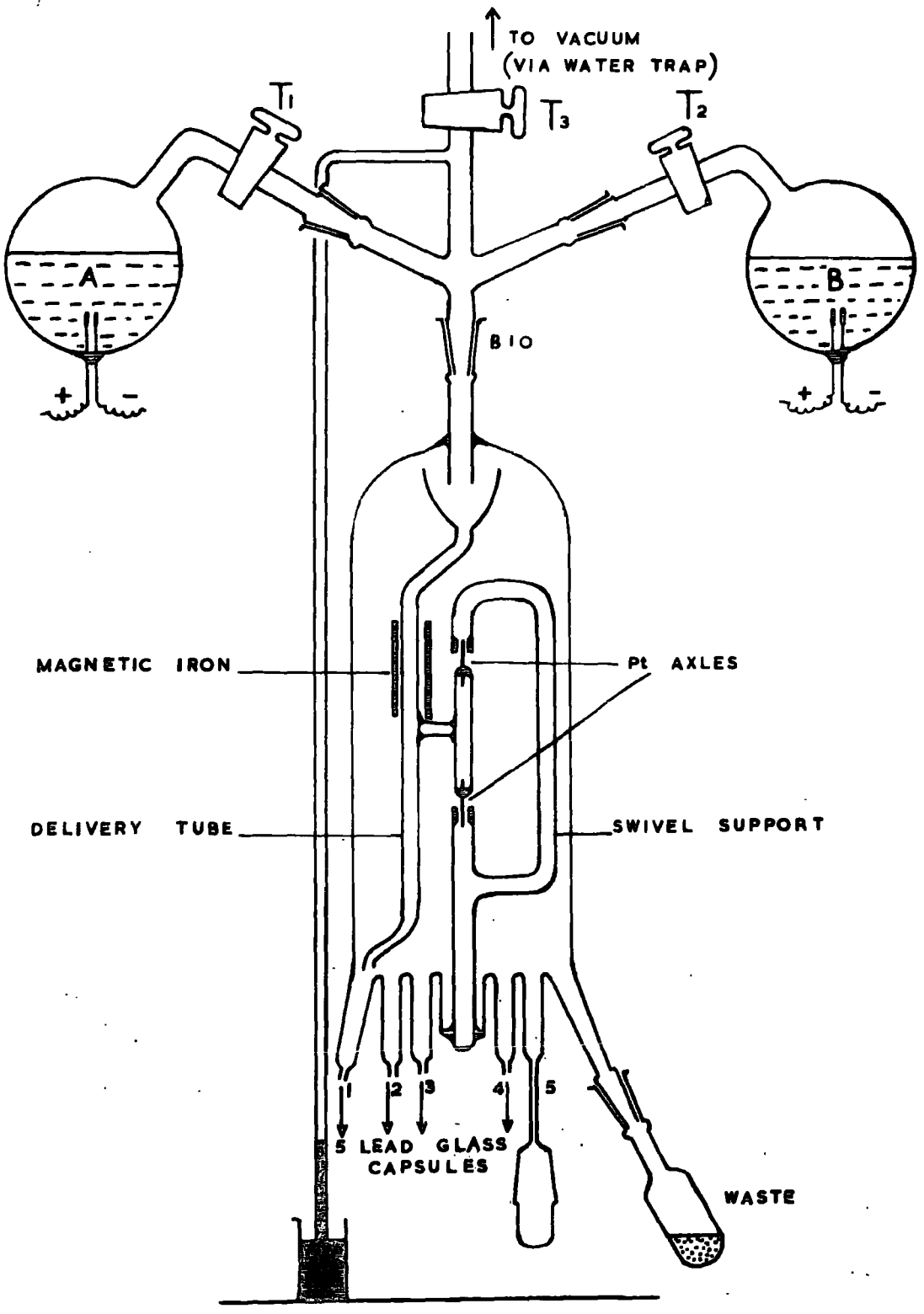
TO VACUUM
(VIA WATER TRAP)
T1
T3
T2
A
B
B10
+
-
+
-
MAGNETIC IRON
Pt AXLES
DELIVERY TUBE
SWIVEL SUPPORT
1
2
3
4
5
5 LEAD GLASS CAPSULES
WASTE

becomes active by the reaction $Na^{23}(n, \gamma)Na^{24}$ (cross section of half a barn) giving rise to handling problems. Lead glass fortunately could be glass-blown directly onto the soda glass of the filling vessel. The capsules consisted of specially made B.14 cones, sealed off behind the cone and drawn out in front to form a narrow tube ready to be sealed off after filling. The volume of the capsule was 4 to 5 ml. They were arranged in a circle around the base of the filling device or 'pig' so that each could be filled in turn through the swivelling delivery tube. Flasks A and B, of about 150 ml., were respectively half full of an uranyl nitrate plus boric acid solution and with slightly acidified water. Each was fitted with two platinum electrodes.

The operation of the apparatus was as follows. The apparatus was first evacuated through tap T_3 with T_1 and T_2 open. The solutions were then outgassed to remove dissolved helium. In the absence of a flushing gas stream, electrolysis has been found to be an effective method by previous workers. However, the uranium solution could not be electrolysed for fear of plating out some of the uranium. Flask B was outgassed in this way, however. T_2 was closed and electrolysis continued for some minutes to build up a pressure of H_2 and O_2 of several centimetres, then T_2 opened to the pumps for a few seconds and the process repeated ten or twelve times. Solution A was outgassed by swirling the flask by rotation in the B.10 socket just beyond T_1 and periodic pumping of the flask through T_1. After periodic pumping for 2 days, the solution was found to be helium free.

The method of filling the capsules was first to obtain a good vacuum in the pig, (with T_1 and T_2 closed). The swivelling

delivery tube was then brought over the waste reservoir by a magnet acting on the iron collar around the tube. Tap T_3 was closed, T_1 opened, and the flask A was turned upwards in the B.10 socket until the solution just commenced to pour through T_1 and down the delivery tube. It was found that the solution could be readily controlled; the delivery tube was positioned over each of the five capsules in turn and about 2 - 3ml. of solution poured into each. The delivery tube was washed out with water from B into the waste reservoir and the narrow capillary tubing connecting the capsules to the pig washed out in turn with water. This was to remove any uranium and boron from the capillary walls before sealing off the capsules with a torch flame.

Five capsules were filled with uranium-boron solution and one with just acidified water. The blank tests and irradiations are described below.

4.4. The analysing vessel

This apparatus was designed for breaking open the capsules under vacuum and flushing out the dissolved helium from the solution with oxygen, as in the dissolution vessel used for iron samples in Section 3.

The apparatus, of about 30 to 40 cc. in volume, was connected to the oxygen line and to the circulating system through two B.10 joints as shown in Fig. 21. The capsule containing the solution from the filling device was fitted into the greased B.14 socket as shown, after a scratch had been made on the capillary tip with a glass knife. The apparatus was then rigourously evacuated through the tap leading to the circulating system. This tap was closed, and the breaking arm slowly turned, while holding the capsule in position

FIGURE 21.

Apparatus for breaking open irradiated capsules under vacuum and for flushing out the dissolved helium

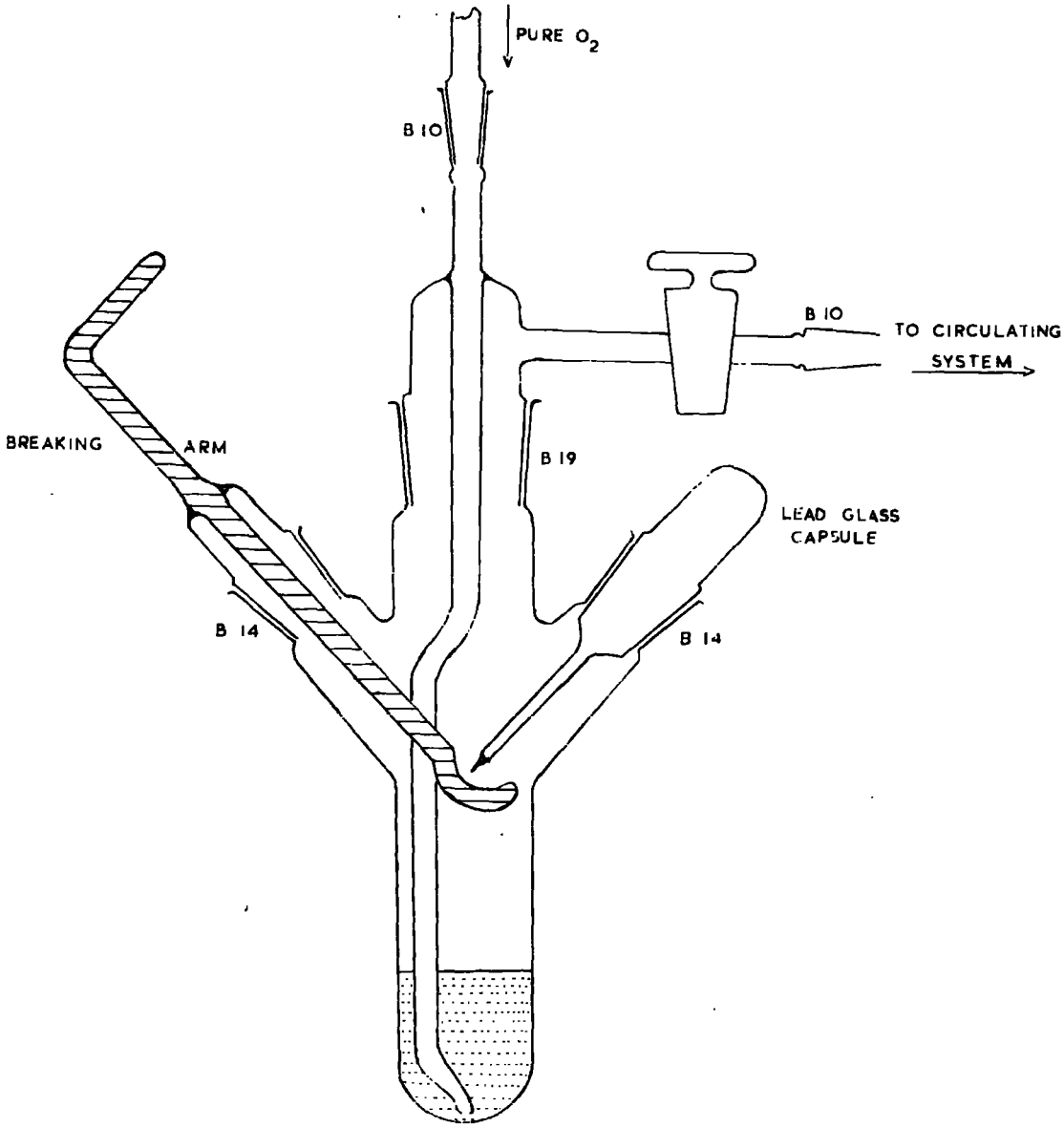
PURE O_2
B 10
B 10
TO CIRCULATING SYSTEM
BREAKING ARM
B 19
LEAD GLASS CAPSULE
B 14
B 14

in the B.14 socket, so that the capillary was broken off at the scratch mark. The liquid then spurted out under the pressure of its vapour leaving only one small drop on the tip of the capillary. The solution was then flushed out with oxygen through the tube passing below the liquid surface to the bottom of the vessel. The flushing procedure was very similar to that outlined in the section on iron sample analysis. The mercury in the ventil of the circulating system was adjusted to allow the oxygen of each flush to bubble past when the connecting tap was opened, and be adsorbed on the cooled charcoal of the circulating system. This process was repeated a further eight times to ensure complete removal of helium from the analysing vessel to the circulating system. The completeness of this transfer was demonstrated by flushing the vessel a further nine times after one of the irradiated capsules had been analysed and no helium was found to have been left behind by the first nine flushes.

Before breaking open the capsule to be analysed, the purity of the oxygen was checked by operating the flushing procedure with the same amount of oxygen as that used on the solution for analysis and detecting the helium present, if any. Typical oxygen blanks were around 2×10^{-9} cc of helium, this being about 0.1% of the actual helium content of the capsules after irradiation.

4.5. Helium contents of the capsules

A complete batch of samples consisted of five capsules filled with uranium-boron mixture and one filled with acidified water. One of the capsules was examined for helium immediately after sealing off the outgassed solutions to check on the completeness of the helium removal. This was termed the 'initial blank', a second

one was kept back to be measured after all the other samples had been irradiated and measured; this 'final blank' showed that no appreciable leakage or diffusion had occurred in the capsules during the three or four weeks that the experiments took. The capsule filled only with water was irradiated with the other three to ensure that the process of irradiation did not give rise to helium.

The helium contents of the six capsules are listed below:

Code	Treatment	He content (cc)
(1) X2	'Initial blank'	$< 1 \times 10^{-9}$
(2) B2	'Final blank'	$< 1 \times 10^{-9}$
(3) X1	Irradiation blank	2.5×10^{-9}
(4) B3	Irradiated	1.309×10^{-6}
(5) B4	Irradiated	2.075×10^{-6}
(6) B5	Irradiated	1.563×10^{-6}

(The different helium contents of B3, B4 and B5 reflected the different amounts of solution each capsule contained).

Each of the irradiated capsule solutions B3 - 5 was then examined radiochemically to determine the number of active atoms of Mo^{99} and Ba^{140} produced in each.

4.6. The nuclear properties of Mo^{99} and Ba^{140}

The β^- decay fission chains in which the two species occur are listed in Katcoff[46] as:

(i) $Zr^{99}(33s.) \longrightarrow Nb^{99}(2.4m.) \longrightarrow Mo^{99}(66.5h.) \longrightarrow Tc^{99m}(6.0h.)$

$Mo^{99} \longrightarrow Tc^{99} \longrightarrow Ru^{99}(\text{stable})$

$(2 \times 10^5 y.)$

(ii) $Xe^{140}(16s.) \longrightarrow Cs^{140}(66s.) \longrightarrow Ba^{140}(12.8d.) \longrightarrow$

$La^{140}(40.2h.) \longrightarrow Ce^{140}(\text{stable})$

Both nuclides are in transient equilibrium with their shorter lived daughters. More details of their modes of decay are listed:

(i)

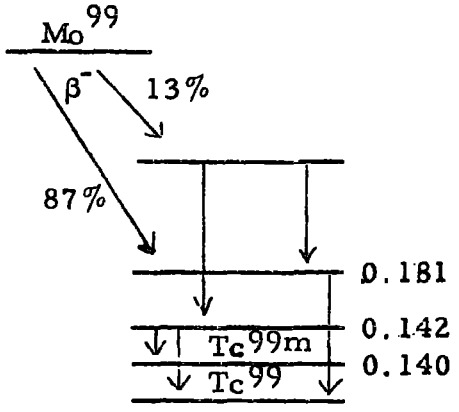

Mo^{99} β^- Energies: 0.45 MeV - 13%; 1.23 MeV - 87%

The half lives used were: Mo^{99}, 66.0 hours; Tc^{99m}, 6.01 hours and Tc^{99} considered as a stable isotope.

(ii)

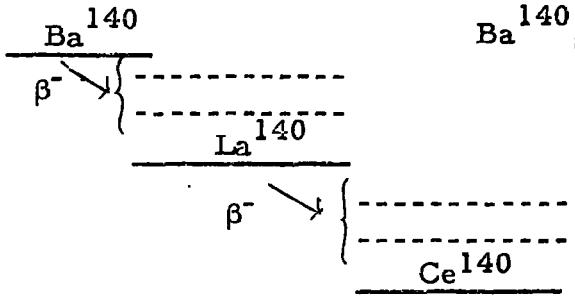

Ba^{140} β^- Energies: 0.48 MeV - 25%; 0.6 MeV - 10%; 0.9 MeV - 5%; 1.02 MeV - 60%

La^{140} β^- Energies: 0.8 MeV - 12%; 1.1 MeV - 25%; 1.38 MeV - 45%; 1.7 MeV - 10%; 2.2 MeV - 7%

Half lives: Ba^{140}, 12.8 days and La^{140}, 40.2 hours.

The half life values quoted were taken from 'Nuclear Data Sheets'[121]; however, there was a spread of values for Mo^{99} between 66 and 67 hours. It was found experimentally from the irradiated MoO_3 used for the counter calibrations that the decay followed a half life of 66.0 hours.

4.7. Radiochemical separation procedures

The analysing vessel containing the irradiated solution after helium analysis was detached from the vacuum line at the B.10 joint. It was thoroughly washed with a 2N nitric acid solution containing accurately known amounts of barium and molybdenum carriers. These consisted of 50 mg. of barium as nitrate, and 50 mg. of molybdenum as ammonium molybdate. The vessel was then washed with 0.5N nitric acid to recover all the carrier, and to produce a combined solution of about 1N nitric acid containing all the added carrier and activity in a volume of about 30 ml. (This strength acid solution was suitable for the initial precipitation of molybdenum). Boiling with a few drops of bromine water ensured radiochemical equilibrium between the active molybdenum and the carrier.

The barium separation consisted of precipitations as the carbonate, the nitrate (twice), the chromate and the chloride (twice); the molybdenum separation of precipitations of the α-benzoin oxime (three times) and the 8-hydroxy quinolinate. This molybdenum procedure is based on that of Ballou[47].

(a) Molybdenum

(1) The solution was cooled in ice and 10 ml. of 2% α-benzoin oxime added with stirring. The supernate after centrifugation forms the barium portion.

(2) The precipitate was washed twice with water and dissolved in 5 ml. of fuming HNO_3. This was diluted to 30 ml., partially neutralized to IN HNO_3 with ammonia solution, cooled in ice, and molybdenum re-precipitated as in (1).

(3) (2) repeated.

(4) The precipitate was converted to MoO_3 by taking almost to dryness with a mixture of concentrated HNO_3 and $HClO_4$.

(5) The oxide was taken up in a little NH_4OH solution, just acidified and 5 mg. iron (Fe^{3+}) carrier added. The solution was re-made alkaline and the scavenge iron precipitate discarded by filtration.

(6) 10 mg. of rhenium 'holdback' carrier were added to the molybdate solution, with 2 ml. of 10% E.D.T.A. solution. The solution was buffered at pH 4.5 with acetic acid-ammonium acetate buffer, and heated almost to boiling. 3% 8-hydroxy-quinoline (alcoholic solution) was added dropwise to excess and the precipitate washed with hot water and 5 ml. of ethyl alcohol.

(7) The precipitate was dissolved in fuming HNO_3, diluted and neutralized to IN acid, and made up to 12 ml. in a volumetric flask, ready for liquid beta counting.

(b) Barium

(1) The supernate from stage (1) of the molybdenum separation was treated with excess solid Na_2CO_3 and the $BaCO_3$ precipitate centrifuged.

(2) The precipitate was dissolved in a little concentrated HNO_3, 25 ml. of fuming HNO_3 were added, and the nitrate precipitated at $0^{\circ}C$ in an ice bath. After centrifugation, the supernate was discarded.

(3) The nitrate was dissolved in a little water, then re-precipitated with fuming HNO_3 as in (2).

(4) The precipitate was dissolved in 10 ml. water and an iron scavenge precipitation performed by addition of 5 mg. Fe^{3+} carrier and then dilute NH_4OH. The solution was filtered and the precipitate discarded.

(5) The solution was just acidified with dilute HNO_3, 5 mg. of strontium 'hold back' carrier were added, and the solution buffered at pH 4.5 with acetic acid-sodium acetate. The chromate was precipitated hot with excess 1.5 M K_2CrO_4 solution added dropwise, and the solution centrifuged after addition of a wetting agent (teepol).

(6) The chromate was washed in hot water and dissolved in 3 ml. of 6N HCl. 25 ml. of HCl-ether reagent were added, the solution was chilled to $0^{\circ}C$ and stirred, and the $BaCl_2.H_2O$ centrifuged. The supernate was discarded.

(7) The chloride was redissolved in the minimum amount of water and reprecipitated as in (6).

(8) The precipitate was filtered onto a glass sinter, and washed with 5 ml. ethyl alcohol containing 5 drops concentrated HCl, three times. The precipitate was washed through into a volumetric flask with water and made up to the mark for liquid counting.

NOTE: The HCl-ether reagent was a 4 : 1 conc. HCl and diethyl ether mixture.

4.8. Counting

4.8.1. Liquid counting

The two nuclides were counted in a calibrated liquid Geiger counter by taking a 10 ml. aliquot of the separated solution after sufficient time had elapsed for transient equilibrium to be re-established (10 daughter half-lives). This method was simple and effective once the counter had been calibrated. The growth and decay of the separated nuclides was followed for several half-lives to check their radionuclidic purities; they were found in all cases to follow their expected decay accurately. Typical count rates of the separated fission products were of the order of several thousand per minute.

The liquid counter was standardized with a solution of the nuclide made up from a known weight of a carrier free solution whose radioactive concentration had been accurately determined by absolute $4\pi\beta^-$ counting. The chemical composition of the standardizing solution in the liquid counter was the same as the separated fission product solution. The preparation of the carrier free parent nuclides for absolute 4π counting to standardize the liquid counter is described below. The necessity for the separation of the parent activity is discussed in Section 4.8.3.

4.8.2. Preparation of 4π films and their counting

The 4π films were prepared from V.Y.N.S. resin (polyvinyl chloride-acetate copolymer), dissolved in cyclohexanone, according to the method of Pate and Yaffé[48]. They were supported by thin flat aluminium rings about 1" in diameter. From information in reference (48), it could be inferred that their thicknesses were

10-20 $\mu g./cm^2$. They were coated with gold on one side of about 5 $\mu g./cm^2$ in an evaporator to make them conducting. The central portion of the film was made hydrophilic by application of a thin coating of insulin (by evaporation of a dilute solution). After the active solution had been weighed out on the film, it was evaporated under an infra-red lamp to produce a dry, thin, evenly spread active source. The source was then transferred to a 4π beta counter. The filler gas used was a dry, oxygen free mixture of 90% argon and 10% methane. The counter was operated as a proportional counter at 1400 volts. Four sources were made and the films interchanged in the counter. This avoided the catastrophe of a single source breaking. The sources were found to be of constant radioactive concentration. The 4π and liquid counts were recorded by a print-out machine on punched tape in binary notation at half hourly intervals. These counts and times were fed directly into a programmed Elliot 803 computer as one of the data tapes. The programme produced a Bunney and Freiling plot[132] and calculated the slope and intercept on a least squares basis for both the 4π and liquid counts.

4.8.3. Preparation of carrier-free Ba^{140} and Bo^{99} solutions for absolute standardizations

Both Ba^{140} and Mo^{99} come to transient equilibrium with their shorter lived daughters, La^{140} and Tc^{99m}. Since it cannot be assumed that both parent and daughter activites count with an 100% efficiency in the 4π counter, in order to estimate their individual contributions to the counting rate, it is necessary to separate the parents and follow the growth of the daughters from the time of

separation. A complete parent separation makes the equations solvable. The results are drawn up in the form of the Bunney plot (see Section 4.8.4. below).

(a) Barium 140

A commercial carrier-free solution of Ba^{140} and La^{140} was bought from the Radiochemical Centre, Amersham. Many methods have been described in the literature for the separation of barium and lanthanum. The production of 4π sources requires that the activity be separated into an almost weightless solution of a reasonably volatile solvent which does not attack the film. The ion exchange methods of Perkins[49] and Farabee[50] fit the condition most easily. The former was chosen since the barium was eluted first from the column, whereas in the latter, a cation exchange method, all the lanthanum must first be eluted.

Perkins' method uses a filtration-precipitation technique on Dowex-1 anion exchange resin. A column, 4 x 200 mm., was first activated with 1N HCl and water in three alternate washings and then converted to the hydroxide form with 20 cc of 1N NaOH. The column was washed until the effluent was neutral to B.D.H. indicator paper. A drop of the concentrated active stock solution of Ba^{140} and La^{140} (as chlorides) was put on top of the column, and leached with water. The trifunctional $La(OH)_3$ was retained strongly by the column, while the Ba was eluted. (The La could be removed from the column by eluting with 6N HNO_3). The effectiveness of the separation was determined by pulse height analysis using a 3 inch flat-top NaI(Tl) crystal with a 100 channel pulse height analyzer. The spectra of Ba^{140} and La^{140} in equilibrium and of separated Ba^{140} are shown in Fig.22. The 0.8 and 1.6 MeV peaks of La^{140} prominent in the

FIGURE 22.

Gamma spectra of Ba^{140} and La^{140}

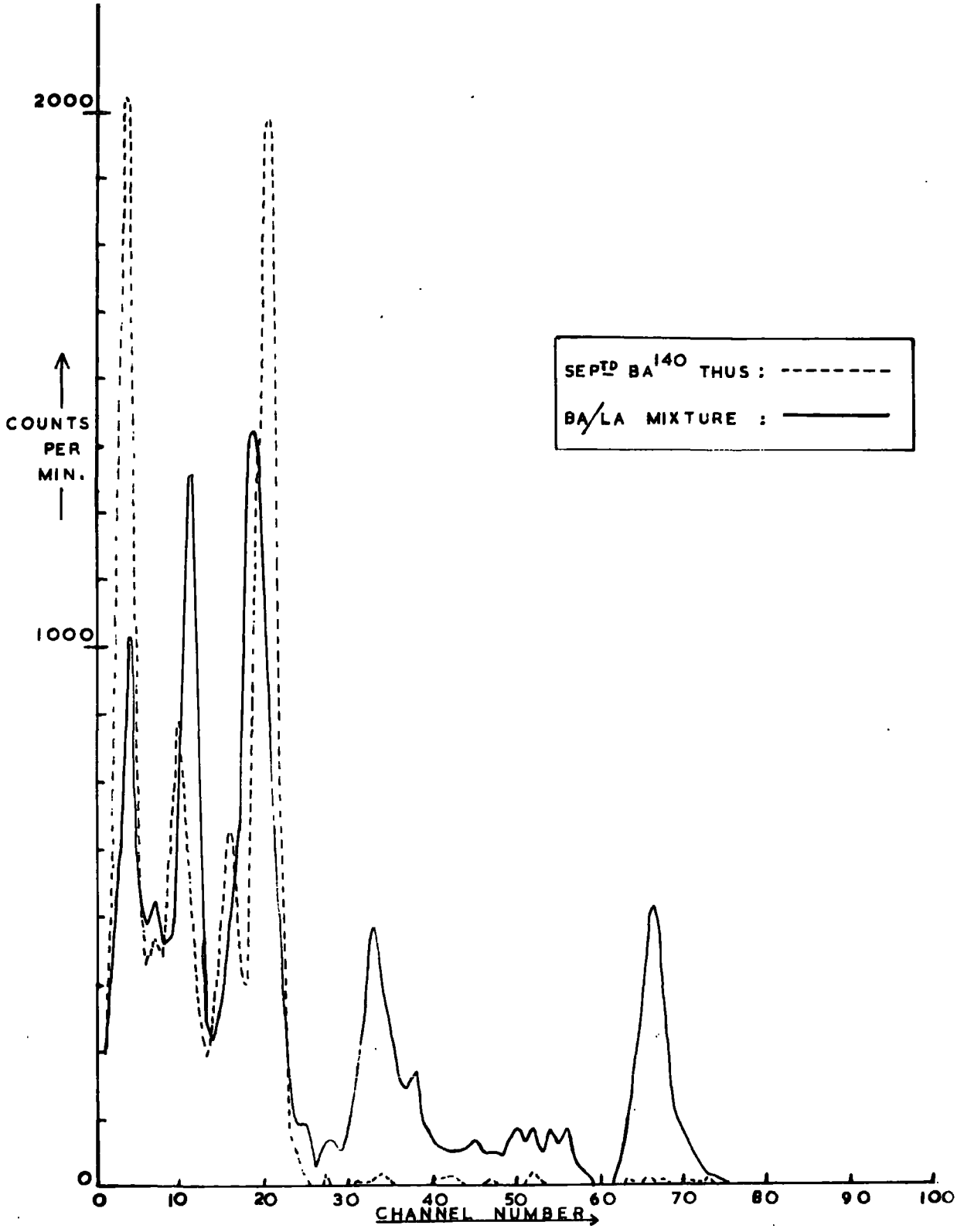
2000
1000
0
COUNTS PER MIN.
SEPTD BA140 THUS : --------
BA/LA MIXTURE : ——
0
10
20
30
40
50
60
70
80
90
100
CHANNEL NUMBER

mixed spectrum have disappeared to no more than background scatter in the Ba^{140} curve. (In fact, the separation is more than twice as good as the ratio of the count rates for the two curves at the La^{140} peaks, since the separated Ba^{140} curve should be normalized to its value in the mixture curve).

The drops of eluted Ba^{140} solution from the column were caught in a polythene capsule and from there sucked up into a polythene dropper bottle with a fine drawn-out neck. Four to six drops of this solution (around 50 mg.) were carefully weighed out onto the prepared 4π films and about one gramme was also weighed out into a 12 cc volumetric flask. The flask already contained Ba carrier, La carrier and HCl such that on making up to the mark with water, the carrier was 1 mg. per cc and the acid concentration 0.5N. A 10 cc aliquot of this solution was pipetted into the clean dry liquid counter and the top closed with a piece of polythene sheet to prevent evaporation. The 4π films, generally four in number, were dried under a lamp and they and the liquid counter were counted as described above.

(b) Molybdenum 99

Mo^{99} was produced by reactor irradiation at Harwell of Johnson Mathey 'Specpure' grade molybdenum trioxide. About 100 mg. of MoO_3 was sealed off in a silica tube for irradiation. A little Nb^{92} (10 day) will also be produced by $Mo^{92}(n, p)Nb^{92}$, which has an average cross section of about 6 mb.[18], and possibly a trace of Nb^{95} from Mo^{95}. The $Mo^{98}(n, \gamma)Mo^{99}$ reaction on the more abundant Mo^{98} isotope has a cross section of about 140 mb.[33]. The method of separation adopted for Mo^{99} from Tc^{99m} also left behind the niobium, however.

Various ion-exchange methods for the carrier-free separation of Mo and Tc have been described. Fisher and Meloche[51] and Boyd and Larson[52] have shown that MoO_4^- can be eluted from TcO_4^- on an anion resin in the ClO_4^- form with 2N NaOH, and Hall and Johns[53] used a very similar technique using a mixture of 0.5 N KOH and 0.5M potassium oxalate as the elutant. However, these elutants are not suitable for the preparation of 4π sources and although they could be altered by passage through a second, hydrogen-form, cation exchanger, it is simpler to use the oxide volatilization technique of Perrier and Segrè[55]. The irradiated MoO_3 was transferred to a silica tube containing a plug of silica wool and through which a slow stream of oxygen was passed. Heating the oxide at 400-500°C preferentially sublimed the Tc through the plug and down the tube into a water filled trap. The MoO_3 was then itself sublimed through the plug by strong heating at around 800°C, leaving behind any non-volatile impurities such as niobium. The section of tube containing the sublimed MoO_3 was cut out and dropped into a small beaker. A little dilute NH_4OH was added and the beaker warmed so that the oxide went into solution as ammonium molybdate and excess ammonia was driven off. A few drops of dilute HCl were added until the solution was just acid. It was found experimentally that if the solution were not acidified, the activity was not homogeneously distributed in the solution.

The Mo^{99} solution was then diluted with water until a few drops contained about 10^4 d.p.m., determined approximately by an end-window gas counter. The activity of the molybdate solution was great enough for this dilution to produce effectively weightless 4π sources. The 4π and liquid sources were prepared as for Ba^{140}, a little rhenium being added as a carrier for Tc in the liquid counter solution.

4.8.4. Bunney plots and liquid counter efficiencies

The Bunney and Freiling plot[132] is an effective method of following the decay of a parent-daughter pair and deriving counter efficiencies. Deviations from linearity in the plot indicate incorrect half-lives assumed or impurities present.

Let the suffix 1 refer to the parent, and the suffix 2 refer to the daughter; let λ be the decay constant; N the number of atoms and A the activity measured. Let the index zero refer to the initial quantities at the time of chemical apparation, t before measurement.

Then $A_1 = C_1 \lambda_1 N_1$ and $A_2 = C_2 \lambda_2 N_2$

where C_1 and C_2 are the respective counting efficiencies.

Hence total activity, A_T is given by

$$A_T = C_1 \lambda_1 N_1 + C_2 \lambda_2 N_2$$

and from the well known parent-daughter expression

$$A_T = C_1 \lambda_1 N_1^{\circ} e^{-\lambda_1 t} + C_2 \lambda_2 \left[\frac{\lambda_1}{\lambda_2 - \lambda_1} N_1^{\circ} (e^{-\lambda_1 t} - e^{-\lambda_2 t}) + N_2^{\circ} e^{-\lambda_2 t} \right]$$

$$\text{or, } A_T e^{\lambda_1 t} = N_1^{\circ} \left[C_1 \lambda_1 + C_2 \frac{\lambda_1 \lambda_2}{\lambda_2 - \lambda_1} \right] + e^{(\lambda_1 - \lambda_2)t} \left[C_2 \lambda_2 N_2^{\circ} - C_2 \frac{\lambda_1 \lambda_1 N_1^{\circ}}{\lambda_2 - \lambda_1} \right] \quad \text{——— (1)}$$

This is the basic equation; if now $A_T e^{\lambda_1 t}$ as ordinate is plotted against $e^{(\lambda_1 - \lambda_2)t}$, then the following holds:

$$\text{slope} = C_2 \lambda_2 \left[N_2^{\circ} - \frac{\lambda_1}{\lambda_2 - \lambda_1} N_1^{\circ} \right] \quad \text{——— (2)}$$

$$\text{intercept} = \lambda_1 N_1^{\circ} \left[C_1 + C_2 \frac{\lambda_2}{\lambda_2 - \lambda_1} \right] \quad \text{——— (3)}$$

Two plots were constructed, one for the 4π counts and one for the liquid counts. Let the indices 4π and L refer to these quantities respectively, and let $w^L/w^{4\pi}$ be the ratio of the source weights. Then we can write

$$\text{slope}^L/\text{slope}^{4\pi} = C_2^L w^L / C_2^{4\pi} w^{4\pi} \qquad (4)$$

$$\text{slope}^{4\pi}/\text{intercept}^{4\pi} = \frac{C_2^{4\pi} \lambda_2 N_2^\circ/\lambda_1 N_1^\circ - C_2^4 \lambda_2/(\lambda_2-\lambda_1)}{C_1^{4\pi} + C_2^{4\pi}\lambda_2/(\lambda_2-\lambda_1)} \qquad (5)$$

$$\text{intercept}^L/\text{intercept}^{4\pi} = \left[\frac{C_1^L + C_2^L \lambda_2/(\lambda_2-\lambda_1)}{C_1^{4\pi} + C_2^{4\pi}\lambda_2/(\lambda_2-\lambda_1)}\right] \cdot \frac{w^L}{w^{4\pi}} \qquad (6)$$

For either the 4π of liquid counter equations, it will be seen that there are four unknowns; N_1°, N_2°, C_1 and C_2, with only two independent equations. Because the initial separation of parent and daughter was complete one can say $N_2^\circ = 0$. To solve, either the parent or daughter efficiencies must be assumed to the unity (for the 4π counts).

Note also that

$$\text{slope} + \text{intercept} = C_1 \lambda_1 N_1^\circ \qquad (7)$$

This may be produced by substitution of $t = 0$ in Equation (1), or re-arrangement of Equation (5). Knowing both $C_1^{4\pi}$ and $C_2^{4\pi}$ it is possible to derive C_1^L and C_2^L from Equations (4) and (6). In fact, counting of the liquid counter when equilibrium has been re-established enables N_1° to be determined for the parent from $C_1^L + C_2^L\left(\frac{\lambda_2}{\lambda_2-\lambda_1}\right)$, [from Equation (6)]. C_1^L and C_2^L are derived separately below, however.

FIGURE 23.

(a) Bunney plot of Mo^{99} and Tc^{99m}

(b) Decay of separated Mo^{99}

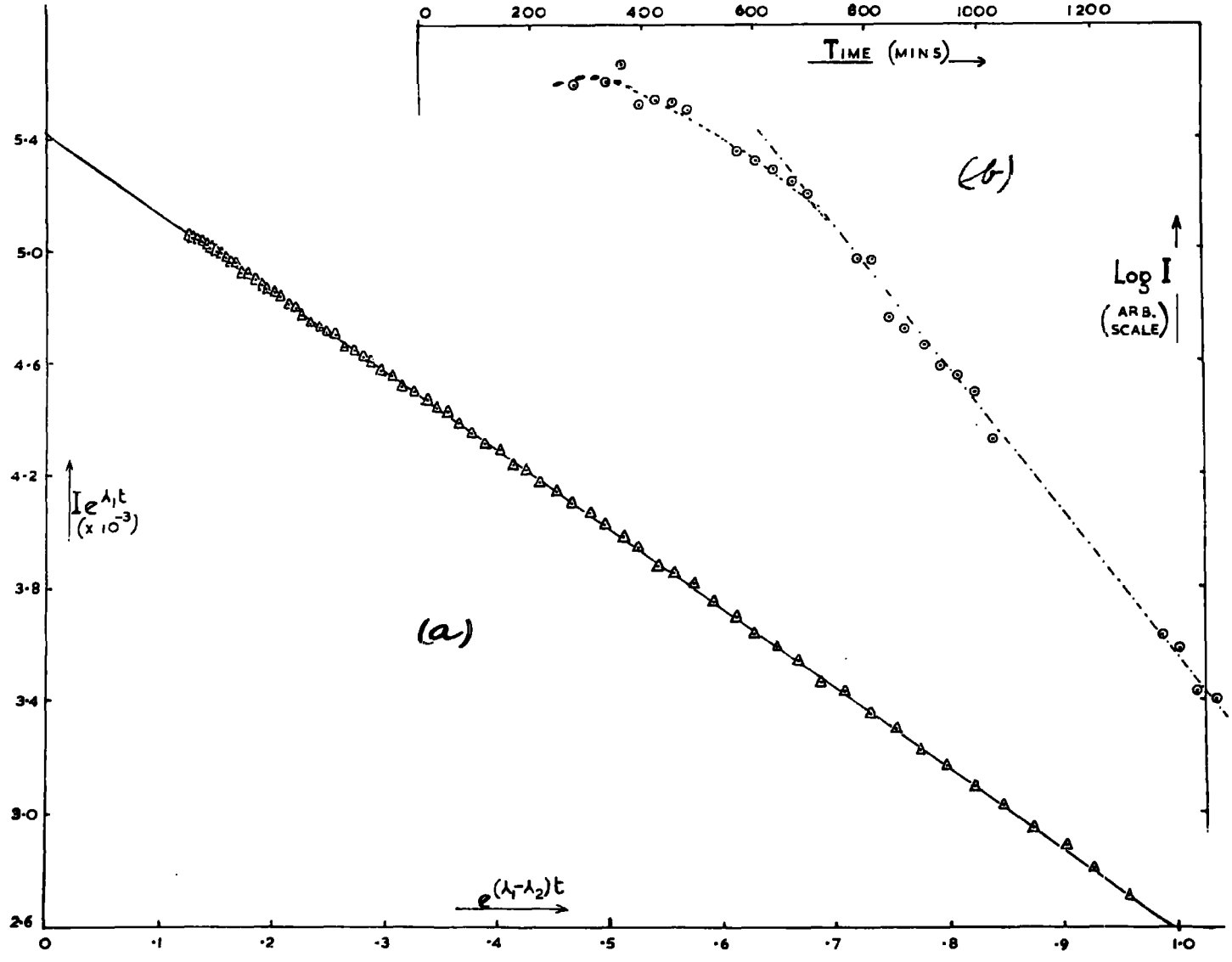
0
200
400
600
800
1000
1200
TIME (MINS)
(b)
Log I
(ARB. SCALE)
5·4
5·0
4·6
4·2
3·8
3·4
3·0
2·6
$Ie^{\lambda_1 t}$
(x 10^{-3})
(a)
$e^{(\lambda_1-\lambda_2)t}$
0
·1
·2
·3
·4
·5
·6
·7
·8
·9
1·0

Shown in Fig. 23(a) is the Bunney plot for Mo^{99} and Tc^{99m}. The computer programme produced the following slopes and intercepts on a 'least squares' basis:

$$\text{Slope}^{4\pi} = -1518 \; ; \qquad \text{Slope}^{L} = -185$$
$$\text{Intercept}^{4\pi} = 11,847 \; ; \qquad \text{Intercept}^{L} = 10,523$$

Assume $C_1^{4\pi} = 1$ and $N_2^{o} = 0$

Then $\lambda_1 N_1^{o} = 10,329$ [from Equation (7)]

Now $\dfrac{\lambda_2}{\lambda_2 - \lambda_1} = 1.100$

Hence $C_2^{4\pi} = 1518/10,329 \times 1.10 = 0.1336$, or 13.36%.

From Equation (4), $C_2^{L} = 0.005125$, or 0.051%

and from Equation (6), $C_1^{L} = 0.0315$, or 3.15%

Two points worth noticing here are: firstly, that Tc^{99m} contributes very little to the liquid counter rate, and secondly, that it has a low 4π efficiency also, due to the extremely low energy of the conversion electrons (1.8 kev). This latter point is demonstrated in Fig. 23(b) which shows the growth in the separated Mo^{99} in the 4π counter.

A second molybdenum trioxide sample was irradiated and the counter calibration repeated. The value of C_1^{L} obtained was 3.14%, in excellent agreement with the first (3.15%).

The corresponding values from the Ba^{140} and La^{140} plots were:-

$$C_1^{L} = 1.06\% \quad (Ba^{140})$$
$$C_2^{L} = 5.20\% \quad (La^{140})$$

In connection with the sensitivity of the Bunney plot to impurities, in an initial calibration, a deviation from linearity was tracked down to the presence of about 1% Sr^{89} in the commercially supplied Ba^{140} solution.

4.8.5. Determination of the paralysis time of the liquid counter

The initial Bunney and Freiling plot for Ba^{140}/La^{140} was not linear as mentioned above. Among the possible causes of non-linearity was numbered an incorrect paralysis or dead-time for the counter. The electronic quench on the probe unit was set at 500 μsec., but it was thought worthwhile investigating this value; an example shows how quite large errors may arise. At a count rate of 10^4 c.p.m., assumption of a 500 μsec. dead time instead of the experimentally determined value of 420 μsec. leads to an error of 1.5% in the count rate.

The method, due to Martin[55], relies on an accurate knowledge of the decay constant of an active source.

If I be the correct count rate,
and A be the observed count rate,
and T the actual dead time, then

$$I(1 - AT) = A$$

also $$I = Ioe^{-\lambda t}$$

so $$A/(1 - AT) = Ioe^{-\lambda t}$$

or $$Ae^{\lambda t} = Io - IoAT \qquad (8)$$

If $Ae^{\lambda t}$ be plotted against A, the slope will be -IoT and the intercept Io, from which T may be calculated.

FIGURE 24.

Plot for the determination of the paralysis time of the liquid counter arrangement

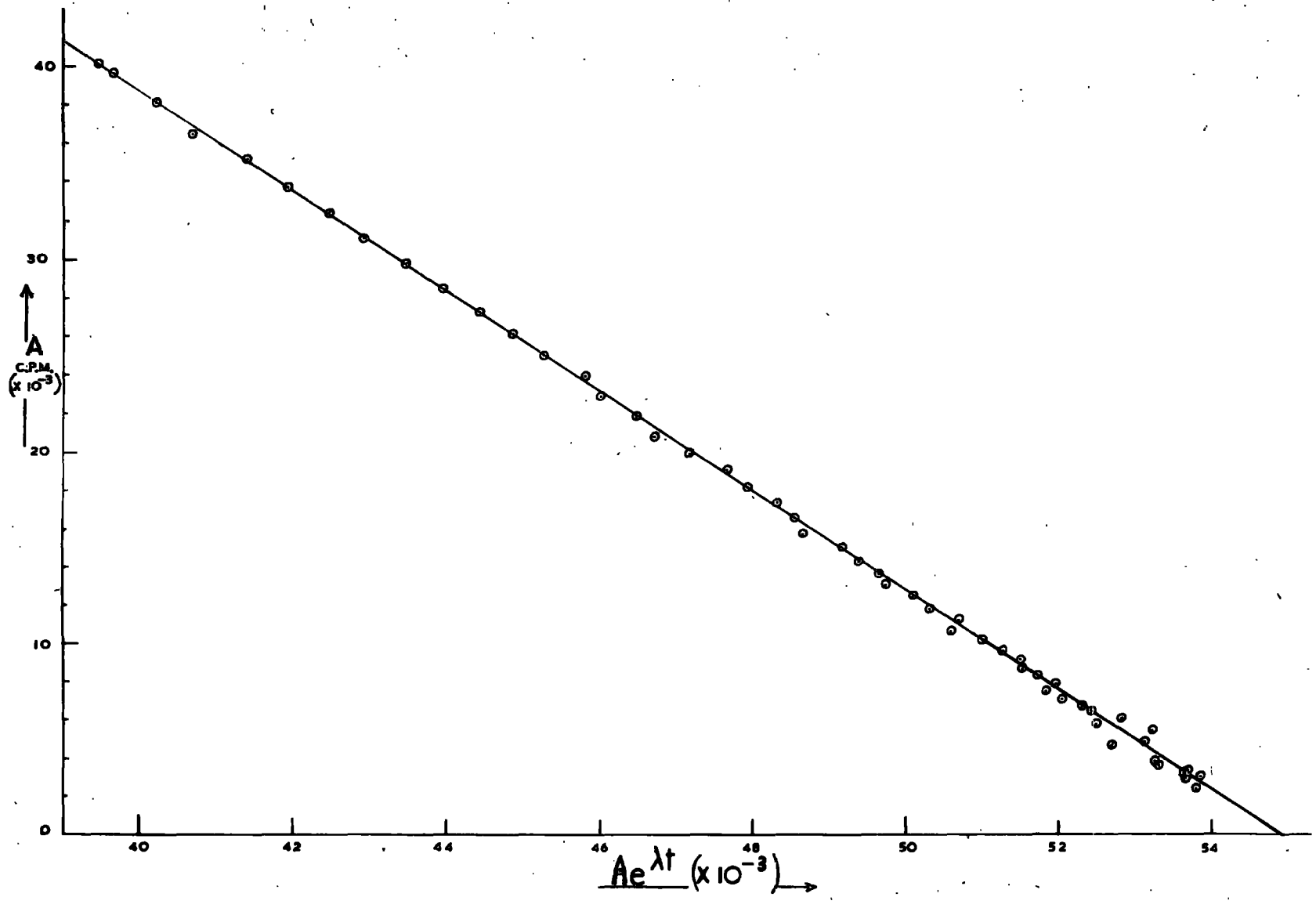
40
30
20
10
0
A
C.P.M.
(x 10^-3)
40
42
44
46
48
50
52
54
Ae^λt (x 10^-3)

Pure iron granules were irradiated with 14 Mev neutrons from the $H^3(d, n)$ reaction, using a Cockcroft-Walton accelerator. The iron was dissolved and transferred to the liquid Geiger counter, the initial activity being about 4×10^4 c.p.m. The plot of the equation above is shown in Fig. 24. From the slope and intercept, the dead time was calculated to be 420 μsec. The linearity of the plot is in agreement with the assumed value of 2.576 hours for the half life of Mn^{56}.

All liquid counting was done with the same equipment and settings.

4.9. Chemical yields in the fission product separations

(a) Molybdenum

Molybdenum can be conveniently determined gravimetrically as the 8-hydroxyquinolinate, often called oxinate, of formula $MoO_2(C_9H_6ON)_2$. Trial precipitations on the carrier solution of ammonium molybdate gave results in excellent agreement with the amount present by weight. The separated molybdenum solution after counting was returned to the 12 cc volumetric flask and duplicate analysis performed on two 5 cc aliquots.

The following procedure was adopted from Wilson and Wilson[56].

(1) The solution was neutralized with dilute NH_4OH, 15 cc of 5% E.D.T.A. solution were added and buffered with 5 cc of acetic acid-ammonium acetate buffer to pH 5 - 6.

(2) It was diluted to 80 cc, boiled and excess 3% alcoholic oxine reagent was added. After several minutes hot digestion, the precipitate was filtered hot and washed with hot water

until the washings were colourless. (A grade 4 sintered glass filter was used).

(3) The precipitate was dried at 80°C for 30 mins. cooled in a dessicator, and weighed to constant weight.

The precipitate contains 23.07% Mo.

The chemical yields found for the three runs were:

$$\left.\begin{array}{lll} B3 & = & 34.14 \\ B4 & = & 10.40 \\ B5 & = & 15.57 \end{array}\right\} \%$$

These yields were surprisingly low and indicated an incomplete precipitation somewhere in the procedure. However, the oxinate precipitation had the advantage of a large ratio of precipitate to molybdenum, so that satisfactorily heavy precipitates were obtained from the 50 mg. of Mo carrier originally added.

(b) Barium

The method of obtaining the chemical yield of barium originally devized entailed the use of tracer Ba^{133}, but it was found difficult to count the low energy γ spectrum of Ba^{133} unambiguously from that of Ba^{140} and La^{140}.

Having decided on a chemical method, some attention was given to the volumetric method for barium devized by Pribil[57]. This relied on a back titration of E.D.T.A. with magnesium using metalphalein indicator screened with methyl red and diazine green dye. This method was found to be excellent for mg. quantities of barium, but unfortunately fails in the presence of lanthanum. (The lanthanum was present in the liquid counter solution as carrier for La^{140}).

The method adopted for two of the three runs was a volumetric determination of homogeneously precipitated $BaSO_4$. $BaSO_4$ has a weight of only 1.7 times its barium content in contrast to the molybdenum oxinate precipitate where the ratio is 4.3. The precipitate would have been difficult to weigh accurately and $BaSO_4$ is prone to co-precipitate impurities from solution. The procedure chosen for the two runs B4 and B5 was based on that of Belcher et al.[58]. The barium was precipitated homogeneously with sulphamic acid according to Wagner[59] (based on Willard's work[60]), filtered off, washed free of La^{3+} and dissolved in excess ammoniacal E.D.T.A. The excess was determined with a magnesium back titration using eriochrome black indicator[61]. The $BaSO_4$ precipitate was washed with a saturated $BaSO_4$ solution to avoid loss of precipitate. Run B3 was known to have a lower chemical yield of barium from the count rate of the solution; unfortunately, spillage had occurred during the separation. Rather unnecessarily perhaps, a separate method was used to obtain the chemical yield. Rather than separate the barium from the lanthanum by precipitation, a differential complexometric titration method was adopted. Lanthanum was titrated at pH 7.0 with E.D.T.A. using eriochrome black according to the method of Lyle and Rahman[62]. The pH was then raised to 10.5 by an ammonia-ammonium chloride buffer and the barium titrated. This was done by addition of excess E.D.T.A. and back titration with magnesium solution as before.

The yields obtained were:

B3 = 15.7 }
B4 = 41.8 } %
B5 = 53.0 }

The yield of B3 was low since spillage had occurred; the yields of B4 and B5 are rather low because the barium procedure was probably unnecessarily lengthy and complex.

4.10. Estimation of uranium and boron

The mixed uranium-boron solution irradiated was made up by weight. Separate uranium and boron solutions were also made up and analysed to see if they conformed to the stoichimetric formulae and purities quoted. This was especially relevant in the case of $UO_2(NO_3)_2.6H_2O$ where loss of water of crystallization might have occurred.

(i) Determination of uranium

This was precipitated as the oxine according to the method of Wilson and Wilson[63]. The conditions were essentially the same as those used in the gravimetric determination of molybdenum. The gravimetric result was 99.8% of the stoichimetric weight. Within experimental error, it was therefore assumed that the uranium content was in accordance with the stoichimetry.

(ii) Determination of boron

The boron was present with the uranium as boric acid. It was estimated, in a separate solution, by titration with alkali in the presence of Mannitol according to the method of Kolthoff and Sandell[64]. The result confirmed the stoichimetry.

4.11. Calculation of fission yields

4.11.1. Values of parameters assumed

(a) Boron

Boron has an isotopic ratio, B^{10}/B^{11}, which is known to vary slightly according to the origin of the sample. Until fairly

recently, the American value on Brookhaven-Argonne boron was 755 barns for the thermal (n, α) cross section. This is the figure quoted in Sher and Moore[65] and Allen[66]. The latter gives the value for Harwell boron as 765 b. The work of the former authors[65] indicated, however, a value of 762 ± 3 for American boron corresponding to a B^{10} abundance of 19.8%. Prosdocimi and Deruyther[123] recently re-determined the cross section as 760.5 ± 2 b. The value assumed in this work is 760 barns.

(b) Uranium

The isotopic abundance of U^{235} in natural uranium was taken as 0.7204% from Bigham's paper at the 2nd Geneva Conference[67]. The thermal fission cross section for U^{235} was taken as 585 b. This is the 'world average' value from the 1st Geneva Conference. Hughes[68] quoted a value of 582 ± 10 more recently.

The results for the fission yields are dependent on the ratio $\sigma[U^{235}(n, f)] / \sigma[B^{10}(n, \alpha)]$ which was here assumed to be 585/760 or 0.770. (This is in close agreement with the value of 0.773 used by Yaffé et al.[42]).

4.11.2. Concentration of uranium and boron in the irradiated solution

The concentrations of boron and uranium required were roughly calculated on the basis of a thermal neutron flux of 10^{9} ncm^{-2}sec^{-1}, and the requirement that about 10^{-6} cc of helium should be produced together with 10^{3} d.p.s. of the fission products. The boron was actually about one third molar boric acid and the uranium about one quarter molar uranyl nitrate hexahydrate.

4.11.3. Calculation of fission yields

Ignoring any finite life time of the precursors of Mo^{99} and Ba^{140}, let Φ be the flux density ($n/cm^2/sec$), and T be the time of irradiation.

Then N_B, σ_B; N_U, σ_U; and N_{He} have the obvious significance; let the subscripts 1 and 2 refer to parent and daughter respectively, and let Y be the fission yield and Θ the chemical yield. Let $I_1^o = \lambda_1 N_1^o$ be the parent activity of the fission nuclide at the end of the irradiation.

$$\text{Then } N_{He} = N_B \sigma_B \Phi T \qquad \text{——————(9)}$$

$$\text{and } I_1^o = \lambda N_1^o = N_U \sigma_U \Phi (1 - e^{-\lambda_1 T}) Y \qquad \text{——————(10)}$$

The parent was separated after t_1 from the end of the irradiation and allowed to grow into equilibrium and counted after an interval t_2. The parent activity after separation, I_1^s, will be

$$I_1^s = N_U \sigma_U \Phi (1 - e^{-\lambda_1 T}) Y \Theta e^{-\lambda_1 t_1} \qquad \text{——————(11)}$$

After equilibrium has been established, the observed count rate A will be

$$A = I_1^s c_1 e^{-\lambda_1 t_2} + I_1^s \frac{c_2 \lambda_2}{(\lambda_2 - \lambda_1)} (e^{-\lambda_1 t_2} - e^{-\lambda_2 t_2}) + I_2^s c_2 e^{-\lambda_2 t_2}$$

from the treatment given previously, where I_2^s represents any daughter not completely removed by the separation.

Then at transient equilibrium one can say

$$A = I_1^s \left(c_1 + \frac{c_2 \lambda_2}{(\lambda_2 - \lambda_1)}\right) e^{-\lambda_1 t_2} \qquad \text{——————(12)}$$

since $e^{-\lambda_2 t_2}$ is negligible. Then from Equation (11)

$$N_U \sigma_U \phi (1 - e^{-\lambda_1 T}) Y \theta e^{-\lambda_1 t_1} = A/(c_1 + \frac{c_2 \lambda_2}{(\lambda_2 - \lambda_1)}) e^{-\lambda_1 t_2}$$

$$\text{or} \quad Y = A/(c_1 + \frac{c_2 \lambda_2}{(\lambda_2 - \lambda_1)}) e^{-\lambda_1 (t_1 + t_2)} (1 - e^{-\lambda_1 T}) N_U \sigma_U \theta$$

Substituting from (9), one obtains

$$Y = A N_B \sigma_B T / N_U \sigma_U \theta (c_1 + \frac{c_2 \lambda_2}{(\lambda_2 - \lambda_1)})(1 - e^{-\lambda_1 T})(e^{-\lambda_1 (t_1 + t_2)}) \quad \text{---(13)}$$

The last term of the denominator may be written $e^{-\lambda_1 t}$ where $t = (t_1 + t_2)$ is the total time from the end of irradiation to counting; thus the time of separation is immaterial if counting is done at equilibrium.

4.11.4. Results

From Equation (13) the following values were derived:

Run	Y for Mo^{99}(%)	Y for Ba^{140}(%)
B3	5.87	5.75
B4	6.01	5.88
B5	5.93	5.98
Average	5.94	5.87

It is instructive to compare these results with the absolute values obtained by other workers.

(a) Mo^{99} - 5.94%

This result is in excellent agreement with previous measurements. In Katcoff's[46] 1960 compilation of fission yields for thermal neutron fission of U^{235}, the value given is 6.06%. This

is an average of the radiochemical results of Terrell et al.[70] of 6.14 ± 0.15% and the radiochemical results of Reed and Turkevitch[69] of 5.98%. The latter workers derived an absolute value of 5.91% for Mo^{99} but then normalized this in the light of relative values to an absolute Sr^{89} yield, which they considered to have a higher accuracy. The discrepancy between this mean value of 6.06% and the result here reported is only a percentage difference of 2.0 which is well within experimental errors.

Errors

The errors involved in the result are:

(a) liquid counter rate 1.0%

(b) helium analysis 1.0%

(c) 4π calibration 1.0%

(d) chemical yield 1.2%

(error of mean in duplicate analysis)

Further errors associated with the result are:

(e) the value of the ratio σ_U/σ_B

(f) decay corrections based on slightly incorrect half lives

(g) systematic errors in the 4π calibration.

The errors (e), (f) and (g) are systematic errors difficult to estimate and are ignored. (c) is an estimate based on statistics and possible loss of counting efficiency.

Treating errors (a) to (d) as standard errors, the total error becomes 2.1%, with possible additional systematic errors. Hence the final yield value of Mo^{99} is (5.94 ± 0.13)%.

(b) Ba^{140} - 5.87%

This result is rather lower than previous values which average around 6.3%:

Reed and Turkevitch[69], 1953	6.35%
Yaffe et al.[42], 1954	6.32 ± 0.24%
Petruska et al.[43], 1955	6.33 ± 0.31%
Santry and Yaffe[71], 1960	6.36 ± 0.12%
Ferrar and Tomlinson[72], 1962	6.25%.

Petruska's value was for Ce^{140}, but the yield will be virtually identical to that of Ba^{140} since the independent yields of nuclides near the end of the β^- chain are negligible. For example, Grummit and Milton[122] found the independent yield of La^{140} to be 4.5×10^{-3}%.

The errors involved are similar to those discussed for Mo^{99}, except that each chemical yield consisted of one determination only and also the accuracy of the method was lower. Assessing the error of the yield determination at 3% (including the determination of the inactive carrier by the same method) and proceeding as before, the final value for Ba^{140} is (5.87 ± 0.21)%.

Although this is lower than the results quoted above, taking into account the standard errors and possible systematic errors, the discrepancy is not large. In view of the Mo^{99} result, it would seem most likely that some systematic error due to (g) was present. Loss of efficiency in the 4π counter would make the liquid counter efficiency too large and so lower the final yield value for Ba^{140}.

Comment

The accuracy of the results is at least comparable to that of mass spectrometric values. The triplicate determinations have a standard error of the mean of 1.2% for Mo^{99} and 1.9% for Ba^{140}, showing that the standard errors quoted are realistic. These results, particularly for Mo^{99}, and where previous values were somewhat scanty, may be fairly said to add to our knowledge of absolute yield values.

SECTION 5.

ABSOLUTE STANDARDIZATION OF PHOTONEUTRON SOURCES

5.1. Introduction

5.1.1. General

The problems of absolute neutron source standardization have been reviewed by Wattenberg[87]; since then the status of absolute comparisons has been described by Hughes[88] (1954), Richmond and Gardner[89] and Larsson[90] in 1958, and Axton[91] in 1961. The latter noted the great strides that have been made towards uniformity in the last decade; ten sources from various national laboratories now have a spread of 3.8%, or about 2% variation about a 'world average' value, compared with a previous spread of 10%. Many workers now claim an accuracy of 1 or $1\frac{1}{2}$% in their absolute calibrations but additional systematic errors must be present.

The photoneutron sources under consideration in the present work were set up as a standard in 1954, following the Oxford Conference on Neutron Standardization. One method of measurement was proposed by a helium technique by Martin and Martin[92]. At that time absolutely calibrated sources had a spread of about 10%[88]. It was proposed that after various standardizations and intercalibrations by other methods had been performed, some of the sources would be destructively analysed for their helium content. This associated particle technique should give a standardization accurate to about 1%. The present account describes the authors' attempt at these measurements.

Before discussing the photoneutron sources further, a

brief background to neutron source measurements is given.

5.1.2. Neutron sources in general

Three main types of neutron source are in general use as standards:-

(1) Photoneutron sources, (γ, n), using the photodisintegration of the beryllium nucleus or occasionally, the deuterium nucleus, (the Oxford Source).

(2) (α, n) sources, usually in the form of mixtures of radium and beryllium (Ra - α - Be), or sometimes as the compound $RaBeF_4$, or some other alpha emitter with beryllium.

(3) Spontaneous fission sources such as Pu^{240} or Cm^{244}.

Halban[93] has described the properties of the ideal neutron source as follows:-

(a) it should have a constant emission rate, or its intensity should change in a known manner with time;

(b) it should be reproducible, that is, two sources prepared by different workers should have the same output;

(c) accurate standardization procedures should be available;

(d) the neutron energy spectrum should be such that the output can be readily compared with the outputs of different types of source;

(e) it should be a low absorber of thermal neutrons (for intercomparisons and experimental uses);

(f) it should be easily transportable and small in size for a reasonable output;

(g) any associated radiation (e.g. γ rays) should not interfere with its uses as a neutron source.

Of course, these are counsels of perfection; in practice, each type has its disadvantages. Consideration (c) is frequently in conflict with some of the more practicable aspects.

Type (1) sources have the advantage of being slightly easier to calibrate absolutely by thermalization techniques than sources of type (2) since at lower neutron energies fast neutron absorption and fast neutron escape is minimized; on the other hand the sources are bulkier and self-absorption is more important. Also, their bulk, low output and high γ background are serious disadvantages.

Type (2) sources have a high output for a small size, are fairly reproducible, and have a more useful energy spectrum. On the other hand their outputs are not constant due to the growth of α-emitting polonium in the radium, though other α-emitters like Am^{241} are now coming more into use.

Type (3) sources have the advantage of a useful energy spectrum, since for many experiments a fission spectrum is required. They suffer from a low output and are difficult to calibrate absolutely. Their uses and calibration have been described by Richmond and Gardner[89].

5.1.3. Neutron source calibration

In order to give the proposed helium method in its context, a short summary of common standardization techniques is here included. Three general methods are possible:

(1) direct determination of the fast neutron output;

(2) measurement of the thermalized neutrons;

(3) the associated particle technique.

Method (1) has never been reported according to Larsson[90], and there is little hope of success, especially in view of the very mixed spectra of most sources. Method (2) has been the most popular, and there are several variations in the method of measuring the thermal neutron density set up by the source in an extended moderator. The main difficulty of this method is that the results are dependent on cross section values. Two main sub-groups may be distinguished;

(a) those using 'mechanical' integration of the neutron density, and

(b) those using 'physical' integration.

There are some other variations of method (2) which we class as group (c).

(a) 'Mechanical' integration simply consists in suspending the source in the middle of a large moderator, (often of oil, water or H_3BO_3 solution) and measuring the radial neutron density with the aid of gold foils or small BF_3 counters or some such detector. The source strength is obtained from absolute counting of foils, or the number of $B^{10}(n,\alpha)Li^7$ reactions or some combination of these methods.

(b) 'Physical' integration is performed automatically by the moderator solution, which usually consists of $MnSO_4$ solution. After irradiation to saturation, the solution is stirred and its activity measured, often with a dip counter. A separate sample of active Mn^{56} solution is counted absolutely (by $4\pi\beta$ or coincidence counting) and added to the tank to calibrate the dip counter.

Both methods (a) and (b) have numerous corrections; for example, for leakage of fast neutrons, self absorption by the source, fast neutron absorption in the moderator, deviations from the 1/v law of the detector, resonance absorption in the foils and foil depression effects [for method (a)].

Typical of method (a) are the publications of DeJuren et al.[94], 1955; or Larsson[95], 1954. Method (b) is exemplified by DeJuren and Chin[96], 1955; Richmond and Gardner[89] in 1957; Bezotosnij and Zamyatnin[97] in 1958; Axton and Cross[98] in 1961 and Noyce et al.[99] in 1963.

These authors[98] measured the outputs of the photo-neutron sources under consideration by method (2)(b) and quote a standard error of $\pm$ 1%, with the possibility of an additional systematic error of up to 1% associated with $4\pi\beta$ counting.

An improvement on the method of Axton and Cross was adopted by Noyce et al.[90]. They calibrated the N.B.S.-I(γ, n) source by comparing its output with that of a Sb-Be(γ, n) source in a $MnSO_4$ tank; the Sb-Be source was then determined absolutely in a heavy water (deuterium) solution of $MnSO_4$, which largely removes the effect of the large hydrogen absorption cross section on the absolute measurement. The dip counter used to measure the Mn^{56} activity was calibrated with an active Mn^{56} solution standardized by $4\pi\beta$-γ coincidence counting, again an improvement on Axton and Cross' $4\pi\beta$ counting. The reason why a Sb-Be(γ, n) source must be used with the deuterium bath is that the γ rays from the Ra-Be source are above the threshold for the photo-disintegration of the deuterium nucleus. The overall uncertainty was 1.1%.

(c) A further variation of the thermalization technique is the use of a large graphite stack or thermal column attached to a reactor. (Erzolimsky and Spivak[100] and Spivak et al. quoted in Larsson[90]).

Method (3), the associated particle technique is a very attractive one in principle though it has received far less attention than method (2). The basis of the method is to detect the other product of the neutron producing reaction, not to measure the neutrons themselves.

This may take the form of counting charged hydrogen or helium nucleii associated with reactions such as $T(d,n)He^4$, $T(p,n)He^3$, $D(d,n)He^3$ or $D(\gamma,n)H$. Florov and Poretskii[101] in 1951 and Larsson[102] in 1955 have described standardizations based on the $T(d,n)He^4$ reaction, while the Oxford Rd-Th(γ,n)H source was standardized by absolute counting of photoprotons associated with the $D(\gamma,n)H$ reaction by Marin et al.[103] in 1954. The $F^{19}(\alpha,n)Na^{22}$ reaction has also received some attention. Geiger[104] in 1959 was able to calibrate a Po^{210}-α-F^{19} source by coincidence counting of the anihilation quanta following positron emission from the Na^{22}. The difficulty is to discriminate against γ rays from the α-emitter, and this is why the short lived Po^{210} had to be adopted.

Proposals using this reaction, but based on the measurement of the Ne^{22} formed from the Na^{22} decay were made by Martin[105] in 1954).

This brings us to the actual method proposed for the measurement of the photoneutron sources. This is an associated particle technique in which He^4 is measured gas volumetrically by the apparatus described earlier in this work.

5.2. Photoneutron sources and the helium method

The method of determining neutron source strengths by a helium measurement was proposed by Glueckauf and Paneth[106] as long ago as 1937. They investigated the photodisintegration of

the beryllium nucleus:

$$Be^{9} + \gamma \longrightarrow Be^{8} + n$$
$$\downarrow$$
$$2He^{4}$$

Prior to their researches, the Be^{8} nucleus was an unknown quantity; they found that the helium produced in beryllium metal, together with other evidence, showed that Be^{8} decayed to $2He^{4}$ with a half life of less than a second. It is now known to have a half life of less than 4×10^{-15} seconds[107].

The photoneutron standard (Durham) is shown in Fig. 25, together with some other photoneutron sources previously alluded to. As already mentioned in the introduction, these are based on the proposals of Martin and Martin[92]. They pointed out that the exact correspondence of every two helium atoms measured to each neutron emitted implies the following:

(i) that each neutron produced is accompanied by two helium atoms, that is
   (a) Be^{8} has no stability,
   (b) no other (γ, α) or (γ, n) reactions are possible in the beryllium or its impurities;

(ii) that all the helium produced is retained in the metal until measurement.

(a) is clearly true[107] and (b) can be seen to be true by consideration of the energies of the γ rays from the radium preparation. The maximum γ energy from Ra and its daughters is 2.4 MeV, from Bi^{214} (RaC), and the only photoneutron reactions with thresholds below this are $Be^{9}(\gamma, n)2He^{4}$ at 1.57 MeV and $H^{2}(\gamma, n)H^{1}$ at 2.23 MeV. There is

FIGURE 25.

Types of (γ, n) sources

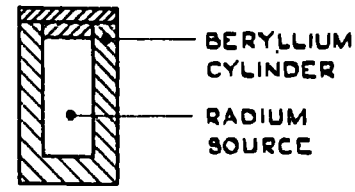

DURHAM

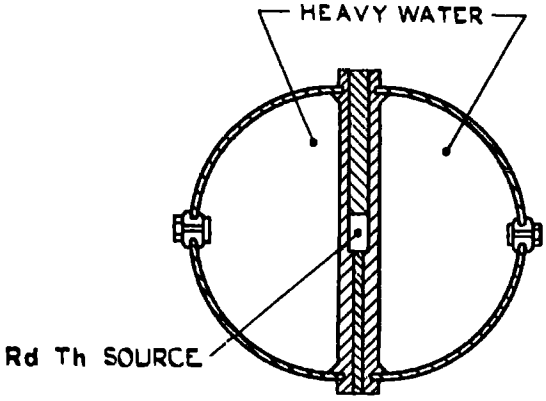

OXFORD

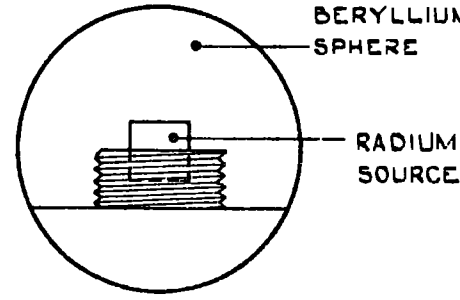

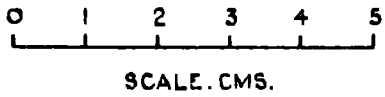

NATIONAL BUREAU
OF STANDARDS.

no deuterium present in cast beryllium. As regards (γ, n) reactions, $Be^9(\gamma, n)He^5 \longrightarrow He^4 + n$ is merely an alternative route to $Be^9(\gamma, n)2He^4$. All other likely impurities have thresholds much too high, e.g. $B^{10}(\gamma, \alpha)Li^6$ at 4.45 MeV.

As regards (ii) there are two points to consider. Firstly, the range of the alphas produced can be shown to be insignificant compared to the dimensions of the beryllium metal. Secondly, it has long been asserted that metals are helium tight at room temperature. Hemingway[11] has recently shown that beryllium and aluminium are indeed completely helium tight at room temperature, losing less than 2% of their helium only on prolonged heating just below their melting points.

There is one further possibility of error, namely, the chance that neutrons produced in the beryllium will react with it or with impurities. The effect of impurities can be dismissed immediately since their concentration in cast beryllium is small[12] and they would need gigantic cross sections to affect the neutron output. As regards reaction with the beryllium itself by (n, α) reaction, the $Be^9(\gamma, n)$ neutron spectrum is of low energy, lying mostly between 0 and 700 keV[124], and from information in Ref. (125) the reaction cross section will be of the order of a millibarn. This is completely negligible in the dimensions of the capsule

The beryllium used in the construction of the cylinders was cast beryllium which had been shown to be free from helium, according to Hall[12], quoting Reasbeck.

5.3. Description of the sources

One of the sources is shown in Fig. 25. The dimensions are about 1.5 cm. diameter by 2.5 cm. high with a wall, base and lid thickness of 0.4 cm. Their weight is around 6.5 g. The six sources are designated 4A, 4N, 3B, 3M, 2C and 2L. N, M and L are for helium measurement. The numbers refer to the radium source. This is a radium bromide preparation of about 400 mc. enclosed in a platinum case. This prevents any (α, n) reactions in the beryllium. However, there are some (α, n) reactions occurring in the source itself and its welded sheath. It was not quite exact above to consider only reactions in the cylinder as sources of, or losses of neutrons. Richmond and Gardner[89], following Eggler, have estimated this effect to contribute 2.5% of the total neutron output from the photoneutron source. This is also the figure that can be derived from the work of Axton and Cross[98], although it is not quite clear whether this was independently measured by them. The following table is taken from their publication and summarises the properties of the sources.

Source	M_{Ra} (g.)	M_{Be} (g.)	Φ (Direct) ($\times 10^{-4}$), n/sec.	Φ(Indirect) ($\times 10^{-4}$), n/sec.	Φ Total incl. α neutrons	$\frac{\text{n/sec.} \times 10^{-4}}{M_{Ra} \times M_{Be}}$
2C	0.3737	6.6572		1.621	1.664	6.52
3B	0.3769	6.3031	1.572		1.615	6.62
4A	0.3769	6.7456	1.671		1.714	6.57
2L	0.3737	6.8186		1.685	1.729	6.61
3M	0.3769	6.8179	1.699		1.743	6.61
4N	0.3769	6.8238		1.701	1.744	6.61

$\dot{\Phi}$(Direct) refers to the directly measured neutron emission from the beryllium; $\dot{\Phi}$(Indirect) is derived from comparative measurements previously made on the sources with BF_3 counters. $\dot{\Phi}$(Total) include the contribution of (α, n) produced neutrons in the radium source. The neutron emission rate derived from measurement of the helium in the beryllium will not of course include the (α, n) contribution from the radium source.

It is interesting to note that the last column, the output divided by the product of the mass of radium and mass of beryllium is constant except for source 2C. This would seem to indicate that a neutron source of this type could be made that would have a reasonably accurately known output without standardization, simply from its known dimensions.

5.4. Method of measurement

The main difficulty is the disproportion between the helium content (about 5×10^{-7} cc) and the size of the sample (about three quarters of a mole of beryllium).

Two main methods seem open.

(a) Vacuum fusion

This has the advantage of not requiring any oxygen flushing system as the evolved gas may be transferred by Toepler pump into the circulating system. On the other hand, it would be difficult to build a furnace system which, when held at above 1400°C for several hours, would not evolve or leak appreciable quantities of helium compared with the helium to be measured. Molten beryllium is also extremely corrosive to crucibles and a potential health hazard in a soft glass vacuum system. However, in the light of

experience of other methods, this system is worthy of reconsideration (see comments at end).

(b) Dissolution and removal of hydrogen

Stoichimetric reaction of the beryllium with acid will produce about 16 litres of hydrogen. A solvent is required which will dissolve the beryllium reasonably rapidly and with the minimum of hydrogen evolution. Some work by McNeil has been done on this problem[108], and she found that solutions of $HgCl_2$ in various alcohols and glycols would reduce the hydrogen evolution to about 15 - 40% of the possible. Unfortunately, reaction was slow and tended to tail-off or stop before completion. Saturated K_2CuCl_4 solution evolves about 40% of the possible hydrogen and dissolves beryllium reasonably rapidly. The metal becomes covered with copper and dissolution is irregular, though experience showed this was not too serious a drawback.

The problem remains of disposing of about 6 to 7 litres of hydrogen. Previous workers have burnt the hydrogen in a combustion vessel with pure oxygen, though the amounts of gas involved were much smaller. Hall[12] who studied the problem under consideration, devized a combustion procedure on a large scale. This required the use of large quantities of pure oxygen, for doing blanks, for flushing and for combustion. He constructed a special oxygen still, in which large quantities of oxygen were prepared immediately before use and which could not be stored.

He obtained an almost satisfactory helium blank on a piece of beryllium of 6.5 g., but found large quantities of neon came off after the helium (presumably from the oxygen), which introduced

some uncertainty into the helium fraction. Unfortunately, time did not permit him to pursue this point further.

The present author used a pilot-scale combustion plant for burning hydrogen and found the flame difficult to control and the process long and tedious.

In principle, the most simple and attractive method of hydrogen removal is to use a palladium diffuser or 'leak'. The main effort was concentrated in this direction. Numerous descriptions exist in the literature of such apparatuses, for example Davis[109], Katz et al.[110] and Lowell et al.[111]. The problem is to have a large enough surface area of the membrane to obtain an adequate diffusion rate at the fairly low pressure differences involved (up to one atmosphere).

A pilot scale apparatus was built with a $^1/_4$" diameter palladium-silver alloy tube heated at around 300°C. This was found capable of diffusion rates of up to one litre per hour of hydrogen at a pressure differential of about 50 - 60 cm. of mercury. The time factor is important since slow diffusion and leakage of helium is occurring in the apparatus continually, especially in sections where some heating of the glass walls occurs. The preliminary experiments indicated that the hydrogen associated with the dissolution of the beryllium could be removed by a $^1/_2$" diameter 'leak' in around three hours or less.

The question then arose of the permeability of silver-palladium alloy to helium. Paneth and Peters[112], in 1928, showed that palladium itself was impermeable to helium even at red heat, under large pressures of helium and helium-hydrogen mixtures. This

question had to be re-investigated for the alloy used, which has a greater permeability to hydrogen than pure palladium.

5.5. The diffusion apparatus

The $^1/_2$" diameter silver-palladium alloy thimble, P, (supplied by Johnson-Mathey), is shown in Fig. 26 with its ancillary apparatus. Unfortunately, a tube of this diameter could not be drawn and was constructed from welded sheet with a seam running up the length of the tube and a nickel top welded onto the end. The lower end was welded onto a supporting Nickel tube N (at the dotted line). This construction led to trouble through leaks in the welded seam.

A silica tube S which fitted snugly into the nickel tube and inside the leak P acted as a support for the walls of P to prevent collapse under large pressure differences. The tube N was hard soldered into two brass B.34 cones as shown. The upper cone fitted into a B.34 socket at the lower end of the glass high vacuum envelope which was connected to the dissolution vessel through tap T_5, the trap C, the non-return valve F and tap T_8. The upper brass cone was hollow and the water circulating in the cooling coil shown wrapped around the nickel tube also passed through the cone. The glass walls surrounding P were also water cooled with a jacket not shown in the figure. The lower brass cone fitted into a socket connected through tap T_6, the trap B and tap T_4 to the secondary pumping line, to remove the diffused hydrogen. The current entered through the sealed-in leads X, and passed through the nichrome heater element inside P. Heating was controlled through a variable A.C. voltage.

FIGURE 26.

Apparatus for the removal of hydrogen through a palladium membrane

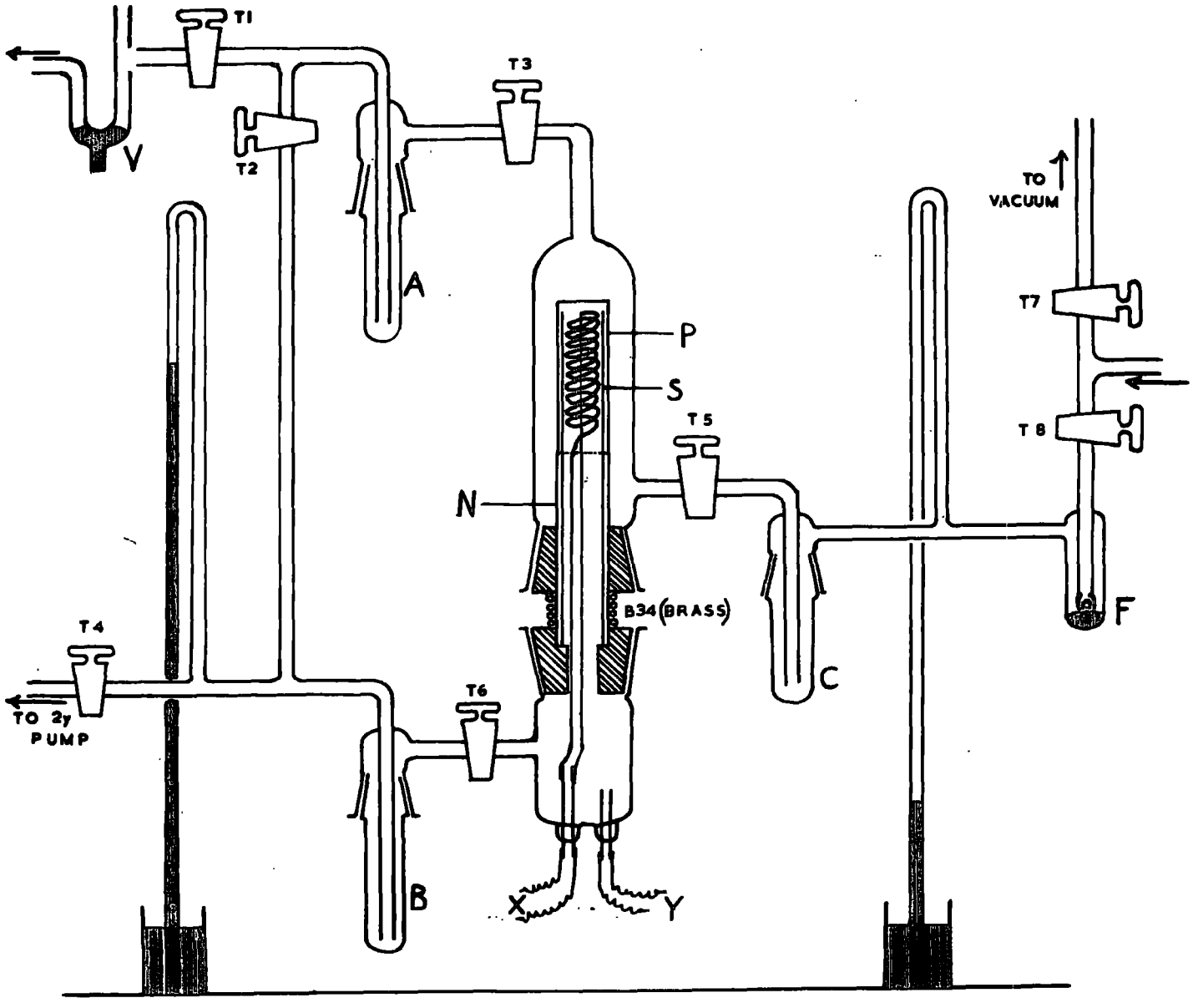
T1
T2
T3
T4
T5
T6
T7
T8
V
A
B
C
F
P
S
N
X
Y
B34 (BRASS)
TO VACUUM
TO 2y PUMP

The temperature of the thimble was measured by a thermocouple between S and P (not shown in the figure) connected to the leads Y. Traps A, B and C were built into the line around P as a precaution against the poisoning of the membrane by mercury vapour. The traps were always filled with liquid nitrogen before opening taps T_3, T_5 and T_6. Tap T_2 was an inter-connecting tap between the high pressure or hydrogen side and secondary side of the palladium tube; through it both sides could be evacuated or let down to air simultaneously. Two manometers served to monitor the hydrogen pressure on the fore and back sides of the thimble.

5.6. The dissolution flask

The dissolution of beryllium in saturated K_2CuCl_4 reagent, assuming the only reaction is the production of cuprous chloride, will require two moles of reagent for every mole of beryllium. Thus, an adequate excess of reagent, for $^3/_4$ of a mole of beryllium, (taking into account the 40% reaction with water to form H_2) will be provided by two moles of reagent. Its solubility is about 550 g. per litre so the flask should be capable of holding just under a litre of reagent solution.

The flask shown in Fig. 27 was of about $1^1/_4$ litres capacity and fitted with three necks, each mounting a B.24 socket. The thin shape was advantageous in obtaining a good flushing action by the oxygen, which passed down the tube in the flask after passing the bubbler B.

The taps T_7, T_8 and the non-return valve F were identical with those shown in Fig. 26. C was a cold trap of the finger type; this was better here than the internal seal type as the large amounts of

FIGURE 27.

The dissolution vessel for the beryllium source cylinders

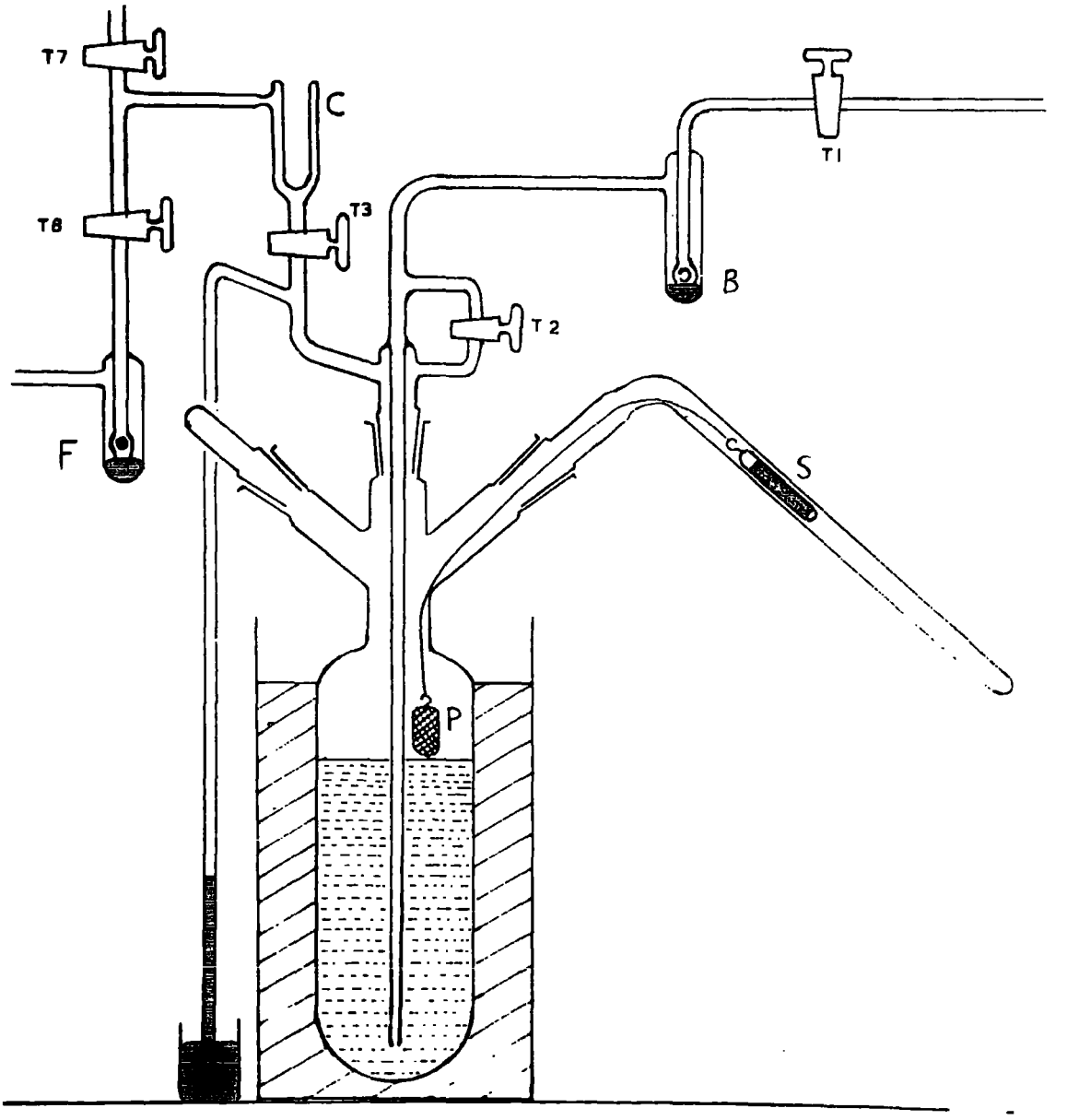
T7
C
T8
T3
T1
B
T2
F
S
P

water which condensed could be returned to the flask through tap T_3 after the finger had been allowed to warm up. P was a platinum gauze cage holding the sample for dissolution, and could be raised or lowered magnetically by movement of the slug S; when S was at its end position at the bottom of the tube, P was drawn up above the cone out of danger of splashing by the solvent during outgassing. The dissolution and flushing procedures were very similar to those previously described in the section on iron in Section 3. The large reagent and flask volume rendered more preliminary flushings necessary to achieve a satisfactory oxygen blank.

5.7. Operation of the diffusion and dissolution apparatus

After the reagent in the flask had been flushed out and a satisfactory oxygen blank obtained, a sample in the cage P was lowered into the reagent. When a hydrogen pressure of about 50 cm. was registered, the sample was withdrawn again. The flask was surrounded by a tank of water to prevent the walls from becoming warm. The hydrogen was then allowed to pass through taps T_3 and T_8 and the non-return valve F, into the previously evacuated palladium section. Taps T_3 and T_7 were kept shut and the traps were cooled in liquid nitrogen before the hydrogen was allowed to come into contact with the palladium thimble. The heater current was switched on and increased until the thermocouple registered about 300°C. The manometer connected to the 'outside' section of the palladium would begin to rise at this point indicating diffusion had begun. It was found that by allowing a small back pressure of hydrogen to accumulate (about 1 - 2 cm.) by not fully opening T_4 to the secondary pump, the rate of diffusion was materially increased. This was probably due to

much improved heat transfer between the filament and the thimble walls. The pressure of hydrogen inside the envelope surrounding the thimble was maintained at 50 - 60 cm. by re-immersing the sample and allowing the gas to pass through T_8, T_3 and F.

By adjustment of the fore and back pressures and the temperature, a diffusion rate of about 2 to $2^1/_2$ litres per hour could be achieved. The diffusion rate was found to be proportional to the square root of the pressure difference, (Ficks first law). The removal of the great bulk of the hydrogen from a $6^1/_2$ g. sample of beryllium (or its equivalent in magnesium as a test run) could be effected in around three hours, but the rate of hydrogen removal became slower as the pressure dropped and very tedious at small pressure differences. Also the limiting process tended to be the rate of dissolution of the last fragments of copper coated beryllium. In practice, therefore, diffusion was terminated when all the beryllium had dissolved and the hydrogen pressure had been reduced to about 2 cm.; this usually took about 4 to $4^1/_2$ hours.

What gas remained was then allowed to bubble into the circulating system through the ventil. The flask and palladium section were then flushed out nine times in the normal manner and the gas collected in the circulating system for helium analysis.

5.8. Experiments and results

(i) The apparatus was checked for helium tightness. A blank on the flask and palladium section of the apparatus was not greater than the normal irreducible minimum of 0.15×10^{-8} cc. The flask and trap were also allowed to stand for five hours unpumped and the helium found to have accumulated was negligible, (less than 0.05×10^{-8} cc).

(ii) In order to test the efficiency of the whole extraction process, a percentage recovery of helium experiment was devized as follows. A piece of magnesium of size sufficient to simulate the hydrogen production of 6.5 g. beryllium and of known or small helium content was dissolved in dilute sulphuric acid in the flask. Simultaneously, a small piece of beryllium disc of known helium content was dissolved to supply a known amount of helium. The hydrogen removal and helium flushing processes should lead to a 100% recovery of the helium added.

As regards the helium content of the magnesium used, small samples were dissolved in the iron sample apparatus (Section 3) to determine this. However, because of the hydrogen production, sample weights had to be restricted to less than 50 mg., and the small amount of helium found, relative to the oxygen blank, gave a large uncertainty in several grammes of magnesium. The result was around 3×10^{-8} cc per gramme. In comparison with the large amount of helium added this did not matter, and later results showed this figure to be too high.

The first percentage recovery experiment gave a result of 99% ($\pm$2%); the uncertainty was due to the fact that the Piranis were not calibrated on the same day, but 2% is the maximum variation of day to day sensitivity. This was extremely encouraging and indicated the method was capable of performing its designed functions.

The amount of helium used in the above experiment was about 4×10^{-6} cc, so small blank errors, leaks, magnesium blanks, etc. up to about 4×10^{-8} cc would hardly matter. However, since the helium content of the sources was about 5×10^{-7} cc, it was

advisable to check the apparatus more carefully at lower helium concentrations, where uncertain blanks must be reduced below 5×10^{-9} cc. Two experiments were devized as part of this programme.

Firstly, a large sample of cast magnesium of the same type as that used in the percentage recovery experiments was dissolved alone and the helium found was 1.7×10^{-9} cc per gramme; much lower than the result above. It was possible that air bubbles were inhomogeneously distributed in the metal.

Secondly, a piece of beryllium metal, labelled 'helium-free' by a previous helium worker, was dissolved alone to determine the limiting size of the helium blank on the whole process. The piece of Be weighed about 5.5 g. and the total helium found on the whole process was 2×10^{-9} cc.

Unfortunately, the value of these last two experiments was thrown into serious doubt by subsequent experiments and discoveries. The former were two more percentage experiments using smaller amounts of helium as suggested above. These gave the surprising results of 5.9 and 4.5% recovery of the dissolved helium. At first it was suspected that the palladium had developed a small crack or hole. And indeed it was found that the palladium tube would allow atmospheric gas to slowly leak from the high to the low pressure side. By immersing the tube in water after demounting it from the apparatus and measuring the pressure, the leak was detected around the welded seal. The tube was dispatched for repair. However, it was found on checking the working of the apparatus with air samples that the column was functioning incorrectly. Mercury was found to be 'tailing' in one of the units forming a bead which

prevented gas passing down the column. Thus it seemed probable that the small percentage figures above were due to this cause and not to the small hole in the palladium. This was why serious doubt was cast upon the two experiments just previously performed (on the magnesium and the 'helium-free' beryllium).

On the arrival of the repaired palladium tube, the sequence of testing experiments was repeated. A helium recovery of 100% was obtained on a fairly large helium sample of about 4×10^{-6} cc. Blanks on 'helium-free' beryllium were again undertaken with renewed confidence.

Results of the Be blanks were:-

(i) 0.26×10^{-8} cc He/g. Be (on 5.4 g. Be)

(ii) 0.24×10^{-8} cc He/g. Be (on 6.5 g. Be)

These results, though in good agreement, are rather high for 'helium-free' beryllium, since the helium present in 6.8 g. would be around 1.7×10^{-8} cc, that is about $3\frac{1}{2}\%$ of the expected helium content produced by (γ, n) reactions in the time for which the sources were irradiated. These values are not in good agreement with the value of Hall[12] of 0.08×10^{-8} cc per gramme. It may be that the helium is not derived from the beryllium but produced during the running of the apparatus. It seems certain that the beryllium used by the various experimenters was of the same origin; and identical to that used in the construction of the sources. There seems to be no record of Reasbeck's measurements on the helium content of the source beryllium.

The percentage of helium recovered by the procedure was then subjected to a more rigorous check with an amount of helium

of the same order as that expected in the sources. The result obtained was 73.6%. The experiment was repeated by using an identical amount of hydrogen, that is, running period, but twice as much helium. The result was very similar at 76.0%. If these low results were due, as seemed likely, to helium being lost through the palladium, then the percentage recovery should be proportional to the reciprocal of the running period. Accordingly to test this, the same amount of beryllium disc was used, i.e. helium, but the hydrogen was halved by using only half the weight of magnesium. With the running period thus reduced from $4^1/_2$ hours to about $2^1/_2$, the percentage recovery was 89.0%.

This seemed to furnish proof of leakage of helium through the palladium during the hydrogen removal process. Unfortunately, it is regretted that time did not allow this section of the work to be concluded.

5.9. Summary and suggestions

It was found that the helium recovery was complete when the palladium tube was new, but after a certain amount of use, holes or micro-cracks or porosity to helium appeared. Katz and Gulbransen[110] who studied the diffusion of hydrogen through palladium, mention the phase change at 150° of PdH, and warn that a long tube life can only be expected if the tube is never cooled below 150°C in the presence of hydrogen. It may be that cycling through the phase change (as was done in the procedure described) produces a crystallinity or cracking which makes the walls porous to helium. Another possibility is that local overheating took place and weak spots in the welding became porous to helium. In view of the

propensity of palladium-silver alloy to leakage, it would appear that the procedure here described is unsuitable.

Hall succeeded in burning the hydrogen with oxygen but admits to great difficulties, and did not achieve an unambiguous blank of satisfactory proportions.

The method which seems to hold out the greatest promise is that of vacuum fusion. Induction furnaces for beryllium have been described in the literature[126, 127] of gas analysis in metals. It is true, however, that many such experiments were not concerned with small and sensitive measurements, and the size of the blank is very important. However, if the blank could be made to be accurately reproducible this would serve as well as a minimal blank.

REFERENCES

(1) Paneth, F.A.; Endeavour, 12, p.3, (1953).

(2) Glueckauf, E.; Proc.Roy.Soc., A185, p.89, (1946).

(3) Glueckauf, E., and Kitt, G.P.; Proc.Roy.Soc., A234, p.557, (1956).

(4) Paneth, F.A., and Peters, K.; Z.Phys.Chem., 34, p.353, (1928).

(5) Glueckauf, E., and Paneth, F.A.; Proc.Roy.Soc., A185, p.98, (1946).

(6) Chackett, K.F., Reasbeck, P., and Wilson, E.J.; Geochim. et Cosmochim.Acta, 3, p.261, (1953).

(7) Reasbeck, P.; Ph.D. Thesis, Durham University, (1953).

(8) Chackett, K.F., Paneth, F.A., and Wilson, E.J.; Nature, 164, p.164, (1949).

(9) Authors (8) in J.Atmos. and Terr.Phys., 1, p.49, (1950).

(10) Wardle, J.; Ph.D. Thesis, Durham University, (1957).

(11) Hemingway, J.D.; unpublished work, (1963).

(12) Hall, D.; Ph.D. Thesis, Durham University, (1958).

(13) Dushman, S.; 'Scientific Foundations of Vacuum Technique', Willey Inc., 2nd Edition, p.280.

(14) Ellet, A., and Zabel, R.M.; Phys.Rev., 37, p.1102, (1931).

(15) Barnes, R.S., et. al.; Proc.Int.Conf. on P.U.A.E. at Geneva (1958), 5, p.543. (Paper P/81).

(16) Rochlin, R.S.; Nucleonics, 17, (No.1), p.54, (1959).

(17) Mellish, C.E.; Nucleonics, 19, (No.3), p.114, (1961).

(18) Boldeman, J. W.; J. Nucl. En., Parts A/B, 18, p.417, (1964).

(19) Hughes, D. J.; 'Pile Neutron Research', p.98, (1953). Addison-Wesley Co., Mass.

(20) Wapstra, A. H.; 'Atomic Masses of Nuclides' in Encyclopaedia of Physics, Vol. 38/1, (1958).

(21) Bethe, H. A.; Rev. Mod. Phys., 9, p.163, (1937).

(22) Hughes, ibid. (19), p.94.

(23) Hughes, ibid. (19), Chapter IV.

(24) Roy, J. C., and Hawton, J. J.; A.E.C.L.1181, (1960).

(25) Mellish, C. E., Payne, J. A., Otlet, R. L.; A.E.R.E. 1/R 2360; also in 'Radioisotopes in Scientific Research', Vol. I., p.35, (1958).

(26) Nash, L. K., and Baxter, G. P.; J. Amer. Chem. Soc., 69, p.2534, (1957).

(27) Brenen, A.; A.E.R.E. Harwell, Private Communication.

(28) Martin, G. R.; Personal Communication.

(29) Birss, J. R.; Private Communication, (1965).

(30) Brookshier and Freund; Anal. Chem., 23, p.1110, (1951).

(31) Vogel; 'Quantitative Analysis', Longmans.

(32) Heath, R. L.; 'Scintillation Spectrometry Gamma-Ray Spectrum Catalogue', Phillips Petroleum Co., Report IDO-16408, (1957).

(33) Freidlander, G., and Kennedy, J. W.; 'Nuclear and Radiochemistry', Appendix C, Wiley Co., (1955).

(34) Mellish, C. E.; Report A.E.R.E.-R/3251, (1960).

(35) Hogg, C. H., and Weber, L. D.; Report I.D.O.-16744, (1962), and Private Communication quoted in (18).

(36) Vogel, 'Quantitative Analysis', p.897, 3rd Edition.

(37) Passell, T.O., and Heath, R.L.;
Nucl.Sci.Eng., 10, p.308, (1961).

(38) Martin, E.B.M.; Personal Communication.

(39) Katcoff, S.; Nucleonics, 16, (No.4), p.78, (1958).

(40) Glendenin, L.E. et al., in 'Radiochemical Studies: The Fission Products', Coryeli and Sugarman Eds., National Nucl.En.Series, IV-9, p.489, McGraw-Hill Co., (1951).

(41) Wahl, A.C.; J.Inorg.and Nucl.Chem., 6, p.263, (1958).

(42) Yaffé, L. et al., Canad.J.Chem., 32, p.1018, (1954).

(43) Petruska, J.A. et al., Canad.J.Phys., 33, p.693, (1955).

(44) Farrar, H. and Tomlinson, R.H.
Nucl.Phys., 34, p.367, (1962)

(45) Fulmer, C.B., and Cohen, B.L.;
Phys.Rev., 108, p.370, (1957).

(46) Katcoff, S.; Nucleonics, 18, (No.11), p.201, (1960).

(47) Ballou, N.E.; as ref.(40), p.1538, (Paper 257).

(48) Pate, B.D., and Yaffé, L.; Canad.J.Chem., 33, p.15, (1955).
See also p.610, ibid.

(49) Perkins, R.W.; Anal.Chem., 29, p.152, (1957).

(50) Farabee, L.B.; Report ORNL-1932, (1955).

(51) Fisher, S.A., and Meloche, V.W.;
Anal.Chem., 24, p.1100, (1952).

(52) Boyd, G.E., and Larson, Q.V.; J.Phys.Chem., 60, p. 1100, (1952).

(53) Hall, N.F., and Johns, D.H.;
J.Amer.Chem.Soc., 75, p.5787, (1963).

(54) Perrier, C., and Segre, E., J. Chem. Phys., 5, p.715, (1937).

(55) Martin, G.R.; J. Nucl. Instr. and Methods, 13, p.263, (1961).

(56) Wilson and Wilson. 'Comprehensive Anal. Chemistry', Vol. I. C., p.592.

(57) Pribil, R.; 'Analytical Uses of E.D.T.A.'. Ed. by Welcher, p.147.

(58) Belcher et al., Chem. and Industry, p.127, (1954).

(59) Wagner et al., Anal. Chem., 24, p.1031, (1952).

(60) Willard, H.H.; Anal. Chem., 22, p.1372, (1950).

(61) Welcher, ibid (57), p.146.

(62) Lyle, S.J., and Rahman, M.; Talanta, 10, p,1177, (1963).

(63) ibid (56), p.614.

(64) Kolthoff, I.M., and Sandell, E.B.; 'A Textbook of Quant. Analysis', p.560, (1947).

(65) Sher, R., and Moore, S.; BNL-607, T.178, Newsletter No.1, Neutron Cross Section Evaluation Group, (June, 1960).

(66) Allen, W.D.; 'Neutron Detection', p.188, Newnes, (1960).

(67) Bigham et al., Vol.16, p.44. Proc. of 2nd Int. Conf. on P.U.A.E. at Geneva, (1958), p.203.

(68) Hughes, D.J.; 'Neutron Cross Sections', p.165, (1957).

(69) Reed, G.W., and Turkevitch, A.; Phys. Rev., 92, p.1473, (1953).

(70) Terrell, J. et al., Phys. Rev., 92, p.1091, (1953).

(71) Santry, D.C., and Yaffe, L.; Canad. J. Chem., 38, p.464, (1960).

(72) Farrar, H., and Tomlinson, R.H., Canad. J. Phys., 40, p.943, and p.1017, (1962).

(73) Thode et al.; Phys.Rev., 78, p.129, (1950).

(74) Halpern, I.; Ann.Rev.Nucl.Sci., p.287, (1959).

(75) Glendenin, L.E.; Mass.Inst.Technol., Tech.Report No.35, (1949).

(76) Glendenin, L.E. et al., Phys.Rev., 84, p.860, (1951).

(77) Glendenin, L.E.; Proc. of 1st Conf. on P.U.A.E., Geneva, (1955). Vol.7, p.614.

(78) Wiles et al., Canad.J.Phys., 31, p.419, (1953).

(79) Pappas; Mass.Inst.Technol., Tec.Report No.63, (1953).

(80) Wanless and Thode; Canad.J.Phys., 33, p.541, (1955).

(81) Perlow, G.J., and Stehney, A.F.; Phys.Rev., 113, p.1269, (1959).

(82) Terrell, J.; Phys.Rev., 127, p.880, (1962).

(83) Fraser, J.S., and Milton, J.C.D.; Phys.Rev., 93, p.818, (1954).

(84) Whetstone, S.; Phys.Rev., 114, p.581, (1959).

(85) Apalin et al., Sov.J.At.Energy, (trans.), 8, p.10, (1961).

(86) Aten, A.H.W.; Physica, 28, p.262, (1962).

(87) Wattenberg, A.; Ann.Rev.Nucl.Sci., 3, p.119, (1953).

(88) Hughes, D.J.; Nucleonics, 12, (No.12), p.26, (1954).

(89) Richmond, R., and Gardner, B.J.; A.E.R.E. R/R 2097, (1957).

(90) Larsson, K.E.; J.Nucl.En., 6, p.322, (1958).

(91) Axton, E.J.; Nucleonics, 19, (No.3), p.60, (1961).

(92) Martin, G.R., and Martin, E.B.M.; in A.E.R.E. NP/R 1577, (1954): Report of Proc. of Int.Conf. on Neutron Sources, Oxford, 1954, (July), edited by Littler, D.J.

(93) Halban, H.; ibid (92).

(94) Dejuren, J.A. et al., J.Res.N.B.S., 40, p.63, (1955).

(95) Larsson, K.E.; Arkiv.Fysik., 7, p.323, (1954).

(96) Dejuren, J.A., and Chin, J.;
J.Res.N.B.S., 40, p.311, (1955).

(97) Bezotsnii, V.M., and Zamyatnin, Y.S.;
J.Nucl.En., 6, p.237, (1958).

(98) Axton, E.J., and Cross, P.; J.Nucl.En., 15, p.22, (1961).

(99) Noyce, R.H. et al., J.Nucl.En., 17, p.313, (1963).

(100) Erzolimsky, B.G., and Spivak, P.E.;
J.Nucl.En., 6, p.243, (1958).

(101) Florov, G.N., and Poretsky, L.B.;
Dokl.Akad.Navk.S.S.S.R., (1951).

(102) Larsson, K.E.; Arkiv.Fysik., 9, p.293, (1955).

(103) Marin, P. et al., in NP/R 1577, (92).

(104) Geiger, K.W.; Canad.J.Phys., 37, p.550, (1959).

(105) Martin, G.R.; in (92).

(106) Glueckauf, E., and Paneth, F.A.,
Proc.Roy.Soc., A.165, p.229, (1938).

(107) Ajzenberg, F., and Lauritsen, T.;
Rev.Mod.Phys., 27, p.77, (1955).

(108) McNeil, J., Unpublished Work.

(109) Davis, W.D.; KAPL-1227, (1954).

(110) Katz, O.M., and Gulbransen, E.A.;
Rev.Sci.Instr., 31, p.615, (1960).

(111) Lowell et al., Rev.Sci.Instr., 31, p.789, (1960).

(112) Paneth, F.A., and Peters; Z.Phys.Chem., Abt.B.,
Band 1, Heft 3/4, p.253, (1928)

(113) Walker and Westenburg; Rev.Sci.Instr., 28, p.789, (1957).

(114) Hoffman, J.H., and Nier, A.O.; Phys.Rev., 112, p.2112, (1958)

(115) Reynolds, J.H.; Rev. Sci. Instr., 27, No.11, p.928, (1956).

(116) Bullock, R.E., and Moore, R.G.; Phys.Rev., 119, p.721, (1960).

(117) Blatt, J.M., and Weisskopf, V.F., 'Theoretical Nuclear Physics', Wiley Co., New York, (1952).

(118) Hanni, H., and Rossel, J.; Helv. Phys. Acta., 23, p.513, (1950).

(119) Lonchamp, J.P.; J. Phys, Rad., 13, p.333, (1952).

(120) Faraggi, H.; J. Phys. Rad., 14, p.160, (1953).

(121) Way, K. et al., 'Nuclear Data Sheets', Nuclear Data Group, National Academy of Sciences, National Research Council, Washington.

(122) Grummitt, W.E., and Milton, G.M.; J. In. Nucl. Chem., 5, p.93, (1957)

(123) Prosdocimi, H., and Deruytter, A.J.; J. Nucl. En., 17, p.86, (1963).

(124) Eggler, C., and Hughes, D.J.; U.S.A.E.C. Report ANL 4476, (1950).

(125) Circular BNL 325, Supplement 1, p.4.

(126) Gregory, J.N., and Mapper; Analyst, 80, p.225, (1955), and ibid p.414, 78, (1953).

(127) Booth and Parker; Analyst, 84, p.546, (1959); and ibid 83, p.241, (1958); 82, p. 57, (1957).

(128) Barrer and Sutherland; Proc. Roy. Soc., A.237, p.439, (1956); and ibid A.258, p.431, (1960).

(129) Barrer and Gibbons; Trans. Farad. Soc., 59, p.2569 and p.2875, (1963); and ibid 57, p.1140 and p.1153, (1961).

(130) Rees, L.V.C., and Williams, C.J.;
Trans.Farad.Soc., 60, p.1973, (1964).

(131) Garden et al.; Proc.Roy.Soc., A234, p.35, (1956).

(132) Bunney, L.R., and Freiling, E.C.;
Nucleonics, 13, (No.9), p.112, (1956).

(133) Lipschutz et al.; J.Geophysical Research,
70, No.6, p.1473, (1965).

(134) Salisbury, S.R., and Chalmers, B.A.;
Phys.Rev., 140, No.2B, p.305, (1965).

(135) Hinves, R., and Parker, K.;
A.W.R.E. Report No. 0-2/60, (1960).

(136) Cranberg, G. et al.; Phys.Rev., 103, p.662, (1956).

(137) Alter, H., and Weber, C.E.;
J.Nucl.Materials, 16, (No.1), p.68-73, (1965).

(138) Carroll, E.E., and Smith, G.G.;
Nucl.Sci.Eng., 22, p.411, (1965).

(139) Van Loef, J.J.; Nucl.Phys., 24, p.340, (1961).

(140) Malmsrog, S., and Lauber, A.; Unpublished Work.

(141) March, P.V., and Morton, W.T.;
Phil.Mag., 3, p.143, (1958).

(142) Allan, D.L.; Nucl.Phys., 10, p.348, (1959).

(143) Pollehn, Von.H., and Neuert, H.;
Z.Naturforsch, 16a, p.227, (1961).

(144) Buttner, H. et al.; Nucl.Phys., 63, p.615, (1965),
and Private Communication.

(145) Cross, W.G., and Clarke, R.L.; A.E.C.L. Report
No. PR-P-53, (1962), Unpublished.

(146) Chittenden, D. M. et al.; Phys. Rev., 122, p.860, (1961).

(147) Allen, W. D.; ibid (66), p.202.

(148) Adamson,; TRG Memo. 2452(D) and Physics Working Party Paper, FRSC/RPWP/P.76, (May, 1964), Dounreay.

(149) Birss, I.R.; Personal Communication, (1966).

(150) Wright, S.B.; A.E.R.E. R/4080, (1962).

(151) Clare, D. M. et al.; Nucl. Sci. Eng., 18, p.448, (Apr. 1964).

(152) Martin, W. H., and Clare, D. M.; Nucl. Sci. Eng., 18, p.465, (Aug. 1964).